

PREFACE

Nguyen, Trinh., INHIBITION OF LET-7I AS A MEANS TO ENHANCE THE NEUROPROTECTIVE EFFICACY OF PROGESTERONE IN THE ISCHEMIC BRAIN. Doctor of Philosophy (Biomedical Sciences), February, 2018, pp 194, 30 illustrations.

The occurrence of ischemic stroke is relatively rare among pre-menopausal women. Strikingly, this risk doubles every 10 years after the menopausal transition; and women are likely to experience worse outcomes and higher mortality post stroke than men. Since both estrogen (E2) and progesterone (P4) levels decline precipitously following the menopause, this hormonal reduction may, at least partially, contribute to the higher risk and worse outcomes. By inference, these hormones could play a critical role in protecting women against ischemic stroke. In this dissertation project, we focus on P4, the relatively understudied of the two hormones. And while P4 has been shown to be a potent neuroprotectant in various experimental models of stroke, the underlying mechanisms remain unclear. One known mediator of P4's protective function is brain-derived-neurotrophic-factor (BDNF), which has an established role in promoting neuronal differentiation, survival, and synaptogenesis. In addition, emerging literature and data from our laboratory strongly support the indispensable role of glia in P4's neuroprotective program and thus, may also play a significant role in post-stroke recovery. We recently reported that P4 induces a significant release of BDNF from primary astrocytes, through a putative membrane-associated progesterone receptor consisting of progesterone-receptor-membrane-component-1 (Pgrmc1). This receptor is abundantly expressed in various regions of brain and mediates such effects of P4 in the central nervous system (CNS) as anti-apoptotic effects, spinogenesis, and BDNF release. What is not known, however, is how the expression of this receptor is regulated. This dissertation was aimed to elucidate what regulates the expression of Pgrmc1 and BDNF in glia and how such regulation influences the neuroprotective function of P4 in the ischemic brain. Based on the observation that Let-7i regulates the expression of Pgrmc1 in a peripheral cell type,

and our *in silico* analysis that revealed that both *Pgrmc1* and BDNF are potential targets of let-7i, we hypothesized that let-7i represses P4's neuroprotective effects by down-regulating the expression of both *Pgrmc1* and BDNF in glia, leading to: 1) suppression of P4-induced BDNF release from glia, and 2) attenuation of the beneficial effects of P4 on neuronal survival and markers of synaptogenesis in the ischemic brain.

Using primary cortical astrocytes as an experimental model, we found that let-7i negatively regulated the expression of *Pgrmc1* and BDNF. This was correlated with a reduction in P4-induced BDNF release from these cells. Under such conditions of reduced expression of both *Pgrmc1* and BDNF, P4 was unable to protect primary neurons against oxygen-glucose-deprivation (OGD) or regulate markers of synaptogenesis. In our *in vivo* model of transient ischemic stroke, we found that protective effects of P4 were greatly enhanced in animals that were concomitantly treated with an inhibitor (antagomir) of let-7i. The combined treatment also enhanced synaptogenesis in the peri-infarct region. Collectively, the data presented here suggested that in the ischemic brain, let-7i negatively influences P4-induced neuroprotection via regulation of the *Pgrmc1*/BDNF axis. As such, inhibition of let-7i maybe an effective means to enhance the efficacy of P4 in treating ischemic stroke.

INHIBITION OF LET-7I AS A MEANS TO ENHANCE THE NEUROPROTECTIVE EFFICACY
OF PROGESTERONE IN THE ISCHEMIC BRAIN.

TRINH NGUYEN, B.S.

APPROVED:

Major Professor

Committee Member

Committee Member

Committee Member

University Member

Chair, Department of Pharmacology & Neuroscience

Dean, Graduate School of Biomedical Sciences

INHIBITION OF LET-7I AS A MEANS TO ENHANCE THE NEUROPROTECTIVE FUNCTION
OF PROGESTERONE IN ISCHEMIC BRAIN

DISSERTATION

Presented to the Graduate Council of the
Graduate School of Biomedical Sciences

University of North Texas

Health Science Center at Fort Worth

In Partial Fulfillment of the Requirements

For the Degree of

DOCTOR OF PHILOSOPHY

By

Trinh Nguyen, B.S

Fort Worth, Texas

February 2018

ACKNOWLEDGEMENTS

First and foremost, I would like to express my deepest gratitude to my mentor, Dr. Meharvan Singh, for his utmost support, guidance, and patience. It has been an honor to be his Ph.D. student. He has always prioritized my training despite his busy schedule and is very supportive of ideas and choices that I make. The joy and enthusiasm he has for research are contagious and inspiring for me, even during difficult times in the Ph.D. training. I am thankful for the excellent example he has provided as a successful scientist and mentor.

I would also like to express my sincere appreciation to my former co-mentor, Dr. Chang Su, who has been a dedicated mentor. Same as Dr. Singh, Dr. Su had always prioritized my training and tried her best to provide guidance and nurturing environment for me to grow as a scientist. She has always amazed me for her absolute dedication to science and family. It holds a special meaning to be her first Ph.D. student.

As an extension of my appreciation, I would like to thank all of my committee members: Dr. Alakananda Basu, Dr. Anuja Ghorpade, Dr. Rebecca Cunningham and Dr. Shaohua Yang for their support. Their guidance and constructive criticism helped to shape this dissertation work and to improve my critical thinking.

My family members have played important roles to me in the pursuit of this project than the members of my family. I would like to thanks my parents, whose love and guidance are with me in whatever I pursue. Most importantly, I am thankful to my loving and supportive husband, Ruslan, who provides unending inspiration and motivation throughout the process.

TABLES OF CONTENTS

LIST OF ILLUSTRATIONS.....	xi
LIST OF ABBREVIATIONS.....	xiv
CHAPTER I. Introduction.....	1
Stroke.....	1
Demographics of Stroke.....	1
Economic Impact of Stroke.....	2
Psychological Impact of Stroke.....	3
Sex Differences in Stroke.....	4
Why Older Women Have a Greater Risk of Stroke Than Men.....	5
Hormone Are Protective.....	6
Estrogen.....	6
Progesterone.....	7
Progesterone Receptors in the Central Nervous System.....	7
Cellular/Molecular Mechanisms of Progesterone-Induced Neuroprotection.....	10
BDNF.....	11
Menopause and The Post-Menopausal Period.....	12
Introduction of microRNA	14

The Let-7 microRNA Family.....	15
Why Let-7i.....	16
Hypothesis.....	17
References.....	23
Chapter II. General Methods.....	42
Primary Neurons and Astrocytes Preparation.....	42
Transfection.....	43
Quantitative RT-PCR.....	43
BDNF Release Assay.....	44
CellTiter-Glo Luminescent Viability Assay.....	45
Oxygen-Glucose Deprivation.....	45
Western Blotting.....	46
Immunofluorescence.....	47
Ovariectomy.....	48
Transient Middle Cerebral Artery Occlusion (MCAo).....	48
Intracerebroventricular (ICV) Injection	49
2,3,5-Triphenyltetrazolium Chloride (TTC) Staining.....	49
Wire Suspension Test.....	50
Synaptophysin (SYP) Optical Density Analysis and Puncta Quantification.....	50
References.....	52

Chapter III. Let-7i Inhibition Potentiates Progesterone’s Action On Functional Recovery in a Mouse Model of Ischemia.....	54
Abstract.....	55
Significance.....	56
Introduction.....	57
Materials and Methods.....	59
Results.....	70
Discussion.....	75
Acknowledgments.....	79
Figures.....	80
References.....	99
 Chapter IV. Pgrmc1/BDNF Signaling Plays a Critical Role in Mediating Glia-Neuron Crosstalk	 104
Abstract.....	105
Introduction.....	106
Materials and Methods.....	109
Results.....	116
Discussion.....	121
Acknowledgments.....	124
Figures.....	125

References.....	143
Chapter V. Additional Data.....	148
Chapter VI. Summary and Future Direction.....	166
Summary.....	166
Future Directions.....	170
Therapeutic Window.....	170
Alternative Delivery Approaches.....	170
Potential Effects in Other CNS Cell Types.....	171
Mechanism Underlies the Conversion of BDNF Protein in Ischemic Brain.....	172
Other CNS Disease Models	173
Conclusion.....	173
References.....	175
Chapter VII. Patent/Publications.....	178

LIST OF ILLUSTRATIONS

The overview of miRNA biogenesis.....	19
The vertebrate let-7 family.....	20
Potential binding sites of let-7i on Pgrmc1 and BDNF.....	21
Central hypothesis.....	22
Let-7i negatively regulates the expression of Pgrmc1 and BDNF in primary cortical astrocytes.....	80
Let-7i and OGD abolished progesterone (P4)-induced BDNF release from primary cortical astrocytes.....	82
Let-7i prevents progesterone (P4)-induced neuroprotection against oxygen- glucose-deprivation (OGD)	84
Let-7i inhibits progesterone (P4) induces synaptophysin (SYP) expression in primary cortical astrocytes.....	86
Combined treatment with progesterone (P4) and the let-7i inhibitor reversed ischemia-induced suppression of Pgrmc1 and BDNF expressions in the peri-infarct region.....	90
Co-administration of let-7i antagomir (anti-let-7i) and progesterone (P4) reduces ischemic injury.....	92
Co-administration of let-7i antagomir (anti-let-7i) and progesterone (P4) enhances	

recovery of motor function/grip strength following stroke.....	94
Inhibition of let-7i enhances progesterone (P4)'s effect on the expression of synaptophysin in the peri-infarct region.....	96
P4 increases the ratio of mature to pro-BDNF released from glia.....	125
P4 did not affect the mRNA levels of GAP43 and SYP in differentiated SH-SY5Y cells.....	127
P4-CM triggers synaptic marker expression in mouse hippocampal neurons.....	129
P4-CM-induced morphological change in SH-SY5Y cells.....	131
Effect of glial-CM on the expression of synaptic markers.....	133
Glial P4-CM increased GAP43 density in both proximal and distal neuritic segments of SH-SY5Y cells.....	135
Blocking of BDNF signaling inhibited glial P4-CM-induced GAP43 density in both proximal and distal neuritic segments of SH-SY5Y cells.....	137
Blocking of BDNF signaling inhibited glial P4-CM-induced GAP43 density in both proximal and distal neuritic segments of primary hippocampal neurons.....	139
P4-CM increased neuronal survival against oxidative stress.....	141
Oxygen-glucose deprivation (OGD) induces expression of let-7i in primary cortical astrocytes.....	148
Oxygen-glucose deprivation (OGD) suppresses the P4-induced BDNF release	

from primary cortical astrocytes.....	150
Transfection duration optimization.....	152
Progesterone (P4) levels in ovariectomized (OVX) mice, with and without P4 pellet Implantation.....	154
The distribution of let-7i inhibitor via the intracerebroventricular injection (ICV)	156
TTC (2,3,5-triphenyltetrazolium chloride) staining of an ischemic brain.....	158
The colocalization of let-7i inhibitor (green fluorescent) with different cell types in ischemic brain	160
The homology of let-7i sequence in mouse vs human.....	164
Binding sites of let-7i on human BDNF and Pgrmc1 genes.....	165

LIST OF ABBREVIATIONS

AD	Alzheimer's disease
AF	Activation function
ALS	Amyotrophic lateral sclerosis
ATP	Adenosine triphosphate
BBB	Blood-brain barrier
BDNF	Brain-derived-neurotrophic-factor
CCA	Common carotid artery
CNS	Central nervous system
CSF	Cerebrospinal fluid
Ct	Cycle threshold
DBD	DNA binding domain
DGCR8	DiGeorge syndrome critical region gene 8
DMEM	Dulbecco's modified Eagle's medium
DMSO	Dimethylsulfoxide
E2	Estrogen
ECA	External carotid artery
FBS	Fetal bovine serum
FSH	Follicle-stimulating hormone

GnRH	Gonadotropin-releasing hormone
HBSS	Hank's balanced salt solution
HD	Huntington's disease
HMGA 2	high-mobility group AT-hook 2
IACUC	Institutional animal care and use committee
ICA	Internal carotid artery
IF	Inhibition function
IL-1 β	Interleukin-1 β
IMP-1	IGF-II mRNA-binding protein 1
KLF8	Kruppel-like factor 8
LDB	Ligand binding domain
LH	Luteinizing hormone
LTD	Long-term-depression
LTP	Long-term-potential
MiRNA	MicroRNAs
MMP	Matrix metalloproteinase
NHANES	National Health and Nutrition Examination Surveys
OGD	Oxygen-glucose-deprivation
OVX	Ovariectomy
P4	Progesterone

PAQR	Progesterin and adipoQ receptor
PD	Parkinson's disease
PEI	Polyethyleneimine
PFA	Paraformaldehyde
Pgrmc1	Progesterone-receptor-membrane-component-1
PRE	Progesterone response element
RISC	RNA-induced silencing complex
RVG	Rabies viral glycoprotein
SYP	Synaptophysin
TBI	Traumatic brain injury
TGF β 2	Transforming growth factor- β 2
tPA	Tissue-type plasminogen activator
WHO	World Health Organization

CHAPTER I

INTRODUCTION

STROKE

A stroke occurs when the flow of oxygen-rich blood to a brain region is interrupted or reduced, leading to cell death due to oxygen and nutrient deprivation (1). There are two main types of stroke: ischemic stroke and hemorrhagic stroke (2). An ischemic stroke occurs when an artery that supplies oxygen to the brain is clotted, while a hemorrhagic stroke is caused by rupture of an artery resulted in blood leakage that damages surrounding brain cells (1). Ischemic stroke is the more common type which accounts for about 87% of all strokes, and the remaining 13% is hemorrhagic (1).

DEMOGRAPHICS OF STROKE

According to the World Health Organization (WHO), 15 million people experience stroke worldwide each year. Of these, 5 million dies and another 5 million are permanently disabled. Thus, stroke is ranked as the second leading cause of death in the world population after ischemic heart disease (3). This global epidemic is not limited to western or high-income countries. In fact, an estimation of 85% of all stroke death occurs in low-to-middle-income countries (4).

The United States (US) Centers for Disease Control and Prevention has also reported stroke as the fifth leading cause of death in the US and is a major cause of serious disability for adults. It is reported that stroke kills about 140,000 Americans each year; that is 1 out of every 20 deaths (5). Each year, more than 795,000 people in the US suffer from stroke, approximately 610,000 of these are first or new strokes (6). And of the remaining 185,000 cases, nearly 1 of 4

are in people who have had a previous stroke (6). As mentioned earlier, stroke is a leading cause of serious long-term disability in the US; it reduces mobility in more than half of stroke survivors age 65 and older (6).

The risk of having a stroke varies with race and ethnicity. For example, it has been reported that the risk of having a first stroke is nearly twice as high for African Americans as for Caucasians, and African Americans have the highest mortality rate due to stroke (5). Even though the stroke mortality rates have declined over the past decade among all race and ethnicities, an increase in mortality rate has been observed within the Hispanic population (5). Age is another substantial risk of stroke; the elderly population accounts for one-third of ischemic stroke cases, and for two-thirds of the overall stroke-related morbidity and mortality (7). Since age is one of the risk factors for stroke, the growing aging population will likely to be at risk. For example, among European countries, Italy has the highest percentage, approximately 19.9%, of the elderly population at the age of 65 years or older (8); and an estimated 153,000 new stroke cases are expected each year in the elderly Italian population (8). Assuming stable incidence rates, a total of 195,000 new stroke cases per year are expected in 2020, simply due to the aging population (9). Although aging is a relevant risk for stroke; however, stroke can and does occur at any age. For example, in 2009, it was reported that 34% of hospitalized stroke patients were less than 65 years old (6).

ECONOMIC IMPACT OF STROKE

An estimate of 50% stroke survivors must cope with physical and cognitive impairment (10, 11). Accordingly, these stroke survivors are in need of support for daily activities that directly impact the quality of life of the stroke patient. The economic burden of stroke is also significant. For example, Evers et al., showed that on average, care for stroke survivors accounted for about

3% of total global healthcare expenditure (12). European countries are estimated to spend a total of €27 billion, €18.5 billion (68.5%) for direct and €8.5 billion (31.5%) for indirect costs, for stroke-related care (13).

In the US, stroke also imposes a substantial economic burden on our healthcare system, with acute ischemic stroke accounting for the bulk of costs. A study in 2008 estimated that the total direct and indirect cost of stroke in the US was \$65.5 billion (11). 67% of this total cost is a direct cost, which includes the cost of health professionals, acute and long-term care and other medical costs; indirect cost accounts for the remaining 33%, which is a result of lost productivity resulting from mortality and morbidity following stroke (11). These number indicates that stroke can be ranked among the most expensive chronic diseases.

PSYCHOSOCIAL IMPACT OF STROKE

Stroke survivors are often suffering from a considerable permanent impairment that leaves long-lasting impacts on their psychological health. For example, several studies have reported that the majority of stroke survivors experience depression, mood swings, irritability and anxiety (14, 15), and these implications sometimes continue up to five years after stroke occurrence (16-18). In addition, depression is one of the factors that contribute to slow recovery of stroke patients (19) and is associated with increased mortality (20). Chronic insomnia is another serious condition that affects about 30-37% of stroke survivors (21). These patients are also likely to experience mild to severe degree of cognitive impairments including difficulties in concentrating, and memory deficits (22-24).

The psychological issues of stroke survivors discussed above arise due to functional disabilities following stroke. Approximately one-third of stroke survivors experience communication difficulties, including dysarthria, aphasia or apraxia (25-27), leading to challenges

with speech comprehension and production, along with difficulties with reading and writing. The overwhelming impact of the communication deficit often causes stroke survivor to become so focused on regaining their communication abilities, to the extent that other physical needs are ignored (28). Communication impairments also lead to social exclusion, feelings of isolation experienced by survivors and sometimes adversely impact their works (16, 18). Stroke survivors often experience a decline in social network relationships due to the loss of opportunities for contact through workplace and recreation. Overall, the experience of decline in social interaction and daily activities (29) makes stroke survivors more vulnerable to depression.

SEX DIFFERENCES IN STROKE

Sex differences have not only been reported in epidemiologic studies that evaluated the prevalence/incidence of stroke, but also in the pathophysiology, outcomes, and their response to treatments. For example, results from the Framingham Heart study revealed sex differences in the reduction of stroke incidence from 1950 to 2004, with 30.3% decrease for men and only 17.8% for women (30). Even though the occurrence of ischemic stroke is relatively rare among premenopause women; strikingly, this risk doubles every 10 years after the menopausal transition; and older women are likely to experience worse outcomes and higher mortality (31, 32). In agreement, Towfighi *et al.*, reported a surge in the prevalence of mid-life stroke among women aged 45 to 54 years in the US (33). The same group also reported higher stroke prevalence in women compared with men 45 to 54 years of age when analyzing the data from the National Health and Nutrition Examination Surveys (NHANES) (34). Similarly, the American Heart Association statistics revealed that global stroke prevalence was 3% in 2008, being most prevalent in men (age-adjusted male/female ratio of 1.41) (35); interestingly, in the older age group (85 years and older), stroke was far more common in women than in men (36). Compared to male counterparts, older women are also likely to experience worse functional outcomes and

slower recovery post-stroke (37-39). Another study analyzed data obtained from the World Health Organization (WHO) and revealed that across European and Central Asian countries, stroke caused a total death of 739,000 women, which was almost double the number in men (487,000 deaths), with 60% of death occurred among subjects at 75 years or older (40). This study (40) also showed that in subjects below 65 years of age, the mortality rate was higher among men (male/female ratio = 1.72), whereas this relationship was reversed in subjects over 75 years of age (male/female ratio = 0.42). Reeves *et al.*, also reported that in the US, there was similar difference in mortality rate between both sexes, among subjects aged 65 or younger such that there were approximately 7,500 more stroke deaths in women aged 75–84 years, and nearly 26,000 more stroke deaths in women aged over 85 years (41).

WHY OLDER WOMEN HAVE A GREATER RISK FOR STROKE THAN MEN

One explanation for the greater risk/prevalence of stroke in older women is thought to be due to their greater life expectancy, thus allowing them to reach the age of greatest stroke risk (40). Another possible reason for observed acceleration of mid-life stroke risk factors for women seems to be associated with the menopausal transition (42, 43), a process that is characterized by dramatic declines in two major ovarian hormones, estradiol (E2) and progesterone (P4). This hypothesis is well supported, where studies have also shown that these hormones can exert neuroprotective effects (44-47), and evidence of more severe neurological deficits associated with menopause (44, 48, 49).

HORMONES ARE PROTECTIVE

ESTROGEN

The effect of estradiol (E2), the biologically most potent and prevalent estrogen in the premenopausal period, on reproduction and sexual behavior has been well studied prior to the 1990's (50, 51). After the mapping of nuclear estrogen receptor in brain regions such as hypothalamus, context, and hippocampus (52, 53), the field started to realize the extended functions of this steroid hormone beyond the confines of the reproductive system. Since then, studies have demonstrated the neuroprotective functions of E2 against a wide variety of injuries including Alzheimer's disease (AD), traumatic brain injury (TBI), hypoxia and excitotoxicity (54-57). In addition, Simpkins and Yang et al., are among the first groups to demonstrate the neuroprotective function of E2 against ischemic stroke (48, 58, 59), followed by others (44, 45, 60-62).

For decades, the field focused on E2 such that the reduced prevalence/risk for stroke in the premenopausal female was thought to be largely due to the protective effects of E2. For this reason, progesterone (P4) has been understudied in the context of neural injuries including ischemic stroke. However, it is worth noting that the levels of P4 also decline precipitously following menopause. As such, increased risk for stroke, worse functional and cognitive impairment, and higher mortality following stroke in post-menopausal women could also be contributed by the loss of P4. Growing literature from studies conducted over the past decade have provided evidence supporting the notion that P4 is a potent neuroprotectant against a variety of neural injuries including cerebral ischemia (63-65).

PROGESTERONE

PROGESTERONE RECEPTORS IN THE CENTRAL NERVOUS SYSTEM

Progesterone (P4) is known to trigger multiple signaling pathways depending on the specific interaction with its receptors. For example, P4 can participate in gene expression regulation by acting via classical progesterone receptors (PR) that belong to the nuclear steroid receptor superfamily. Cellular/physiological responses resulted from the PR-mediated signaling are relatively slow, considering the time required for the process of gene transcription, followed by translational modification, to create protein products, that in turn, exert their physiological effects. In contrast, studies have shown that P4 can also elicit rapid and non-genomic actions through putative cell membrane-associated receptors, resulting in the activation of intracellular signaling pathways more commonly associated with growth factors (66-68).

The classical PR exists as two major isoforms: PR-A and PR-B. These two isoforms are transcribed from two distinct promoter regions of a single gene and differ by a 164-amino-acid segment in the N-terminal region of PR-B (69, 70). The structure of PR infers four functional domains including an N-terminal regulatory domain, a DNA binding domain (DBD), hinge region and a C-terminus ligand binding domain (LBD) (71). In addition, it also contains transcription activation function (AF) and inhibition function (IF) domains (72), which serve as binding sites for nuclear coregulators. Concerning functionalities, despite sharing similar affinities for hormone and DNA-binding, the actions of PR-A and PR-B are remarkably different, and they target distinct gene networks (73-75). And in some instances, the two isoforms even exert opposite effects on the same gene promoter such as human gonadotrophin-releasing hormone receptor, uteroferrin, catechol-O-methyltransferase, and corticotrophin-releasing hormones genes (75-79). The exact mechanisms by which the two isoforms exert their specific transcriptional regulation, however, remain unclear. It has been speculated that transcription factors and nuclear coregulator proteins

flanking the progesterone response element (PRE) might attribute to the transcriptional regulatory specificity of these isoforms (75).

According to the classical view, gene transcription requires the dimerization of PRs and its subsequent binding to the PRE of target genes in the nucleus (71). However, this model has been questioned because of recent evidence suggesting that PR monomers may even be more efficient trans-activators than dimers (75, 80). PR expression is regulated by both E2 and P4 in a region-specific manner. For example, E2 induces PR expression in hypothalamic and limbic regions, including the nucleus of the stria terminalis, the CA1 region of the hippocampus and amygdaloid nucleus (81, 82), but not in other brain regions such as cerebral cortex, caudate putamen, midbrain, cerebellum, dentate gyrus and the CA3 region of the hippocampus (81, 82). Interestingly, studies showed that P4 only downregulates expression of PR in regions where E2 elicits an increase in its expression. However, it has no effect on PR expression in brain regions that are not responsive to E2 (83-85).

As mentioned above, P4 can exert rapid, non-genomic actions by activating membrane receptors belonging to the progestin and adipoQ receptor (PAQR) family, referred as membrane progesterone receptors (mPRs) (86-88). mPRs are G-protein coupled receptors that exhibit seven transmembrane-spanning domains and are divided into three classes based on their ligand binding and structural properties (89, 90). Among these three classes, only members in class II are present in vertebrates, including mPR α , mPR β , mPR γ , mPR δ and mPR ϵ , which were cloned and characterized by Thomas and colleagues (86, 87, 91). Among these, mPR β , mPR γ , mPR δ are G_i-protein-coupled receptors, whereas mPR α and mPR ϵ are coupled to G_s proteins (86, 87, 91). These mPRs have been mapped in the human brain, and their levels and expression patterns vary across brain regions. For example, highest levels of mPR α were detected in the medulla, pituitary gland, and temporal lobe. mPR β is highly expressed in hippocampus, hypothalamus, corpus callosum, substantia nigra, and cerebellum. mPR γ is less abundant than other mPRs in many brain regions, with highest relative expression in the choroid plexus and pons. mPR δ is

mostly expressed in the forebrain, corpus callosum, hypothalamus, amygdala, whereas mPR ϵ is abundant in the hypothalamus and pituitary gland (86, 87, 91). mPRs are also expressed in mouse and rat brain. For example, mPR α was widely detected in many regions including the striatum, cortex, hypothalamus, thalamus, cerebellum, and hippocampus (92). mPR β has been mapped to the mediobasal hypothalamus (93), and it is also highly expressed in the forebrain, midbrain, cortex, thalamus, and hypothalamus (94). The expression of mPR γ in the mouse brain is low and was only detected using the RT-PCR method, but not by in-situ hybridization (95). Knowledge on the regulation of these mPRs, however, is still limited. Expression of mPR α and mPR β in the brain have been shown to vary with hormonal changes during the estrous cycle, with highest mPR expression noted at proestrus (a period of high E2 levels), suggesting these two mPRs could potentially be downregulated by progesterone and upregulated by estrogen (96). Regulation of the remaining mPRs is still not uncharacterized. Information on the functionalities of mPRs also remains limited. mPR α has been shown to mediate progesterone's antiapoptotic function in granulosa and breast cancer cells (97, 98), and is likely to be involved in inhibition of gonadotropin-releasing hormone (GnRH) release from rodent GnRH neurons (99). It has also been suggested that mPR β may have similar steroid binding and signaling characteristics as seen with mPR α (100, 101). For example, these two mPRs were shown to have similar functions in mediating P4's transactivation of the classical PR in human myometrial cells (101); and these two mPRs have been implicated in the progesterone's action in the ventral tegmental area (VTA) leading to facilitation of lordosis in rats (102). Functions of the remaining three mPRs are still unclear.

Another known putative receptor that mediates P4's rapid, non-genomic action is the progesterone-membrane-receptor-component 1 (Pgrmc1), also known as 25-Dx. Pgrmc1 was first cloned from porcine liver microsomes in 1996 (103). Its structure is composed of 194 amino acids and consists of a single transmembrane domain (103, 104). Pgrmc1 was detected with low expression throughout the cortex and striatum, while highly expressed in other brain regions that

include the hypothalamus, amygdala, ventromedial hypothalamus, paraventricular nucleus, supraoptic nucleus, arcuate nucleus, and hippocampus (105). Various functions have been proposed for this putative receptor. For example, Pgrmc1 can act as an adaptor protein to transport mPR α to the cell membrane, and this Pgrmc1/mPR α complex acts as a membrane progesterone receptor to mediate progestin-induced anti-apoptosis (106). It also mediates P4-induced proliferation of neural progenitor cells (107), P4's antagonism of ion channels in epithelial cells (108), P4's inhibition of calcium oscillations in hypothalamic neurons (109), and osmoregulation in traumatic brain injury (110). Another important function of Pgrmc1 in P4's protective effects, and characterized by our laboratory, is its involvement in the release of brain-derived-neurotrophin-factor (BDNF) (111). Despite Pgrmc1's wide distribution in brain and its potential importance in mediating P4-induced protection, knowledge regarding the regulation of Pgrmc1 in brain and the consequence of such regulation is limited.

CELLULAR/MOLECULAR MECHANISMS OF PROGESTERONE-INDUCED NEUROPROTECTION

Numerous mechanisms have been proposed to underlie the neuroprotective effects of progesterone (P4). For example, P4 elicits protection by activating signaling pathways such as the MAP/ERK (112, 113) and Akt (114) pathway in neurons; these pathways are known to associate with neuroprotection (114, 115). In addition to its direct effect on neurons, P4 can also exert neuroprotection by acting on non-neuronal populations. For instance, P4 can dampen glial activation (116), suppress inflammation and the production of nitric oxide synthase (64), and increases myelination (117), all of which may indirectly confer neuroprotection.

P4-induced neuroprotection may also be attributed to its genomic action – i.e., through the regulation of gene expression. For example, P4 increases the expression of BDNF (118, 119), which in turn, could lead to cell survival. It is also worth noting that neurotrophin signaling is a necessary element in P4-induced neuroprotection (120). P4 is also capable of modulating

expression of inflammatory cytokines such as interleukin-1 β (IL-1 β) and transforming growth factor- β 2 (TGF β 2) (64), which may contribute to their suppression during the injury-induced inflammatory response.

Alternatively, P4 may also act on cell surface novel receptors such as mPRs or Pgrmc1, where it can elicit the activation of rapid signaling transduction pathways that in turn, regulate cellular events that are relevant and critical for neuroprotection. For example, as stated above, P4 can activate signaling pathways including MAPK (ERK1/2) (112, 121), the PI-3K/Akt pathway (114) and the cAMP/PKA (91, 122), all of which have been implicated in neuroprotection. The activation of MAPK and Akt pathways have been shown to upregulate anti-apoptotic protein such as Bcl-2 (113). Moreover, Pgrmc1/mPR α complex plays a role in mediating P4-induced anti-apoptotic function (106). Importantly, recently published work from our laboratory reported P4 induced BDNF release from glia, and that this glial-derived BDNF was neuroprotective and resulted in an enhancement on synaptogenic markers (111).

BDNF

BDNF, another known mediator of P4's protective function, has been gaining attention due to its essential role in many important processes that are required to maintain healthy function of the central nervous system (CNS). BDNF belongs to the neurotrophin family, and it is synthesized in both neurons and glia (123, 124). BDNF is initially synthesized as a glycosylated precursor (pre-pro-BDNF), processed into a 35 kDa pro-BDNF, which can then be converted into the 14 kDa mature BDNF (125, 126). The pro- and mature form of BDNF preferentially act on different receptors that elicit opposite biological functions, such that mature BDNF binds to the TrkB receptor and influence neuronal survival, differentiation, and promote long-term-potentialiation (LTP) (124, 125, 127), whereas pro-BDNF binds to p75NTR and can promote neuronal apoptosis and long-term-depression (LTD) (126). Studies have linked a deficit in BDNF to stroke

pathophysiology (128, 129). In addition, it has been suggested that neuronal dysfunction or atrophy observed in aging or age-associated diseases may be attributed to decreases in mature neurotrophic factor expression or function (130, 131). BDNF has an established role in promoting neuronal differentiation, survival, synaptic plasticity (123, 132) and synaptogenesis [19-21]. Synaptogenesis occurring in the peri-infarct region is known to strongly contribute to enhanced functional recovery from stroke [22-25]. Based on these observations, it is plausible that the P4/BDNF signaling-mediated enhanced synaptogenesis and neuroprotection may contribute to P4's protective effects during post-stroke brain repair.

Another mechanism by which P4 can induce protective effect is through its metabolite, allopregnanolone (or 3 α , 5 α tetrahydro-progesterone), which binds to GABA_A receptor, leading to the potentiation of GABA-induced chloride conductance (133). Emerging evidence has suggested that allopregnanolone plays a role in mediating the protective effect of P4 (134-136). In addition to acting on GABA_A receptor system, allopregnanolone may also exert neuroprotection through its actions on the mitochondria (137). For example, Sayeed et al., have reported that allopregnanolone inhibits currents associated with the opening of the mitochondrial permeability transition pore (mtPTP) and therefore, may help reduce the occurrence of apoptosis as a consequence of injury-induced mtPTP opening (136). Allopregnanolone has also been shown to be a potent mPR δ agonist that triggers an increased cAMP production and the promotion of anti-apoptotic function in hippocampal neurons (91).

MENOPAUSE AND THE POST-MENOPAUSAL PERIOD

The menopause is marked as one of the most significant events in a woman's life, bringing along various physiological changes that permanently affect the reproductive ability of a woman. It is defined as the termination of menstruation leading to ovarian failure characterized by the loss of ovarian follicle development (138). Menopause begins at the time of the final menstruation,

followed by 12 months of amenorrhea; the post-menopausal period is defined as the period following the final menses (139). The average age of menopause in the U.S. is 51 years. Interestingly, the age at menopause seems to be genetically predetermined and is not affected by race, socioeconomic status or number of prior ovulation (140). However, it appears that factors which are toxic to the ovary may lead to an earlier age of menopause. For example, smoking has been implicated in women reaching their menopause sooner (141). Moreover, those who have undergone an oophorectomy, with or without a hysterectomy, may also experience early menopause, termed surgical menopause (142). In humans, while the menopause is associated with changes in hypothalamic and pituitary hormones, it is not a central event, but rather secondary to the primary event of ovarian failure (140). During the menopause, there is a depletion of ovarian follicles, which makes the ovary no longer responsive to the pituitary hormones such as follicle-stimulating hormone (FSH) and luteinizing hormone (LH); which in turn, leads to the cessation of ovarian estrogen (E2) and progesterone (P4) production. Levels of E2 and P4 decline dramatically following menopause, imposing some major health concerns often known as post-menopausal syndrome. The postmenopausal syndrome can be accompanied by hot flashes, insomnia, mood swings, dry vagina, sexual dysfunction, stress and urge incontinences, depression, difficulty concentrating, and osteoporotic symptoms. (140). It is worth noting that the menopausal transition is a period when women's risk for cardiovascular, cognitive impairment and osteoporosis increase significantly, such that the incidence of these diseases increase substantially (143). As such, the next 30 years (translating to approximately one-third of a women's life) is spent in an estrogen- and progesterone-deprived state, the consequence of which is to put women at greater risk for a number of serious health issues.

INTRODUCTION OF microRNA

MicroRNAs (miRNA) are a novel class of short (~18-25 nucleotides), non-coding RNAs that are expressed in all eukaryotes, and predicted to post-transcriptionally regulate at least half of the human transcriptome (144). Approximately 50% of miRNA-coding genes are located within the intergenic region and have their own regulatory elements (145); while another 40% of miRNA genes are situated within introns, and the remaining 10% are positioned in exon terminals (146). As such, expression of miRNAs are often dependent on the regulation of their host gene, suggesting they may be involved in controlling the genetic networks related to the function of the host gene product (147). Interestingly, many miRNA genes are clustered together, with an intergenic space ranging from 0.1 to 50 kb, and display similar expression pattern (148).

miRNA biogenesis starts with miRNA gene transcription in the nucleus by RNA polymerase II or III, resulting in the generation of a primary miRNA (pri-miRNA) transcripts, consisting of a large (3-4 kb in length) stem-loop structure with a 5'cap and a 3' polyA tail (149). These pri-miRNAs are then recognized and further processed by a molecular complex comprising of RNase III Drosha, DGCR8 (DiGeorge syndrome critical region gene 8), the RNA-binding protein (RBP) (150, 151) and auxiliary factors (i.e., p72 and KH-type splicing regulatory protein) (152), generating a ~ 60-70-nucleotide long hairpin precursor miRNAs (pre-miRNA) (152). Pre-miRNAs are actively transported out of the nucleus to the cytoplasm, via export receptor Exportin 5 in a GTP-dependent manner (153). Once in the cytoplasm, pre-miRNAs are cleaved into ~22-nucleotide-long miRNA/miRNA* duplexes by Dicer/TRBP (the human immunodeficiency virus (HIV)-1 transactivating response RNA-binding protein) complex (154). Finally, only the mature "guide" strand of the miRNA/miRNA* duplex is associated with an Argonaute (Ago) protein and loaded into the RNA-induced silencing complex (RISC), ready to bind to its mRNA target via complementary binding (155). The overview of the miRNA biogenesis is demonstrated in illustration 1 at the end of this chapter (156).

The gene regulatory action of miRNA is achieved by its binding to the 3'-untranslated region (3'UTR) of targeted mRNA, consequently regulating the mRNA stability and protein translation (157, 158). Due to its regulation of a large number of genes, miRNA has been shown to coordinate key cellular processes including DNA repair, metabolism, proliferation, and apoptosis (reviewed in (157-159)). Dysregulation of miRNAs has been implicated in a variety of pathologies including cancers (160), stroke (see (161) for review) and neurodegenerative disorders such as Parkinson's disease (PD)(162, 163), Alzheimer's disease (AD)(164, 165), Huntington's disease (HD)(166, 167), and Amyotrophic lateral sclerosis (ALS) (168, 169). It is worth noting that every miRNA has a unique sequence and expression pattern in different cell types (160, 170).

THE LET-7 microRNA FAMILY

The lethal-7 (let-7) was among the first miRNAs discovered (171), and its sequence is highly conserved across species (172). Not only are the sequences and temporal expression patterns conserved across species, but the clustering and genomic organization of let-7 miRNAs are also well-conserved (146, 173, 174), suggesting the importance of these genes and the need to sustain their expression patterns both temporally and spatially.

In vertebrates, the let-7 family comprises more members than in *D. melanogaster* and *C. elegans* (175). The mature sequences of the let-7 members are shown in illustration 2 (176), which includes multiple isoforms resulting from post-transcriptional modification (177). Being members of the same miRNA family, these miRNAs share a similar seeding sequence, defined as a highly-conserved region within the miRNA (nucleotides 2 to 8), which is critical for targeted mRNA recognition (178). This also suggests that members of the let-7 family may share at least some targets and functions. For example, both pre-let-7d and pre-let-7g have been shown to

regulate expression of IMP-1 (IGF-II mRNA-binding protein 1) expression in A549 carcinoma cells (179). Interestingly, Obad and colleagues also reported that all let-7 members could effectively repress the reporter activity of the high-mobility group AT-hook 2 (HMGA 2) 3' UTR in Huh-7 hepatocarcinoma cells (180). In animals, some of the known biological functions of the let-7 family include limb development in chicken and mouse (181, 182), the regulation of stem cell differentiation in *C. elegans* (183), cell proliferation and differentiation (184-186), and neuro-musculature development and adult behaviors in flies (187). This miRNA family is also well-known for their tumor-suppressing functions in cancers (184, 188).

In the CNS, let-7 miRNAs are expressed in both embryonic and adult brains (189-191). Studies have reported their elevated expressions and maturation during neural cell specification (186, 192). The role of let-7 has been studied extensively in cancers. However, knowledge of their functions in the brain is limited. One known function of the let-7 miRNAs is their involvement in neural cell specification. For example, let-7a has been reported to play a role in the differentiation of embryonic neural progenitors (193), and let-7b is capable of reducing the self-renewal process of aging neural stem cells (194), while let-7i is a potent inhibitor of neuronal differentiation (195). Other studies have reported the protective role of let-7c in a traumatic brain injury model, while let-7a and let-7f have deleterious function following ischemic injury (196, 197).

WHY LET-7i

Herein, we focus on the role of let-7i in the overall protective function of progesterone (P4) in ischemia due to its potential connections with *Pgrmc1* and BDNF, the two key players in P4's action in the brain as discussed earlier. Let-7i has been reported to regulate the expression of *Pgrmc1* in ovarian cancer cells (198). In addition, our *in silico* analysis revealed that both *Pgrmc1* and BDNF are potential targets of let-7i (see illustration 3) and a reduction of BDNF level has

been observed in ischemic brain (197), suggesting that in the ischemic brain, let-7i may play a role in influencing P4's mechanism of protection via regulating the expression of Pgrmc1 and BDNF, which have both been reported by our laboratory as key mediators of P4's protective effects on brain cells.

HYPOTHESIS

Our central hypothesis is that let-7i represses P4's neuroprotective effects by down-regulating the expression of both Pgrmc1 and BDNF in glia, leading to 1) suppression of P4-induced BDNF release from glia, and 2) attenuation of the beneficial effects of P4 on neuronal survival and markers of synaptogenesis in the ischemic brain. A schematic representation of this central hypothesis is shown in illustration 4.

Our long-term goal is to harness the therapeutic benefit that is offered by P4 in preventing and treating stroke and neurodegenerative disorders. Our overall objective, which is the next step in pursuit of that goal, is to determine how Pgrmc1 expression is regulated in glia and the consequence of such regulatory mechanisms on P4's efficacy towards stroke recovery.

The rationale for the proposed research is that, because glial Pgrmc1 and BDNF are shown to mediate several beneficial effects of P4, understanding how their expression is regulated by miRNA in the CNS could reveal insight into how alteration of their expression might be a viable method of treating stroke, and possibly other neurodegenerative disorders. We proposed to test our central hypothesis and, thereby, accomplish our overall objective for this project through the completion of two specific aims:

Specific Aim 1: Determine whether let-7i attenuates P4-induced neuroprotection and markers of synaptogenesis by suppressing the Pgrmc1/BDNF pathway in glia. Based on our preliminary data, our working hypothesis is that let-7i attenuates P4-induced neuroprotection and

reduces markers of synaptogenesis by suppressing the expression of Pgrmc1 and BDNF in glia, which ultimately results in an overall decrease in the availability of BDNF (released from glia) to act on the neighboring neurons.

Specific Aim 2: Determine the involvement of let-7i in P4's protective effects in a mouse middle cerebral artery occlusion (MCAo) model of ischemia. Our working hypothesis is that in the ischemic brain, let-7i attenuates P4-induced neuroprotection and synaptogenesis, hence decreasing animal functional recovery after stroke. Conversely, inhibition of Let7i is expected to enhance the protective effects of P4.

Following successful completion of the studies proposed, we expect to not only advance our fundamental understanding of the receptor pharmacology associated with P4's effects in the CNS but to also reveal the role of a major miRNA in the regulation of P4's protective effects. Equally important, new and important mechanistic details will become available that will be relevant to the development of novel miRNA-based therapeutic strategies in mitigating the structural and functional deficits associated with stroke.

Illustration 1. The overview of miRNA biogenesis (156). Adapted from Winter, J., et al., Many roads to maturity: microRNA biogenesis pathways and their regulation. Nat Cell Biol, 2009

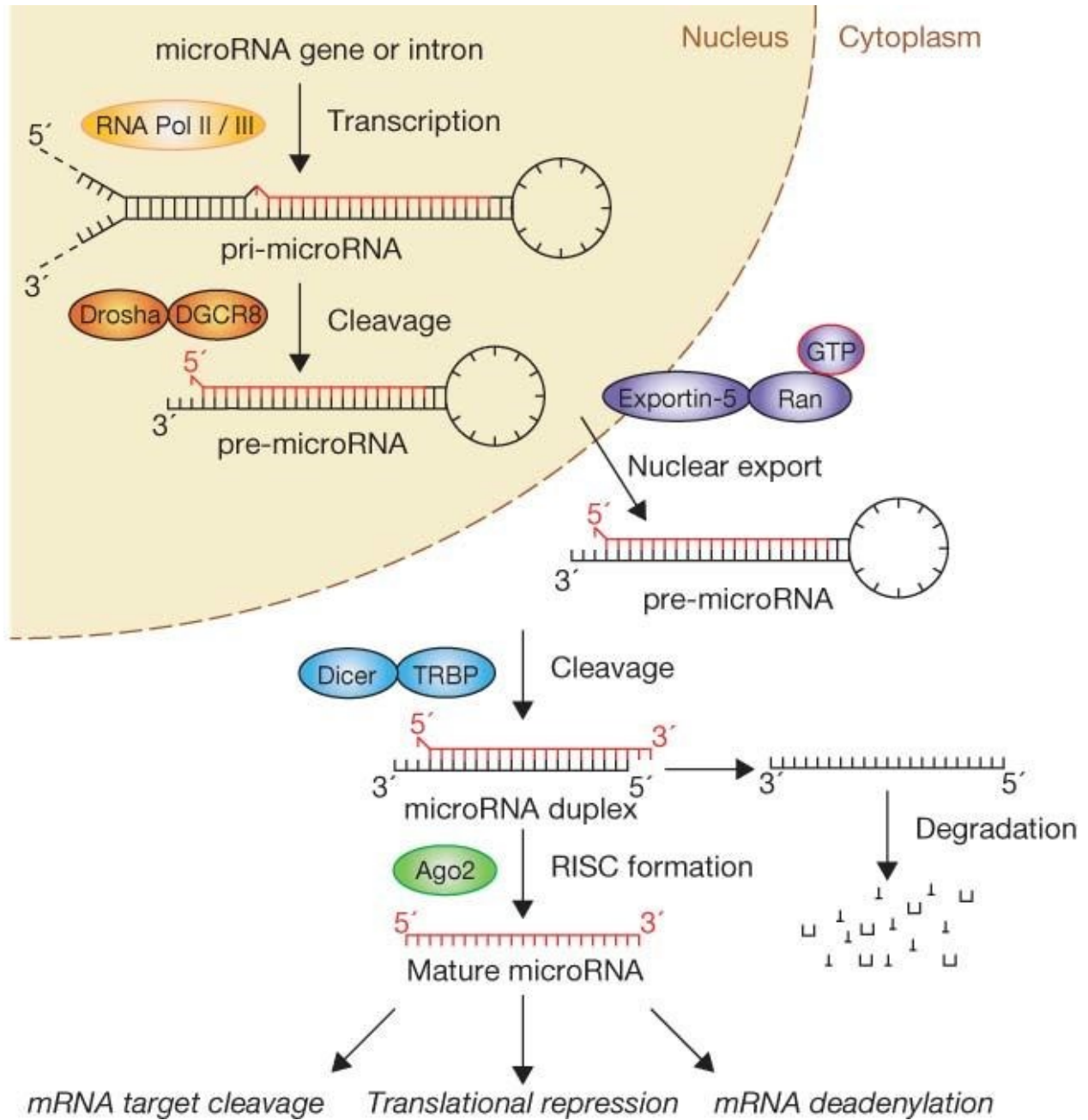


Illustration 3. Potential binding sites of let-7i on Pgrmc1 and BDNF mRNAs.

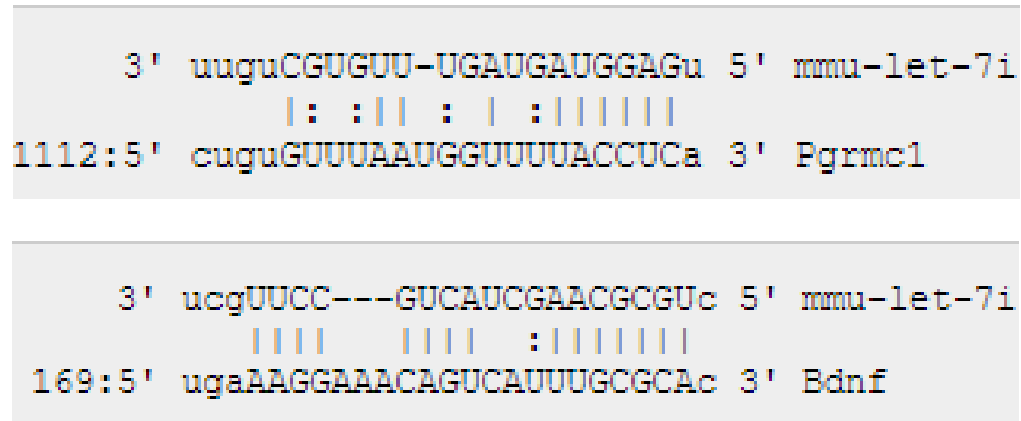
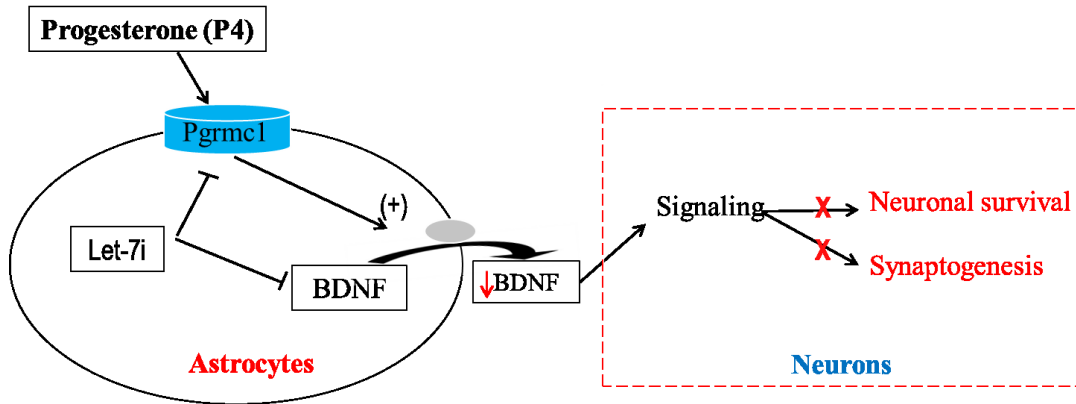


Illustration 4. Central hypothesis. let-7i represses P4's neuroprotective effects by down-regulating the expression of both Pgrmc1 and BDNF in glia, leading to 1) suppression of P4-induced BDNF release from glia, and 2) attenuation of the beneficial effects of P4 on neuronal survival and markers of synaptogenesis in the ischemic brain

CENTRAL HYPOTHESIS



STROKE BRAIN

REFERENCES

1. Haast, R.A., D.R. Gustafson, and A.J. Kiliaan, *Sex differences in stroke*. J Cereb Blood Flow Metab, 2012. **32**(12): p. 2100-7.
2. Amarenco, P., et al., *Classification of stroke subtypes*. Cerebrovasc Dis, 2009. **27**(5): p. 493-501.
3. Strong, K., C. Mathers, and R. Bonita, *Preventing stroke: saving lives around the world*. Lancet Neurol, 2007. **6**(2): p. 182-7.
4. Lopez, A.D., et al., *Global and regional burden of disease and risk factors, 2001: systematic analysis of population health data*. Lancet, 2006. **367**(9524): p. 1747-57.
5. Yang, Q., et al., *Vital Signs: Recent Trends in Stroke Death Rates - United States, 2000-2015*. MMWR Morb Mortal Wkly Rep, 2017. **66**(35): p. 933-939.
6. Benjamin, E.J., et al., *Heart Disease and Stroke Statistics-2017 Update: A Report From the American Heart Association*. Circulation, 2017. **135**(10): p. e146-e603.
7. Ly, J. and P. Maquet, *[Stroke and aging]*. Rev Med Liege, 2014. **69**(5-6): p. 315-7.
8. Di Carlo, A., *Human and economic burden of stroke*. Age Ageing, 2009. **38**(1): p. 4-5.
9. Di Carlo, A., et al., *Stroke in an elderly population: incidence and impact on survival and daily function. The Italian Longitudinal Study on Aging*. Cerebrovasc Dis, 2003. **16**(2): p. 141-50.
10. Leys, D., et al., *Poststroke dementia*. Lancet Neurol, 2005. **4**(11): p. 752-9.
11. Young, J. and A. Forster, *Review of stroke rehabilitation*. BMJ, 2007. **334**(7584): p. 86-90.
12. Evers, S.M., et al., *International comparison of stroke cost studies*. Stroke, 2004. **35**(5): p. 1209-15.
13. Atlas Writing, G., et al., *European Society of Cardiology: Cardiovascular Disease Statistics 2017*. Eur Heart J, 2017.

14. Eastwood, M.R., et al., *Mood disorder following cerebrovascular accident*. Br J Psychiatry, 1989. **154**: p. 195-200.
15. Spalletta, G., et al., *Predictors of cognitive level and depression severity are different in patients with left and right hemispheric stroke within the first year of illness*. J Neurol, 2002. **249**(11): p. 1541-51.
16. Murray, J., et al., *Developing a primary care-based stroke model: the prevalence of longer-term problems experienced by patients and carers*. Br J Gen Pract, 2003. **53**(495): p. 803-7.
17. Murray, J., J. Young, and A. Forster, *Review of longer-term problems after a disabling stroke*. Reviews in Clinical Gerontology, 2008. **17**(04): p. 277.
18. Hare, R., et al., *What do stroke patients and their carers want from community services?* Fam Pract, 2006. **23**(1): p. 131-6.
19. West, R., et al., *Psychological disorders after stroke are an important influence on functional outcomes: a prospective cohort study*. Stroke, 2010. **41**(8): p. 1723-7.
20. Morris, P.L., et al., *Association of depression with 10-year poststroke mortality*. Am J Psychiatry, 1993. **150**(1): p. 124-9.
21. Glozier, N., et al., *The Course and Impact of Poststroke Insomnia in Stroke Survivors Aged 18 to 65 Years: Results from the Psychosocial Outcomes In Stroke (POISE) Study*. Cerebrovasc Dis Extra, 2017. **7**(1): p. 9-20.
22. Robinson, R.G., et al., *Depression influences intellectual impairment in stroke patients*. Br J Psychiatry, 1986. **148**: p. 541-7.
23. Dam, H., *Depression in stroke patients 7 years following stroke*. Acta Psychiatr Scand, 2001. **103**(4): p. 287-93.
24. Verdelho, A., et al., *Depressive symptoms after stroke and relationship with dementia: A three-year follow-up study*. Neurology, 2004. **62**(6): p. 905-11.

25. Arboix, A., J.L. Marti-Vilalta, and J.H. Garcia, *Clinical study of 227 patients with lacunar infarcts*. Stroke, 1990. **21**(6): p. 842-7.
26. Donkervoort, M., et al., *Prevalence of apraxia among patients with a first left hemisphere stroke in rehabilitation centres and nursing homes*. Clin Rehabil, 2000. **14**(2): p. 130-6.
27. Engelter, S.T., et al., *Epidemiology of aphasia attributable to first ischemic stroke: incidence, severity, fluency, etiology, and thrombolysis*. Stroke, 2006. **37**(6): p. 1379-84.
28. Ch'ng, A.M., D. French, and N. McLean, *Coping with the challenges of recovery from stroke: long term perspectives of stroke support group members*. J Health Psychol, 2008. **13**(8): p. 1136-46.
29. Hilari, K., *The impact of stroke: are people with aphasia different to those without?* Disabil Rehabil, 2011. **33**(3): p. 211-8.
30. Carandang, R., et al., *Trends in incidence, lifetime risk, severity, and 30-day mortality of stroke over the past 50 years*. JAMA, 2006. **296**(24): p. 2939-46.
31. Lisabeth, L. and C. Bushnell, *Stroke risk in women: the role of menopause and hormone therapy*. Lancet Neurol, 2012. **11**(1): p. 82-91.
32. Roquer, J., A.R. Campello, and M. Gomis, *Sex differences in first-ever acute stroke*. Stroke, 2003. **34**(7): p. 1581-5.
33. Towfighi, A., et al., *A midlife stroke surge among women in the United States*. Neurology, 2007. **69**(20): p. 1898-904.
34. Towfighi, A., D. Markovic, and B. Ovbiagele, *Persistent sex disparity in midlife stroke prevalence in the United States*. Cerebrovasc Dis, 2011. **31**(4): p. 322-8.
35. Roger, V.L., et al., *Heart disease and stroke statistics--2011 update: a report from the American Heart Association*. Circulation, 2011. **123**(4): p. e18-e209.
36. Appelros, P., B. Stegmayr, and A. Terent, *Sex differences in stroke epidemiology: a systematic review*. Stroke, 2009. **40**(4): p. 1082-90.

37. Kim, J.S., et al., *Gender differences in the functional recovery after acute stroke*. J Clin Neurol, 2010. **6**(4): p. 183-8.
38. Kong, F.Y., et al., *Predictors of one-year disability and death in Chinese hospitalized women after ischemic stroke*. Cerebrovasc Dis, 2010. **29**(3): p. 255-62.
39. Vibo, R., J. Korv, and M. Roose, *One-year outcome after first-ever stroke according to stroke subtype, severity, risk factors and pre-stroke treatment. A population-based study from Tartu, Estonia*. Eur J Neurol, 2007. **14**(4): p. 435-9.
40. Redon, J., et al., *Stroke mortality and trends from 1990 to 2006 in 39 countries from Europe and Central Asia: implications for control of high blood pressure*. Eur Heart J, 2011. **32**(11): p. 1424-31.
41. Reeves, M.J., et al., *Sex differences in stroke: epidemiology, clinical presentation, medical care, and outcomes*. Lancet Neurol, 2008. **7**(10): p. 915-26.
42. Sutton-Tyrrell, K., et al., *Sex-hormone-binding globulin and the free androgen index are related to cardiovascular risk factors in multiethnic premenopausal and perimenopausal women enrolled in the Study of Women Across the Nation (SWAN)*. Circulation, 2005. **111**(10): p. 1242-9.
43. Sutton-Tyrrell, K., et al., *Carotid atherosclerosis in premenopausal and postmenopausal women and its association with risk factors measured after menopause*. Stroke, 1998. **29**(6): p. 1116-21.
44. Alkayed, N.J., et al., *Gender-linked brain injury in experimental stroke*. Stroke, 1998. **29**(1): p. 159-65; discussion 166.
45. Alkayed, N.J., et al., *Estrogen and Bcl-2: gene induction and effect of transgene in experimental stroke*. J Neurosci, 2001. **21**(19): p. 7543-50.
46. Morali, G., et al., *Post-ischemic administration of progesterone in rats exerts neuroprotective effects on the hippocampus*. Neurosci Lett, 2005. **382**(3): p. 286-90.

47. Cervantes, M., et al., *Neuroprotective effects of progesterone on damage elicited by acute global cerebral ischemia in neurons of the caudate nucleus*. Arch Med Res, 2002. **33**(1): p. 6-14.
48. Yang, S.H., et al., *Estradiol exerts neuroprotective effects when administered after ischemic insult*. Stroke, 2000. **31**(3): p. 745-9; discussion 749-50.
49. Yao, J., et al., *Decline in mitochondrial bioenergetics and shift to ketogenic profile in brain during reproductive senescence*. Biochim Biophys Acta, 2010. **1800**(10): p. 1121-6.
50. Arnold, A.P., *The organizational-activational hypothesis as the foundation for a unified theory of sexual differentiation of all mammalian tissues*. Horm Behav, 2009. **55**(5): p. 570-8.
51. Wilson, C.A. and D.C. Davies, *The control of sexual differentiation of the reproductive system and brain*. Reproduction, 2007. **133**(2): p. 331-59.
52. Handa, R.J., et al., *Gonadal steroid hormone receptors and sex differences in the hypothalamo-pituitary-adrenal axis*. Horm Behav, 1994. **28**(4): p. 464-76.
53. Miranda, R.C. and C.D. Toran-Allerand, *Developmental expression of estrogen receptor mRNA in the rat cerebral cortex: a nonisotopic in situ hybridization histochemistry study*. Cereb Cortex, 1992. **2**(1): p. 1-15.
54. Emerson, C.S., J.P. Headrick, and R. Vink, *Estrogen improves biochemical and neurologic outcome following traumatic brain injury in male rats, but not in females*. Brain Res, 1993. **608**(1): p. 95-100.
55. Fillit, H., et al., *Observations in a preliminary open trial of estradiol therapy for senile dementia-Alzheimer's type*. Psychoneuroendocrinology, 1986. **11**(3): p. 337-45.
56. Komesaroff, P.A., M.D. Esler, and K. Sudhir, *Estrogen supplementation attenuates glucocorticoid and catecholamine responses to mental stress in perimenopausal women*. J Clin Endocrinol Metab, 1999. **84**(2): p. 606-10.

57. Bishop, J. and J.W. Simpkins, *Estradiol treatment increases viability of glioma and neuroblastoma cells in vitro*. Mol Cell Neurosci, 1994. **5**(4): p. 303-8.
58. Simpkins, J.W., et al., *Estrogens may reduce mortality and ischemic damage caused by middle cerebral artery occlusion in the female rat*. J Neurosurg, 1997. **87**(5): p. 724-30.
59. Yang, S.H., et al., *17-beta estradiol can reduce secondary ischemic damage and mortality of subarachnoid hemorrhage*. J Cereb Blood Flow Metab, 2001. **21**(2): p. 174-81.
60. Alkayed, N.J., et al., *Neuroprotective effects of female gonadal steroids in reproductively senescent female rats*. Stroke, 2000. **31**(1): p. 161-8.
61. Dubal, D.B., et al., *Estradiol modulates bcl-2 in cerebral ischemia: a potential role for estrogen receptors*. J Neurosci, 1999. **19**(15): p. 6385-93.
62. Rau, S.W., et al., *Estradiol differentially regulates c-Fos after focal cerebral ischemia*. J Neurosci, 2003. **23**(33): p. 10487-94.
63. Kumon, Y., et al., *Neuroprotective effect of postischemic administration of progesterone in spontaneously hypertensive rats with focal cerebral ischemia*. J Neurosurg, 2000. **92**(5): p. 848-52.
64. Gibson, C.L., et al., *Progesterone suppresses the inflammatory response and nitric oxide synthase-2 expression following cerebral ischemia*. Exp Neurol, 2005. **193**(2): p. 522-30.
65. Aggarwal, R., et al., *Neuroprotective effect of progesterone on acute phase changes induced by partial global cerebral ischaemia in mice*. J Pharm Pharmacol, 2008. **60**(6): p. 731-7.
66. Revelli, A., M. Massobrio, and J. Tesarik, *Nongenomic actions of steroid hormones in reproductive tissues*. Endocr Rev, 1998. **19**(1): p. 3-17.
67. Watson, C.S. and B. Gametchu, *Membrane-initiated steroid actions and the proteins that mediate them*. Proc Soc Exp Biol Med, 1999. **220**(1): p. 9-19.

68. Norman, A.W., M.T. Mizwicki, and D.P. Norman, *Steroid-hormone rapid actions, membrane receptors and a conformational ensemble model*. Nat Rev Drug Discov, 2004. **3**(1): p. 27-41.
69. Kastner, P., et al., *Two distinct estrogen-regulated promoters generate transcripts encoding the two functionally different human progesterone receptor forms A and B*. EMBO J, 1990. **9**(5): p. 1603-14.
70. Conneely, O.M. and J.P. Lydon, *Progesterone receptors in reproduction: functional impact of the A and B isoforms*. Steroids, 2000. **65**(10-11): p. 571-7.
71. Schumacher, M., et al., *Revisiting the roles of progesterone and allopregnanolone in the nervous system: resurgence of the progesterone receptors*. Prog Neurobiol, 2014. **113**: p. 6-39.
72. Wardell, S.E., et al., *Jun dimerization protein 2 functions as a progesterone receptor N-terminal domain coactivator*. Mol Cell Biol, 2002. **22**(15): p. 5451-66.
73. Al-Sabbagh, M., E.W. Lam, and J.J. Brosens, *Mechanisms of endometrial progesterone resistance*. Mol Cell Endocrinol, 2012. **358**(2): p. 208-15.
74. Conneely, O.M., et al., *Reproductive functions of progesterone receptors*. Recent Prog Horm Res, 2002. **57**: p. 339-55.
75. Jacobsen, B.M. and K.B. Horwitz, *Progesterone receptors, their isoforms and progesterone regulated transcription*. Mol Cell Endocrinol, 2012. **357**(1-2): p. 18-29.
76. Cheng, K.W., C.K. Cheng, and P.C. Leung, *Differential role of PR-A and -B isoforms in transcription regulation of human GnRH receptor gene*. Mol Endocrinol, 2001. **15**(12): p. 2078-92.
77. Ni, X., et al., *Progesterone receptors A and B differentially modulate corticotropin-releasing hormone gene expression through a cAMP regulatory element*. Cell Mol Life Sci, 2004. **61**(9): p. 1114-22.

78. Tsuchiya, S., et al., *Identification and characterization of a novel progesterone receptor-binding element in the mouse prostaglandin E receptor subtype EP2 gene*. *Genes Cells*, 2003. **8**(9): p. 747-58.
79. Zhang, X.L., et al., *Selective interactions of Kruppel-like factor 9/basic transcription element-binding protein with progesterone receptor isoforms A and B determine transcriptional activity of progesterone-responsive genes in endometrial epithelial cells*. *J Biol Chem*, 2003. **278**(24): p. 21474-82.
80. Jacobsen, B.M., et al., *ALU repeats in promoters are position-dependent co-response elements (coRE) that enhance or repress transcription by dimeric and monomeric progesterone receptors*. *Mol Endocrinol*, 2009. **23**(7): p. 989-1000.
81. MacLusky, N.J. and B.S. McEwen, *Oestrogen modulates progesterin receptor concentrations in some rat brain regions but not in others*. *Nature*, 1978. **274**(5668): p. 276-8.
82. MacLusky, N.J. and B.S. McEwen, *Progesterin receptors in rat brain: distribution and properties of cytoplasmic progesterin-binding sites*. *Endocrinology*, 1980. **106**(1): p. 192-202.
83. Camacho-Arroyo, I., C. Guerra-Araiza, and M.A. Cerbon, *Progesterone receptor isoforms are differentially regulated by sex steroids in the rat forebrain*. *Neuroreport*, 1998. **9**(18): p. 3993-6.
84. Guerra-Araiza, C., A. Coyoy-Salgado, and I. Camacho-Arroyo, *Sex differences in the regulation of progesterone receptor isoforms expression in the rat brain*. *Brain Res Bull*, 2002. **59**(2): p. 105-9.
85. Guerra-Araiza, C., et al., *Changes in progesterone receptor isoforms content in the rat brain during the oestrous cycle and after oestradiol and progesterone treatments*. *J Neuroendocrinol*, 2003. **15**(10): p. 984-90.

86. Zhu, Y., et al., *Cloning, expression, and characterization of a membrane progesterin receptor and evidence it is an intermediary in meiotic maturation of fish oocytes*. Proc Natl Acad Sci U S A, 2003. **100**(5): p. 2231-6.
87. Zhu, Y., J. Bond, and P. Thomas, *Identification, classification, and partial characterization of genes in humans and other vertebrates homologous to a fish membrane progesterin receptor*. Proc Natl Acad Sci U S A, 2003. **100**(5): p. 2237-42.
88. Thomas, P., et al., *Steroid and G protein binding characteristics of the seatrout and human progesterin membrane receptor alpha subtypes and their evolutionary origins*. Endocrinology, 2007. **148**(2): p. 705-18.
89. Tang, Y.T., et al., *PAQR proteins: a novel membrane receptor family defined by an ancient 7-transmembrane pass motif*. J Mol Evol, 2005. **61**(3): p. 372-80.
90. Garitaonandia, I., et al., *Adiponectin identified as an agonist for PAQR3/RKTG using a yeast-based assay system*. J Recept Signal Transduct Res, 2009. **29**(1): p. 67-73.
91. Pang, Y., J. Dong, and P. Thomas, *Characterization, neurosteroid binding and brain distribution of human membrane progesterone receptors delta and {epsilon} (mPRdelta and mPR{epsilon}) and mPRdelta involvement in neurosteroid inhibition of apoptosis*. Endocrinology, 2013. **154**(1): p. 283-95.
92. Meffre, D., et al., *Distribution of membrane progesterone receptor alpha in the male mouse and rat brain and its regulation after traumatic brain injury*. Neuroscience, 2013. **231**: p. 111-24.
93. Liu, B. and L.A. Arbogast, *Gene expression profiles of intracellular and membrane progesterone receptor isoforms in the mediobasal hypothalamus during pro-oestrus*. J Neuroendocrinol, 2009. **21**(12): p. 993-1000.
94. Zuloaga, D.G., et al., *Distribution and estrogen regulation of membrane progesterone receptor-beta in the female rat brain*. Endocrinology, 2012. **153**(9): p. 4432-43.

95. Guennoun, R., et al., *Progesterone and allopregnanolone in the central nervous system: response to injury and implication for neuroprotection*. J Steroid Biochem Mol Biol, 2015. **146**: p. 48-61.
96. Dressing, G.E., et al., *Membrane progesterone receptor expression in mammalian tissues: a review of regulation and physiological implications*. Steroids, 2011. **76**(1-2): p. 11-7.
97. Dressing, G.E., et al., *Membrane progesterone receptors (mPRs) mediate progestin induced antimorbidity in breast cancer cells and are expressed in human breast tumors*. Horm Cancer, 2012. **3**(3): p. 101-12.
98. Dressing, G.E., et al., *Progestin signaling through mPRalpha in Atlantic croaker granulosa/theca cell cocultures and its involvement in progestin inhibition of apoptosis*. Endocrinology, 2010. **151**(12): p. 5916-26.
99. Sleiter, N., et al., *Progesterone receptor A (PRA) and PRB-independent effects of progesterone on gonadotropin-releasing hormone release*. Endocrinology, 2009. **150**(8): p. 3833-44.
100. Hanna, R.N. and Y. Zhu, *Controls of meiotic signaling by membrane or nuclear progestin receptor in zebrafish follicle-enclosed oocytes*. Mol Cell Endocrinol, 2011. **337**(1-2): p. 80-8.
101. Karteris, E., et al., *Progesterone signaling in human myometrium through two novel membrane G protein-coupled receptors: potential role in functional progesterone withdrawal at term*. Mol Endocrinol, 2006. **20**(7): p. 1519-34.
102. Frye, C.A., et al., *Membrane progestin receptors in the midbrain ventral tegmental area are required for progesterone-facilitated lordosis of rats*. Horm Behav, 2013. **64**(3): p. 539-45.
103. Meyer, C., et al., *Purification and partial sequencing of high-affinity progesterone-binding site(s) from porcine liver membranes*. Eur J Biochem, 1996. **239**(3): p. 726-31.

104. Falkenstein, E., et al., *Full-length cDNA sequence of a progesterone membrane-binding protein from porcine vascular smooth muscle cells*. *Biochem Biophys Res Commun*, 1996. **229**(1): p. 86-9.
105. Krebs, C.J., et al., *A membrane-associated progesterone-binding protein, 25-Dx, is regulated by progesterone in brain regions involved in female reproductive behaviors*. *Proc Natl Acad Sci U S A*, 2000. **97**(23): p. 12816-21.
106. Thomas, P., Y. Pang, and J. Dong, *Enhancement of cell surface expression and receptor functions of membrane progesterin receptor alpha (mPRalpha) by progesterone receptor membrane component 1 (PGRMC1): evidence for a role of PGRMC1 as an adaptor protein for steroid receptors*. *Endocrinology*, 2014. **155**(3): p. 1107-19.
107. Liu, L., et al., *Progesterone increases rat neural progenitor cell cycle gene expression and proliferation via extracellularly regulated kinase and progesterone receptor membrane components 1 and 2*. *Endocrinology*, 2009. **150**(7): p. 3186-96.
108. Johannessen, M., et al., *Antagonist action of progesterone at sigma-receptors in the modulation of voltage-gated sodium channels*. *Am J Physiol Cell Physiol*, 2011. **300**(2): p. C328-37.
109. Bashour, N.M. and S. Wray, *Progesterone directly and rapidly inhibits GnRH neuronal activity via progesterone receptor membrane component 1*. *Endocrinology*, 2012. **153**(9): p. 4457-69.
110. Guennoun, R., et al., *The membrane-associated progesterone-binding protein 25-Dx: expression, cellular localization and up-regulation after brain and spinal cord injuries*. *Brain Res Rev*, 2008. **57**(2): p. 493-505.
111. Sun, F., et al., *Pgrmc1/BDNF Signaling Plays a Critical Role in Mediating Glia-Neuron Cross Talk*. *Endocrinology*, 2016. **157**(5): p. 2067-79.

112. Nilsen, J. and R.D. Brinton, *Impact of progestins on estrogen-induced neuroprotection: synergy by progesterone and 19-norprogesterone and antagonism by medroxyprogesterone acetate*. *Endocrinology*, 2002. **143**(1): p. 205-12.
113. Nilsen, J. and R.D. Brinton, *Divergent impact of progesterone and medroxyprogesterone acetate (Provera) on nuclear mitogen-activated protein kinase signaling*. *Proc Natl Acad Sci U S A*, 2003. **100**(18): p. 10506-11.
114. Singh, M., *Ovarian hormones elicit phosphorylation of Akt and extracellular-signal regulated kinase in explants of the cerebral cortex*. *Endocrine*, 2001. **14**(3): p. 407-15.
115. Singer, C.A., et al., *The mitogen-activated protein kinase pathway mediates estrogen neuroprotection after glutamate toxicity in primary cortical neurons*. *J Neurosci*, 1999. **19**(7): p. 2455-63.
116. Grossman, K.J., C.W. Goss, and D.G. Stein, *Effects of progesterone on the inflammatory response to brain injury in the rat*. *Brain Res*, 2004. **1008**(1): p. 29-39.
117. Koenig, H.L., et al., *Progesterone synthesis and myelin formation by Schwann cells*. *Science*, 1995. **268**(5216): p. 1500-3.
118. Kaur, P., et al., *Progesterone increases brain-derived neurotrophic factor expression and protects against glutamate toxicity in a mitogen-activated protein kinase- and phosphoinositide-3 kinase-dependent manner in cerebral cortical explants*. *J Neurosci Res*, 2007. **85**(11): p. 2441-9.
119. Gonzalez Deniselle, M.C., et al., *Progesterone modulates brain-derived neurotrophic factor and choline acetyltransferase in degenerating Wobbler motoneurons*. *Exp Neurol*, 2007. **203**(2): p. 406-14.
120. Jodhka, P.K., et al., *The differences in neuroprotective efficacy of progesterone and medroxyprogesterone acetate correlate with their effects on brain-derived neurotrophic factor expression*. *Endocrinology*, 2009. **150**(7): p. 3162-8.

121. Migliaccio, A., et al., *Activation of the Src/p21ras/Erk pathway by progesterone receptor via cross-talk with estrogen receptor*. EMBO J, 1998. **17**(7): p. 2008-18.
122. Collado, M.L., G. Rodriguez-Manzo, and M.L. Cruz, *Effect of progesterone upon adenylate cyclase activity and cAMP levels on brain areas*. Pharmacol Biochem Behav, 1985. **23**(4): p. 501-4.
123. Causing, C.G., et al., *Synaptic innervation density is regulated by neuron-derived BDNF*. Neuron, 1997. **18**(2): p. 257-67.
124. Pruginin-Bluger, M., D.L. Shelton, and C. Kalcheim, *A paracrine effect for neuron-derived BDNF in development of dorsal root ganglia: stimulation of Schwann cell myelin protein expression by glial cells*. Mech Dev, 1997. **61**(1-2): p. 99-111.
125. Matsumoto, T., et al., *Biosynthesis and processing of endogenous BDNF: CNS neurons store and secrete BDNF, not pro-BDNF*. Nat Neurosci, 2008. **11**(2): p. 131-3.
126. Lu, B., P.T. Pang, and N.H. Woo, *The yin and yang of neurotrophin action*. Nat Rev Neurosci, 2005. **6**(8): p. 603-14.
127. Minichiello, L., *TrkB signalling pathways in LTP and learning*. Nat Rev Neurosci, 2009. **10**(12): p. 850-60.
128. Liu, L., et al., *The neuroprotective effects of Tanshinone IIA are associated with induced nuclear translocation of TORC1 and upregulated expression of TORC1, pCREB and BDNF in the acute stage of ischemic stroke*. Brain Res Bull, 2010. **82**(3-4): p. 228-33.
129. Sato, Y., et al., *White matter activated glial cells produce BDNF in a stroke model of monkeys*. Neurosci Res, 2009. **65**(1): p. 71-8.
130. Phillips, H.S., et al., *BDNF mRNA is decreased in the hippocampus of individuals with Alzheimer's disease*. Neuron, 1991. **7**(5): p. 695-702.
131. Connor, B., et al., *Brain-derived neurotrophic factor is reduced in Alzheimer's disease*. Brain Res Mol Brain Res, 1997. **49**(1-2): p. 71-81.

132. Coffey, E.T., K.E. Akerman, and M.J. Courtney, *Brain derived neurotrophic factor induces a rapid upregulation of synaptophysin and tau proteins via the neurotrophin receptor TrkB in rat cerebellar granule cells*. *Neurosci Lett*, 1997. **227**(3): p. 177-80.
133. Deutsch, S.I., J. Mastropaolo, and A. Hitri, *GABA-active steroids: endogenous modulators of GABA-gated chloride ion conductance*. *Clin Neuropharmacol*, 1992. **15**(5): p. 352-64.
134. Ardeshiri, A., et al., *Mechanism of progesterone neuroprotection of rat cerebellar Purkinje cells following oxygen-glucose deprivation*. *Eur J Neurosci*, 2006. **24**(9): p. 2567-74.
135. Djebaili, M., S.W. Hoffman, and D.G. Stein, *Allopregnanolone and progesterone decrease cell death and cognitive deficits after a contusion of the rat pre-frontal cortex*. *Neuroscience*, 2004. **123**(2): p. 349-59.
136. Sayeed, I., et al., *Direct inhibition of the mitochondrial permeability transition pore: a possible mechanism for better neuroprotective effects of allopregnanolone over progesterone*. *Brain Res*, 2009. **1263**: p. 165-73.
137. Robertson, C.L., et al., *Physiologic progesterone reduces mitochondrial dysfunction and hippocampal cell loss after traumatic brain injury in female rats*. *Exp Neurol*, 2006. **197**(1): p. 235-43.
138. Spinelli, M.G., *Depression and hormone therapy*. *Clin Obstet Gynecol*, 2004. **47**(2): p. 428-36.
139. Soules, M.R., et al., *Executive summary: Stages of Reproductive Aging Workshop (STRAW)*. *Fertil Steril*, 2001. **76**(5): p. 874-8.
140. Dalal, P.K. and M. Agarwal, *Postmenopausal syndrome*. *Indian J Psychiatry*, 2015. **57**(Suppl 2): p. S222-32.
141. Adena, M.A. and H.G. Gallagher, *Cigarette smoking and the age at menopause*. *Ann Hum Biol*, 1982. **9**(2): p. 121-30.

142. Siddle, N., P. Sarrel, and M. Whitehead, *The effect of hysterectomy on the age at ovarian failure: identification of a subgroup of women with premature loss of ovarian function and literature review*. Fertil Steril, 1987. **47**(1): p. 94-100.
143. Marko, K.I. and J.A. Simon, *Clinical trials in menopause*. Menopause, 2018. **25**(2): p. 217-230.
144. Friedman, R.C., et al., *Most mammalian mRNAs are conserved targets of microRNAs*. Genome Res, 2009. **19**(1): p. 92-105.
145. Corcoran, D.L., et al., *Features of mammalian microRNA promoters emerge from polymerase II chromatin immunoprecipitation data*. PLoS One, 2009. **4**(4): p. e5279.
146. Rodriguez, A., et al., *Identification of mammalian microRNA host genes and transcription units*. Genome Res, 2004. **14**(10A): p. 1902-10.
147. O'Carroll, D. and A. Schaefer, *General principals of miRNA biogenesis and regulation in the brain*. Neuropsychopharmacology, 2013. **38**(1): p. 39-54.
148. Baskerville, S. and D.P. Bartel, *Microarray profiling of microRNAs reveals frequent coexpression with neighboring miRNAs and host genes*. RNA, 2005. **11**(3): p. 241-7.
149. Lee, Y., et al., *MicroRNA genes are transcribed by RNA polymerase II*. EMBO J, 2004. **23**(20): p. 4051-60.
150. Denli, A.M., et al., *Processing of primary microRNAs by the Microprocessor complex*. Nature, 2004. **432**(7014): p. 231-5.
151. Lee, Y., et al., *The nuclear RNase III Drosha initiates microRNA processing*. Nature, 2003. **425**(6956): p. 415-9.
152. Han, J., et al., *The Drosha-DGCR8 complex in primary microRNA processing*. Genes Dev, 2004. **18**(24): p. 3016-27.
153. Yi, R., et al., *Exportin-5 mediates the nuclear export of pre-microRNAs and short hairpin RNAs*. Genes Dev, 2003. **17**(24): p. 3011-6.

154. Chendrimada, T.P., et al., *TRBP recruits the Dicer complex to Ago2 for microRNA processing and gene silencing*. Nature, 2005. **436**(7051): p. 740-4.
155. Schwarz, D.S., et al., *Asymmetry in the assembly of the RNAi enzyme complex*. Cell, 2003. **115**(2): p. 199-208.
156. Winter, J., et al., *Many roads to maturity: microRNA biogenesis pathways and their regulation*. Nat Cell Biol, 2009. **11**(3): p. 228-34.
157. Ambros, V., *The functions of animal microRNAs*. Nature, 2004. **431**(7006): p. 350-5.
158. Bartel, D.P., *MicroRNAs: genomics, biogenesis, mechanism, and function*. Cell, 2004. **116**(2): p. 281-97.
159. Croce, C.M. and G.A. Calin, *miRNAs, cancer, and stem cell division*. Cell, 2005. **122**(1): p. 6-7.
160. Lu, J., et al., *MicroRNA expression profiles classify human cancers*. Nature, 2005. **435**(7043): p. 834-8.
161. Koutsis, G., G. Siasos, and K. Spengos, *The emerging role of microRNA in stroke*. Curr Top Med Chem, 2013. **13**(13): p. 1573-88.
162. Gehrke, S., et al., *Pathogenic LRRK2 negatively regulates microRNA-mediated translational repression*. Nature, 2010. **466**(7306): p. 637-41.
163. Kim, J., et al., *A MicroRNA feedback circuit in midbrain dopamine neurons*. Science, 2007. **317**(5842): p. 1220-4.
164. Wang, W.X., et al., *The expression of microRNA miR-107 decreases early in Alzheimer's disease and may accelerate disease progression through regulation of beta-site amyloid precursor protein-cleaving enzyme 1*. J Neurosci, 2008. **28**(5): p. 1213-23.
165. Smith, P., et al., *In vivo regulation of amyloid precursor protein neuronal splicing by microRNAs*. J Neurochem, 2011. **116**(2): p. 240-7.
166. Sinha, M., et al., *Altered microRNAs in STHdh(Q111)/Hdh(Q111) cells: miR-146a targets TBP*. Biochem Biophys Res Commun, 2010. **396**(3): p. 742-7.

167. Jin, J., et al., *Interrogation of brain miRNA and mRNA expression profiles reveals a molecular regulatory network that is perturbed by mutant huntingtin*. J Neurochem, 2012. **123**(4): p. 477-90.
168. Haramati, S., et al., *miRNA malfunction causes spinal motor neuron disease*. Proc Natl Acad Sci U S A, 2010. **107**(29): p. 13111-6.
169. De Felice, B., et al., *A miRNA signature in leukocytes from sporadic amyotrophic lateral sclerosis*. Gene, 2012. **508**(1): p. 35-40.
170. Landgraf, P., et al., *A mammalian microRNA expression atlas based on small RNA library sequencing*. Cell, 2007. **129**(7): p. 1401-14.
171. Sulston, J.E. and H.R. Horvitz, *Post-embryonic cell lineages of the nematode, Caenorhabditis elegans*. Dev Biol, 1977. **56**(1): p. 110-56.
172. Pasquinelli, A.E., et al., *Conservation of the sequence and temporal expression of let-7 heterochronic regulatory RNA*. Nature, 2000. **408**(6808): p. 86-9.
173. Sempere, L.F., et al., *Temporal regulation of microRNA expression in Drosophila melanogaster mediated by hormonal signals and broad-Complex gene activity*. Dev Biol, 2003. **259**(1): p. 9-18.
174. Bashirullah, A., et al., *Coordinate regulation of small temporal RNAs at the onset of Drosophila metamorphosis*. Dev Biol, 2003. **259**(1): p. 1-8.
175. Lagos-Quintana, M., et al., *Identification of novel genes coding for small expressed RNAs*. Science, 2001. **294**(5543): p. 853-8.
176. Roush, S. and F.J. Slack, *The let-7 family of microRNAs*. Trends Cell Biol, 2008. **18**(10): p. 505-16.
177. Reid, J.G., et al., *Mouse let-7 miRNA populations exhibit RNA editing that is constrained in the 5'-seed/ cleavage/anchor regions and stabilize predicted mmu-let-7a:mRNA duplexes*. Genome Res, 2008. **18**(10): p. 1571-81.

178. Lim, L.P., et al., *The microRNAs of Caenorhabditis elegans*. Genes Dev, 2003. **17**(8): p. 991-1008.
179. Boyerinas, B., et al., *Identification of let-7-regulated oncofetal genes*. Cancer Res, 2008. **68**(8): p. 2587-91.
180. Obad, S., et al., *Silencing of microRNA families by seed-targeting tiny LNAs*. Nat Genet, 2011. **43**(4): p. 371-8.
181. Lancman, J.J., et al., *Analysis of the regulation of lin-41 during chick and mouse limb development*. Dev Dyn, 2005. **234**(4): p. 948-60.
182. Schulman, B.R., A. Esquela-Kerscher, and F.J. Slack, *Reciprocal expression of lin-41 and the microRNAs let-7 and mir-125 during mouse embryogenesis*. Dev Dyn, 2005. **234**(4): p. 1046-54.
183. Reinhart, B.J., et al., *The 21-nucleotide let-7 RNA regulates developmental timing in Caenorhabditis elegans*. Nature, 2000. **403**(6772): p. 901-6.
184. Esquela-Kerscher, A. and F.J. Slack, *Oncomirs - microRNAs with a role in cancer*. Nat Rev Cancer, 2006. **6**(4): p. 259-69.
185. Yu, F., et al., *let-7 regulates self renewal and tumorigenicity of breast cancer cells*. Cell, 2007. **131**(6): p. 1109-23.
186. Wulczyn, F.G., et al., *Post-transcriptional regulation of the let-7 microRNA during neural cell specification*. FASEB J, 2007. **21**(2): p. 415-26.
187. Sokol, N.S., et al., *Drosophila let-7 microRNA is required for remodeling of the neuromusculature during metamorphosis*. Genes Dev, 2008. **22**(12): p. 1591-6.
188. Shi, X.B., C.G. Tepper, and R.W. deVere White, *Cancerous miRNAs and their regulation*. Cell Cycle, 2008. **7**(11): p. 1529-38.
189. Kapsimali, M., et al., *MicroRNAs show a wide diversity of expression profiles in the developing and mature central nervous system*. Genome Biol, 2007. **8**(8): p. R173.

190. Miska, E.A., et al., *Microarray analysis of microRNA expression in the developing mammalian brain*. Genome Biol, 2004. **5**(9): p. R68.
191. Sempere, L.F., et al., *Expression profiling of mammalian microRNAs uncovers a subset of brain-expressed microRNAs with possible roles in murine and human neuronal differentiation*. Genome Biol, 2004. **5**(3): p. R13.
192. Rybak, A., et al., *A feedback loop comprising lin-28 and let-7 controls pre-let-7 maturation during neural stem-cell commitment*. Nat Cell Biol, 2008. **10**(8): p. 987-93.
193. Schwamborn, J.C., E. Berezikov, and J.A. Knoblich, *The TRIM-NHL protein TRIM32 activates microRNAs and prevents self-renewal in mouse neural progenitors*. Cell, 2009. **136**(5): p. 913-25.
194. Nishino, J., et al., *Hmga2 promotes neural stem cell self-renewal in young but not old mice by reducing p16Ink4a and p19Arf Expression*. Cell, 2008. **135**(2): p. 227-39.
195. Cimadamore, F., et al., *SOX2-LIN28/let-7 pathway regulates proliferation and neurogenesis in neural precursors*. Proc Natl Acad Sci U S A, 2013. **110**(32): p. E3017-26.
196. Wang, Z.K., et al., *Let-7a gene knockdown protects against cerebral ischemia/reperfusion injury*. Neural Regen Res, 2016. **11**(2): p. 262-9.
197. Selvamani, A., et al., *An antagomir to microRNA Let7f promotes neuroprotection in an ischemic stroke model*. PLoS One, 2012. **7**(2): p. e32662.
198. Wendler, A., et al., *Involvement of let-7/miR-98 microRNAs in the regulation of progesterone receptor membrane component 1 expression in ovarian cancer cells*. Oncol Rep, 2011. **25**(1): p. 273-9.

CHAPTER II

GENERAL METHODS

PRIMARY NEURONS AND ASTROCYTES PREPARATION

Dissociated cortical neurons were prepared and maintained as previously described (1). Briefly, cortices were removed from neonatal mouse brains (postnatal day 2–4, mixed gender) and dissociated with 0.25% trypsin. Cortical neurons were then plated on glass coverslip or plastic culture dishes coated with poly-D-lysine (Sigma). The culture medium used was Neurobasal (ThermoFisher Scientific), supplemented with Glutamax and B27 serum-free supplement (ThermoFisher Scientific). On the 3rd day in vitro (DIV3), 5 μ M (final concentration) of 1- β -arabinofuranosylcytosine (AraC) (Sigma) was added to the neuronal cultures to prevent glial proliferation. Half of the medium was replaced with fresh medium every four days. For viability assay, cortical neurons were plated onto 96-well plates (Corning) at a concentration of 1.2×10^5 cells/cm². For immunocytochemistry, cortical neurons were plated onto 12mm glass coverslip (Neuvitro) at a density of 4×10^4 cells/cm². Treatments of primary cortical neurons started at DIV12.

Primary cortical astrocytes were prepared and maintained as previously described (2), with some modifications. Briefly, cortices of post-natal day 2-4 mouse pups were dissociated with 0.25% trypsin and plated onto 75 cm² tissue culture flask. The culture medium used was Dulbecco's modified Eagle's medium (DMEM) (ThermoFisher Scientific), supplemented with 10% fetal bovine serum (FBS) (GE Healthcare Life Sciences) and 10000U/ml Penicillin-Streptomycin (ThermoFisher Scientific). After reaching confluence, mixed glial cultures were placed on the

shaker for 48 h to dislodge microglia, resulting in cultures enriched with more than 95% pure astrocyte population.

TRANSFECTION

Transfection of miRNA mimics and inhibitors was performed using the Hiperfect transfection reagent (Qiagen) according to manufacturer's instructions. Cells were transfected with miRNA mimics and inhibitors for 48 h. This duration was chosen since it resulted in an optimal effect on targets-of-interest, based on our preliminary data (Chapter V, figure 3). Synthetic miRNA mimics (Syn-mmu-let-7i-5p, Syn-mmu-let-7f-5p) and inhibitors (Anti-mmu-let-7i-5p, Anti-mmu-let-7f-5p) were purchased from Qiagen.

QUANTITATIVE RT-PCR

Total RNA was isolated from primary cortical astrocytes and mouse brains using the MiRNeasy Mini Kit (Qiagen) according to the manufacturer's instructions. Concentrations of extracted RNA were determined using absorbance values at 260 nm. The purity of RNA was assessed by ratios of absorbance values at 260 and 280 nm (A_{260}/A_{280} ratios of 1.9 –2.0 were considered acceptable).

For miRNA expression measurements, total RNA (10ng) was reverse transcribed into cDNA in a total volume of 15 μ l using the microRNA cDNA Archive Kit (ThermoFisher Scientific) according to the manufacturer's instructions. The reaction mixture contained water, 2x quantitative PCR Master Mix (Eurogentec), and 20x Assay-On-Demand for each target gene. A separate reaction mixture was prepared for the endogenous control, U6. The reaction mixture was aliquoted in a 96-well plate, and cDNA added to give a final volume of 20 μ l. Each sample was analyzed in triplicate. The comparative cycle threshold (Ct) method ($2^{-\Delta\Delta Ct}$) was used to calculate the relative changes in target miRNA expression.

For mRNA expression measurements, total RNA (1.6 µg) was reverse transcribed into cDNA in a total volume of 20 µl using the High-Capacity cDNA Archive Kit (ThermoFisher Scientific) according to the manufacturer's instructions. The reaction mixture contained water, 2x quantitative PCR Master Mix (Eurogentec), and 20x Assay-On-Demand for each target gene. A separate reaction mixture was prepared for the endogenous control, GAPDH. The reaction mixture was aliquoted in a 96-well plate, and cDNA (30 ng RNA converted to cDNA) was added to give a final volume of 30 µl. Each sample was analyzed in triplicate. The comparative cycle threshold (Ct) method ($2^{-\Delta\Delta Ct}$) was used to calculate the relative changes in target gene expression.

PCR primers were purchased as Assay-On-Demand from ThermoFisher Scientific. The assays were supplied as a 20 mix of PCR primers (900 nM) and TaqMan probes (200 nM). The let-7i (002221), U6 (001973), BDNF (Mm00432069_m1), GAP-43 (Mm00500404_m1), GAPDH (Mm99999915_g1), PSD-95 (Mm00492193_m1), Pgrmc1 (Mm00443985_m1) and SYP (Mm00436850_m1) assays contain FAM (6-carboxy-fluorescein phosphoramidite) dye label at the 5' end of the probes and minor groove binder and nonfluorescent quencher at the 3' end of the probes.

BDNF RELEASE ASSAY

To determine the amount of endogenous BDNF released with P4 treatment, we performed an in-situ ELISA using the BDNF Emax® ImmunoAssay Systems (Promega), as previously described (3). In brief, a 96-well Nunc MaxiSorp surface polystyrene flat-bottom immunoplate was precoated with an anti-BDNF monoclonal antibody [diluted 1:1,000 in coating buffer (25 mM sodium bicarbonate and 25 mM sodium carbonate, pH 9.7)]. After blocking nonspecific binding, primary cortical astrocytes were then plated, followed by appropriate treatments application. BDNF standards, ranging in concentration from 1.95 to 500 pg/ml, were added to parallel wells. At the end of hormone treatment, cells were carefully washed with TBST. The plate was then

incubated with the polyclonal anti-human BDNF antibody. The amount of specifically bound polyclonal antibody was then detected through the use of the anti-IgY-horseradish peroxidase (HRP) tertiary antibody, which when exposed to the chromogenic substrate (TMB reagent), changes color in proportion to the amount of BDNF present in the sample. The color intensity was quantified by measuring the absorbance at 450 nm with a Viktor3 ELISA plate reader (Perkin Elmer). Only values within the linear range of the standard curve, and above the lowest standard, were considered valid. This method allowed detection of as little as 2pg/ml BDNF release in control cultures to ~250 pg/ml in P4-treated cultures.

CELLTITER-GLO LUMINESCENT VIABILITY ASSAY (Promega)

This assay uses the level of adenosine triphosphate (ATP) as an indicator of metabolically active cells and is directly proportional to the number of living cells (4, 5). The assay was performed according to manufacturer's instruction. In brief, cell plate was first equilibrated to room temperature for 30 minutes. A volume of the kit reagent equal to the volume of cell culture present was then added to each well. The plate was then placed on an orbital shaker for 2 minutes to induce cell lysis, followed by 10 minutes of incubation at room temperature. Luminescence was recorded using a plate reader.

OXYGEN-GLUCOSE DEPRIVATION (OGD)

OGD was performed according to an established protocol, as described elsewhere, with minor modifications (6). Briefly, primary cortical neurons were carefully washed five times with Hank's balanced salt solution (HBSS, ThermoFisher Scientific) to remove residual glucose. Glucose-free DMEM (ThermoFisher Scientific) was then added to the cultures, and the plates were transferred into a hypoxic chamber (0.1% oxygen) for 1h. At the end of hypoxia, glucose-free DMEM was replaced with regular maintaining media. Re-oxygenation was initiated by transferring the cells to normoxic 5% CO₂ cell culture incubator.

WESTERN BLOTTING

Primary cortical astrocytes and mouse brains were lysed with RIPA (radio-immunoprecipitation assay) lysis buffer containing protease and phosphatase inhibitors, as previously described (1). After homogenization, samples were centrifuged at 120,000 x g for 30 min at 4°C and supernatants were collected. Total protein concentrations were determined using the Bio-Rad DC protein assay kit (Bio-Rad Laboratories). Cell lysates were separated by SDS-PAGE and transferred onto a polyvinylidene fluoride (PVDF) membrane (Bio-Rad Laboratories) by electroblotting. Membranes were blocked with 5% skim milk in tris-buffered saline containing 0.2% Tween 20 (TBS-T) for 1h at room temperature, followed by overnight incubation with the primary antibody, at 4°C. The following primary antibodies were used: rabbit polyclonal anti-PSD 95 (1:1000, ab18258, Abcam), rabbit polyclonal anti-Synaptophysin (1:1000, ab14692, Abcam), rabbit monoclonal anti-GAP43 (1:200000, ab75810, Abcam), rabbit monoclonal anti-GAPDH (1:1000, 14C10, Cell Signaling), rabbit polyclonal anti-BDNF (1:300, sc546, Santa Cruz) and goat polyclonal anti-Pgrmc1 (1:500, ab48012, Abcam). After washing three times with Tris-buffered saline containing 0.2% Tween-20 (TBS-T), membranes were incubated with anti-goat IgG or anti-rabbit IgG conjugated with horseradish peroxidase (Millipore) for 1hr at room temperature. After three washes with TBS-T, immunoreactive bands were visualized with the ECL detection system (ThermoFisher Scientific). The chemiluminescent signal was captured using a luminescent image analyzer (Alpha Innotech). Densitometric analysis of visualized bands was conducted using ImageJ (National Institutes of Health) software (7).

IMMUNOHISTOFLUORESCENCE

Cortical neurons were fixed with 4% paraformaldehyde (PFA) for 15 min, followed by incubation in Tris-buffered saline (TBS) containing 0.2% Triton X-100 for 15 min at room temperature for permeabilization. Cultures were then blocked with 5% donkey serum/1% bovine serum albumin (BSA) in TBS for 1 h at room temperature and incubated with rabbit monoclonal

anti-Synaptophysin (1:500, ab32127, Abcam) for 48 h at 4°C. After extensive rinsing with TBS/0.05%Tween 20, cultures were incubated with Alexa Fluor 647-conjugated secondary antibody (1:500, Jackson ImmunoResearch Laboratories) for 2h at room temperature. After extensive washing with TBS to remove unbound secondary antibody, the coverslips were mounted onto glass slides (VWR Scientific) using Vectashield mounting medium with DAPI (Vector Laboratories). The slides were observed under a confocal fluorescence microscope (FV1200, Olympus) with a 60x objective.

Mouse brains were fixed in 4% PFA overnight at 4°C and subsequently cryoprotected in 30% sucrose solution. The brains were then sectioned into 40- μ m thick coronal slices and subjected to immunostaining using an established protocol described elsewhere, with some modifications (8). In brief, brain sections were blocked in 5% donkey serum/1%BSA/TBS solution for 2h at room temperature. In staining using mouse primary antibody, sections were subsequently blocked using the F(ab) fragment of donkey anti-mouse IgG (50ug/ml, Jackson ImmunoResearch Laboratories) for 2 h at room temperature to reduce background caused by secondary antibody binding to endogenous mouse IgG in the tissue. After the blocking step, brain sections were then incubated in the primary antibody solution at 4°C for 72 h. Primary antibodies used were as follows: mouse monoclonal anti-NeuN (1:500, ab104224, Abcam); rabbit polyclonal anti-GFAP (1:1000, ab7260, Abcam); rabbit monoclonal anti-Synaptophysin (1:500, ab32127, Abcam) and goat polyclonal anti-Pgrmc1 (1:200, ab48012, Abcam). Alexa Fluor 647, Alexa Fluor 594 or Rhodamine Red-conjugated secondary antibodies (Jackson ImmunoResearch Laboratories) were used at 1:500 dilution. After immunostaining, sections were mounted onto microscope slides with Vectashield mounting medium (Vector Laboratories) and observed under a confocal fluorescence microscope (FV1200, Olympus) with a 63x objective.

MICE AND TREATMENTS

Animals were treated humanely and with regard for alleviation of suffering according to protocols approved by the Institutional Animal Care and Use Committee of University of North Texas Health Science Center. All institutional and national guidelines for the care and the use of animals were followed. Female C57BL/6J mice (18-week-old) were purchased from Jackson Laboratory. Animals were habituated to housing conditions one week prior to experiments.

All mice were first ovariectomized to deplete endogenous ovarian hormone levels. Two weeks after ovariectomy (OVX), P4 pellets were subcutaneously implanted into these animals to replenish their progesterone levels. In parallel, different groups received cholesterol pellet implantations to serve as vehicle control. One week after pellet implantation, stroke was induced in these mice using middle cerebral artery occlusion (MCAo) procedure. In parallel, different groups received sham operation (non-stroke). 30 min after MCAo, 5 μ g of either scrambled or let-7i inhibitor was injected into each animal brain via intracerebroventricular (ICV) injection. Experimental groups included sham-operated mice with cholesterol pellet implantation (sham), stroked mice with cholesterol pellet implantation and scrambled ICV injection (cholesterol + scrambled), stroked mice with P4 pellet implantation and scrambled ICV injection (P4 + scrambled), and stroked mice with P4 pellet implantation and let-7i inhibitor ICV injection (P4 + scrambled).

OVARIECTOMY

Bilateral ovariectomy (OVX) was performed using a dorsal approach under isoflurane anesthesia, as described elsewhere (9). Briefly, small incisions were made bilaterally to expose ovaries. The arteries adjacent to ovaries were ligated before the removal of the ovaries. Incisions were then closed using 4-0 Vicryl absorbable suture. All surgical procedures included the post-

operative monitoring and management of stress and pain and were approved by the institutional animal care and use committee (IACUC).

TRANSIENT MIDDLE CEREBRAL ARTERY OCCLUSION (MCAo)

MCAo was performed to induce transient focal cerebral ischemia, as previously described (10). In brief, mice were anesthetized with isoflurane inhalation. A mid-line incision was made on the neck. Left common carotid artery (CCA), external carotid artery (ECA) and internal carotid artery (ICA) were dissected from the connective tissue. The left MCA was occluded by a 6-0 monofilament suture (Doccol Corporation) introduced via internal carotid artery. After 45 minutes occlusion, the suture was withdrawn for reperfusion. In sham-operated animals, monofilament was advanced to MCA region and withdraw immediately without MCA occlusion. All surgical procedures included the post-operative monitoring and management of stress and pain and were approved by the institutional animal care and use committee (IACUC).

INTRACEREBROVENTRICULAR (ICV) INJECTION

5 μg of either scrambled or let-7i inhibitor (GE Healthcare Dharmacon) was suspended in 0.5 μL of PBS and injected into lateral ventricles using a stereotaxic instrument, as previously described, with minor modifications (11). In brief, the solution was injected using a 5- μL Hamilton syringe attached to the Ultra Micro Pump UMP3 system (World Precision Instruments) at a flow rate of 0.2 $\mu\text{L}/\text{min}$. Coordinates used for ICV injection were: anteroposterior axis, relative to the bregma suture (AP) -0.58 mm, mediolateral axis, relative to the lambda suture (ML) ± 1.2 mm, dorsoventral axis, relative to the intra-aural line (DV) -2.1 mm. All surgical procedures included the post-operative monitoring and management of stress and pain and were approved by the institutional animal care and use committee (IACUC).

2,3,5-TRIPHENYLTETRAZOLIUM CHLORIDE (TTC) STAINING

TTC staining was performed to assess ischemic injury among groups, as described in an established protocol (12). Briefly, 24 h after MCAo, mouse brains were harvested and sectioned into 2-mm thick coronal sections. These sections were immersed in 2% TTC solution for 30 min at 37°C and then fixed in 10% formalin. The stained slices were photographed and subsequently measured for the surface area of the slices and the ischemic lesion (Image-Pro Plus 3.0.1, Silver Springs, MD, U.S.A.). Images of stained sections were captured and infarct sizes were analyzed using ImageJ (National Institutes of Health) software (7).

WIRE SUSPENSION TEST

In order to assess motor function in animals exposed to different treatments, wire suspension test, a test of grip strength and endurance, was used, as described elsewhere (13). In brief, mice were allowed to suspend their bodies on a single wire that was elevated above a padded platform. The latency for animals to fall off the wire was recorded. Mice were trained two days prior to MCAo to establish a baseline across groups. Training was achieved with several rounds of habituation and trials. In the actual testing phase, each mouse was tested 3 times, and average performance was taken as final values. Performances of these mice was evaluated at day 3, 7 and 14 post stroke.

SYNAPTOPHYSIN (SYP) OPTICAL DENSITY ANALYSIS AND PUNCTA QUANTIFICATION

For experiments using primary cortical neurons, mounted coverslips were imaged using a confocal fluorescence microscope (FV1200, Olympus) with a 63x objective. Healthy cells that were at least two cell diameters from their nearest neighbor were identified and selected at random by eye by DAPI fluorescence. Ten non-overlapping fields per sample were imaged. Quantification of SYP immunoreactivity (IR) was performed using ImageJ (National Institutes of Health) software (7). Average IR was calculated by dividing total IR value by the number of cells presented in the captured image. Synaptophysin puncta quantification was analyzed with a

custom plug-in (written by Barry Wark; available upon request from c.eroglu@cellbio.duke.edu) for ImageJ program. The details of this imaging and quantification method can be found in a previous publication (14).

To quantify SYP fluorescence intensity and number of puncta in mouse brain, three independent coronal brain sections per animal were stained with SYP. 5- μm confocal scans were performed (optical section width, 0.33 μm ; 15 optical sections each) at 63x magnification, as previously described (15). Maximum projections of three consecutive optical sections corresponding to 1- μm sections were analyzed by using the ImageJ puncta analyzer option to quantify for numbers of SYP puncta (≥ 5 optical sections per brain section and ≥ 15 total images per brain). Average SYP puncta density per imaged area was calculated for each treatment group.

REFERENCES

1. Sun F, et al. (2016) Pgrmc1/BDNF Signaling Plays a Critical Role in Mediating Glia-Neuron Cross Talk. *Endocrinology* 157(5):2067-2079.
2. Roy Choudhury G, et al. (2015) Methylene blue protects astrocytes against glucose oxygen deprivation by improving cellular respiration. *PLoS One* 10(4):e0123096.
3. Su C, Cunningham RL, Rybalchenko N, & Singh M (2012) Progesterone increases the release of brain-derived neurotrophic factor from glia via progesterone receptor membrane component 1 (Pgrmc1)-dependent ERK5 signaling. *Endocrinology* 153(9):4389-4400.
4. Crouch SP, Kozlowski R, Slater KJ, & Fletcher J (1993) The use of ATP bioluminescence as a measure of cell proliferation and cytotoxicity. *J Immunol Methods* 160(1):81-88.
5. Parker CG, et al. (2017) Ligand and Target Discovery by Fragment-Based Screening in Human Cells. *Cell* 168(3):527-541 e529.
6. Ryou MG, et al. (2015) Methylene blue-induced neuronal protective mechanism against hypoxia-reoxygenation stress. *Neuroscience* 301:193-203.
7. Rueden CT, et al. (2017) ImageJ2: ImageJ for the next generation of scientific image data. *BMC Bioinformatics* 18(1):529.
8. Jin K, et al. (2004) Increased hippocampal neurogenesis in Alzheimer's disease. *Proc Natl Acad Sci U S A* 101(1):343-347.
9. Singh M, Meyer EM, Millard WJ, & Simpkins JW (1994) Ovarian steroid deprivation results in a reversible learning impairment and compromised cholinergic function in female Sprague-Dawley rats. *Brain Res* 644(2):305-312.

10. Li W, et al. (2014) PTEN degradation after ischemic stroke: a double-edged sword. *Neuroscience* 274:153-161.
11. Ni J, et al. (2015) MicroRNA let-7c-5p protects against cerebral ischemia injury via mechanisms involving the inhibition of microglia activation. *Brain Behav Immun* 49:75-85.
12. Yang SH, et al. (2001) 17-beta estradiol can reduce secondary ischemic damage and mortality of subarachnoid hemorrhage. *J Cereb Blood Flow Metab* 21(2):174-181.
13. Hauben U, D'Hooge R, Soetens E, & De Deyn PP (1999) Effects of oral administration of the competitive N-methyl-D-aspartate antagonist, CGP 40116, on passive avoidance, spatial learning, and neuromotor abilities in mice. *Brain Res Bull* 48(3):333-341.
14. Ippolito DM & Eroglu C (2010) Quantifying synapses: an immunocytochemistry-based assay to quantify synapse number. *J Vis Exp* (45).
15. Kucukdereli H, et al. (2011) Control of excitatory CNS synaptogenesis by astrocyte-secreted proteins Hevin and SPARC. *Proc Natl Acad Sci U S A* 108(32):E440-449.

CHAPTER III

LET-7I INHIBITION POTENTIATES PROGESTERONE'S ACTION ON FUNCTIONAL RECOVERY IN A MOUSE MODEL OF ISCHEMIA

TRINH NGUYEN, CHANG SU, MEHARVAN SINGH*

Department of Pharmacology and Neuroscience, University of North Texas Health Science
Center, Fort Worth, Texas 76107

Corresponding author:

Meharvan Singh, Ph.D.

Department of Pharmacology and Neuroscience

University of North Texas Health Science Center at Fort Worth

3400 Camp Bowie Blvd.

Fort Worth, Texas. 76107

Phone: +1-8177355429

Fax: +1-8177350408

Email: meharvan.singh@unthsc.edu

Submitted to the Proceedings of the National Academy of Sciences (PNAS)

ABSTRACT

Progesterone (P4) is a potent neuroprotectant and a promising therapeutic for stroke treatment. However, the underlying mechanism(s) remain unclear. Our laboratory has recently reported that brain-derived neurotrophic factor (BDNF) is a critical mediator of P4's protective actions and that P4 enhances BDNF release from cortical astrocytes is mediated by a novel membrane-associated progesterone receptor, Pgrmc1. Here, we report that the microRNA (miRNA), let-7i, is a negative regulator of Pgrmc1 and BDNF in glia, and that let-7i disrupts P4-induced BDNF release and P4's beneficial effects on cell viability and markers of synaptogenesis. Using an *in vivo* model of ischemia, we demonstrate that inhibiting let-7i enhances P4 induced neuroprotection and facilitates functional recovery following stroke. The discovery of such factors that regulate the cytoprotective effects of P4 may lead to the development of biomarkers to differentiate/predict those likely to respond favorably to P4 versus those that do not.

SIGNIFICANCE

We and others have found that *Pgrmc1* plays an important role in mediating progesterone's protective effects. Currently, knowledge regarding the regulation of *Pgrmc1* in brain and the consequence of such regulation is limited. In this study, we identified microRNA (miRNA) *let-7i* as a negative regulator of *Pgrmc1* and BDNF. We also discovered that through such regulation, *let-7i* is able to suppress P4-induced BDNF release from astrocytes and attenuated the P4's neuroprotective effects as well as its positive regulation of synaptogenic endpoints in the ischemic brain. Additionally, we show that *let-7i* inhibition enhanced P4's beneficial effects in ischemic brain. These findings are significant because they provide a strong scientific framework/foundation for the identification and development of a novel, miRNA-targeting approach for the treatment of ischemic stroke which could also impact the effectiveness of hormone-based therapeutic approaches. At the very minimum, a better understanding of the cellular/molecular factors that influence the brain's response to P4 may lead to more informed decisions on who should (or should not) be considered for hormone therapy, thus supporting a personalized, precision-medicine approach for post-menopausal women.

INTRODUCTION

Stroke has been reported as one of the leading causes of death and a major cause of disability in the US (1), costing approximately \$34 Billion annually (according to the Center for Disease Control). A number of studies have shown that ovarian hormone, progesterone (P4), is neuroprotective in a variety of experimental models of stroke (2-4). However, the underlying mechanisms for P4's protective effects remain unclear.

One known mediator of P4's protective function is brain-derived-neurotrophic-factor (BDNF) (5). A deficit in BDNF has been linked to a more severe stroke pathophysiology (6, 7). This neurotrophin also has an established role in promoting neuronal differentiation, survival, synaptic plasticity (8-10) and synaptogenesis (11-13). Synaptogenesis occurring in the penumbra is known to strongly contribute to enhanced functional recovery from stroke (14-17). Based on these observations, it is plausible that the P4/BDNF signaling-mediated enhanced synaptogenesis and neuroprotection may contribute to P4's protective effects during post-stroke brain repair.

We recently reported that P4 elicits the release of BDNF from primary astrocytes via a putative membrane progesterone receptor consisting of progesterone-receptor-membrane-component-1 (Pgrmc1) (18). Our results also suggest that conditioned medium derived from P4-treated astrocytes, when applied to primary cortical neurons, increases the expression of synaptic markers in these neural cells and enhances their survival against oxidative stress. These findings support the model whereby P4 elicits its (neuro)protective effects through a mechanism that involves Pgrmc1-dependent BDNF release from glia.

While it is clear that *Pgrmc1* plays an important role in P4's protective effects on the brain, knowledge regarding the regulation of *Pgrmc1* in the brain and the consequence of such regulation is limited. Studies suggest that microRNA (miRNA) might be involved (19, 20). MicroRNAs are a class of small non-coding RNAs with mature transcripts consisting of 18-25 nucleotides (21). Indeed, there exists support for the role of miRNA in stroke (21-23) where manipulation of miRNA in experimental models of stroke resulted in neuroprotection (19, 22-24).

In the present study, we aimed to investigate the role of a miRNA, *let-7i*, in regulating the protective function of progesterone in ischemia. Using an *in vitro* two-cell model system, which consisted of astrocytes and neurons, we found that *let-7i* negatively regulates expression of both *Pgrmc1* and BDNF in glia, leading to suppression of P4-induced BDNF release from glia and attenuation of P4's beneficial effects on cell viability and markers of synaptogenesis. In our *in vivo* model of ischemia (temporary middle cerebral artery occlusion, followed by reperfusion), combined treatment of P4 and the *let-7i* inhibitor/antagomir led to reduced ischemic injury and complete recovery of motor function. These findings support the therapeutic value of *let-7i* inhibition as a novel approach to enhance P4's protective efficacy in ischemic brain.

MATERIALS AND METHODS

Primary cultures

Dissociated cortical neurons were prepared and maintained as previously described (28). Briefly, cortices were removed from neonatal mouse brains (postnatal day 2–4, mixed gender) and dissociated with 0.25% trypsin. Cortical neurons were then plated on glass coverslip or plastic culture dishes coated with poly-D-lysine (Sigma). The culture medium used was Neurobasal (ThermoFisher Scientific), supplemented with Glutamax and B27 serum-free supplement (ThermoFisher Scientific). At day in vitro (DIV) 3, 5 μM final concentration of 1- β -arabinofuranosylcytosine (AraC) (Sigma) was added to the neuronal cultures to prevent glial proliferation. Half of the medium was replaced with fresh medium every four days. For viability assay, cortical neurons were plated onto 96-well plates (Corning) at the concentration of 1.2×10^5 cells/cm². For immunocytochemistry, cortical neurons were plated onto 12mm glass coverslip (Neuvitro) at the density of 4×10^4 cells/cm². Treatments of primary cortical neurons started at DIV12.

Primary cortical astrocytes were prepared and maintained as previously described (31), with some modifications. Briefly, cortices of post-natal day 2-4 mouse pups were dissociated with 0.25% trypsin and plated onto 75 cm² tissue culture flask. The culture medium used was Dulbecco's modified Eagle's medium (DMEM) (ThermoFisher Scientific), supplemented with 10% fetal bovine serum (FBS) (GE Healthcare Life Sciences) and 10000U/ml Penicillin-Streptomycin (ThermoFisher Scientific). After reaching confluence, mixed glial cultures were placed on the shaker for 48 h to dislodge microglia, resulting in cultures enriched with astrocyte population.

Treatment of primary cultures

To determine the miRNA regulation of downstream targets in primary cortical astrocytes, miRNA mimics and inhibitors were transfected into these cells for 48 hrs. After transfection, total RNA and proteins were isolated for gene and protein expression analysis. Mock transfection was used as the control for these experiments.

To study the effect of miRNA on P4-induced BDNF release from astrocytes, BDNF *in-situ* ELISA were performed. Expression of miRNA was first manipulated by transfection as described above. 24 h after transfection, 10 nM P4 was added to primary cortical astrocytes for additional 24 h without changing media containing transfection complexes. Vehicle controls were performed in parallel such that control cultures were exposed to 0.1% dimethylsulfoxide (DMSO). The 10 nM concentration of P4 used in studies described here was chosen because it has been reported to elicit a maximal release of BDNF from astrocytes (18).

In experiments evaluating the effect of miRNA on P4-induced neuroprotection and the synaptogenic marker, synaptophysin, we first transfected miRNA mimic and inhibitor into primary cortical astrocytes for 24 h. Afterward, P4 (10nM) was added to these cultures for additional 24 h to generate P4-treated-astrocytes-derived-conditioned-media (P4-ACM). In parallel, treatment of 0.1% DMSO was performed to generate DMSO-treated-astrocytes-derived-conditioned-media (DMSO-ACM), which served as vehicle controls. In neuroprotection assay, astrocytes-conditioned-media were added to primary cortical neurons with prior exposure to one hour of oxygen-glucose-deprivation (OGD), an *in-vitro* model of ischemic-like insult. Based on our preliminary data (not shown here), 1 h of OGD was enough to induce 50% neuronal cell death. BDNF (50ng/ml) was directly added to different groups after OGD to serve as positive control. Neuronal cultures exposed to normoxia were used as the control for these data sets. 24 h after the applications of BDNF or conditioned-media, CellTiter-Glo Luminescent cell viability assay (Promega) was performed to measure neuroprotection. In synaptogenic marker measurement assay, BDNF and astrocytes-derived-conditioned-media were directly added to primary cortical

neurons for 24 hrs. Synaptophysin expression and number of synaptophysin puncta in these neuronal cultures were assessed by immunocytochemistry, followed by confocal imaging and analyzed using ImageJ (National Institutes of Health) software (32).

Transfection

Transfection of miRNA mimics and inhibitors was performed using the Hiperfect transfection reagent (Qiagen) according to manufacturer's instructions. Cells were transfected with miRNA mimics and inhibitors for 48 h. This duration was chosen since it resulted in an optimal effect on targets-of-interest, based on our preliminary data (not shown here). Synthetic miRNA mimics (Syn-mmu-let-7i-5p, Syn-mmu-let-7f-5p) and inhibitors (Anti-mmu-let-7i-5p, Anti-mmu-let-7f-5p) were purchased from Qiagen.

Quantitative RT-PCR

Total RNA was isolated from primary cortical astrocytes and mouse brains using the MiRNeasy Mini Kit (Qiagen) according to the manufacturer's instructions. Concentrations of extracted RNA were determined using absorbance values at 260 nm. The purity of RNA was assessed by ratios of absorbance values at 260 and 280 nm (A₂₆₀/A₂₈₀ ratios of 1.9 –2.0 were considered acceptable).

For miRNA expression measurements, total RNA (10ng) was reverse transcribed into cDNA in a total volume of 15 µl using the microRNA cDNA Archive Kit (ThermoFisher Scientific) according to the manufacturer's instructions. The reaction mixture contained water, 2x quantitative PCR Master Mix (Eurogentec), and 20x Assay-On-Demand for each target gene. A separate reaction mixture was prepared for the endogenous control, U6. The reaction mixture was aliquoted in a 96-well plate, and cDNA added to give a final volume of 20 µl. Each sample was analyzed in triplicate. The comparative cycle threshold (Ct) method ($2^{-\Delta\Delta Ct}$) was used to calculate the relative changes in target miRNA expression.

For mRNA expression measurements, total RNA (1.6 µg) was reverse transcribed into cDNA in a total volume of 20 µl using the High-Capacity cDNA Archive Kit (ThermoFisher Scientific) according to the manufacturer's instructions. The reaction mixture contained water, 2x quantitative PCR Master Mix (Eurogentec), and 20x Assay-On-Demand for each target gene. A separate reaction mixture was prepared for the endogenous control, GAPDH. The reaction mixture was aliquoted in a 96-well plate, and cDNA (30 ng RNA converted to cDNA) was added to give a final volume of 30 µl. Each sample was analyzed in triplicate. The comparative cycle threshold (Ct) method ($2^{-\Delta\Delta Ct}$) was used to calculate the relative changes in target gene expression.

PCR primers were purchased as Assay-On-Demand from ThermoFisher Scientific. The assays were supplied as a 20 mix of PCR primers (900 nM) and TaqMan probes (200 nM). The let-7i (002221), U6 (001973), BDNF (Mm00432069_m1), GAP-43 (Mm00500404_m1), GAPDH (Mm99999915_g1), PSD-95 (Mm00492193_m1), Pgrmc1 (Mm00443985_m1) and SYP (Mm00436850_m1) assays contain FAM (6-carboxy-fluorescein phosphoramidite) dye label at the 5' end of the probes and minor groove binder and nonfluorescent quencher at the 3' end of the probes.

CellTiter-Glo Luminescent cell viability assay (Promega)

This assay uses the level of adenosine triphosphate (ATP) as an indicator of metabolically active cells and is directly proportional to the number of living cells (33, 34). The assay was performed according to manufacture's instruction. In brief, cell plate was first equilibrated to room temperature for 30 minutes. A volume of the kit reagent equal to the volume of cell culture present was then added to each well. The plate was then placed on an orbital shaker for 2 minutes to induce cell lysis, followed by 10 minutes of incubation at room temperature. Luminescence was recorded using a plate reader.

BDNF Immuno Assay *In situ*

To determine the amount of endogenous BDNF released with P4 treatment, we performed ELISA *in situ* assay, as previously described (18). In brief, a 96-well Nunc MaxiSorp surface polystyrene flat-bottom immunoplate was precoated with an anti-BDNF monoclonal antibody [diluted 1:1,000 in coating buffer (25 mM sodium bicarbonate and 25 mM sodium carbonate, pH 9.7)]. After blocking nonspecific binding, primary cortical astrocytes were then plated, followed by appropriate treatments application. BDNF standards, ranging in concentration from 1.95 to 500 pg/ml, was added to parallel wells. At the end of hormone treatment, cells were carefully washed with TBST. The plate was then incubated with the polyclonal anti-human BDNF antibody. The amount of specifically bound polyclonal antibody was then detected through the use of the anti-IgY-horseradish peroxidase (HRP) tertiary antibody, which when exposed to the chromogenic substrate (TMB reagent, Promega), changes color in proportion to the amount of BDNF present in the sample. The color intensity was quantified by measuring the absorbance at 450 nm with a Viktor3 ELISA plate reader (Perkin Elmer). Only values within the linear range of the standard curve, and above the lowest standard, were considered valid. This method allowed detection of as little as 2pg/ml BDNF release in control cultures to ~250 pg/ml in P4-treated cultures.

Oxygen-glucose Deprivation (OGD)

OGD was performed according to an established protocol, as described elsewhere, with minor modifications (35). Briefly, primary cortical neurons were carefully washed five times with Hank's balanced salt solution (HBSS, ThermoFisher Scientific) to remove residual glucose. Glucose-free DMEM (ThermoFisher Scientific) was then added to the cultures, and the plates were transferred into a hypoxic chamber (0.1% oxygen) for 1h. At the end of hypoxia, glucose-free DMEM was replaced with regular maintaining media. Reoxygenation was initiated by transferring the cells to normoxic 5% CO₂ cell culture incubator.

Western blotting

Primary cortical astrocytes and mouse brains were lysed with RIPA lysis buffer containing protease and phosphatase inhibitors, as previously described (28). After homogenization, samples were centrifuged at 45,000rpm for 30 min at 4°C and supernatants were collected. Total protein concentrations were determined using the Bio-Rad DC protein assay kit (Bio-Rad Laboratories). Cell lysates were separated by SDS-PAGE and transferred onto polyvinylidene fluoride membrane (Bio-Rad Laboratories) by electroblotting. Membranes were blocked with 5% skim milk in tris-buffered saline containing 0.2% Tween 20 (TBS-T) for 1h at room temperature, followed by overnight incubations of primary antibodies at 4°C. The following primary antibodies were used: rabbit polyclonal anti-PSD 95 (1:1000, ab18258, Abcam), rabbit polyclonal anti-Synaptophysin (1:1000, ab14692, Abcam), rabbit monoclonal anti-GAP43 (1:200000, ab75810, Abcam), rabbit monoclonal anti-GAPDH (1:1000, 14C10, Cell Signaling), rabbit polyclonal anti-BDNF (1:300, sc546, Santa Cruz) and goat polyclonal anti-Pgrmc1 (1:500, ab48012, Abcam). After washing three times with TBS-T, membranes were incubated with anti-goat IgG or anti-rabbit IgG conjugated with horseradish peroxidase (Millipore) for 1hr at room temperature. After triple washes with TBS-T, immunoreactive bands were visualized with the ECL detection system (ThermoFisher Scientific) and were captured using a luminescent image analyzer (Alpha Innotech). Densitometric analysis was conducted using ImageJ (National Institutes of Health) software (32).

Immunofluorescence

The cortical neurons were fixed in 4% paraformaldehyde (PFA) for 15 min, followed by incubation in 0.2% Triton X-100 in Tris-buffered saline (TBS) for 15 min at room temperature for permeabilization. Cultures were then blocked with 5% donkey serum/1% bovine serum albumin (BSA) in TBS for 1 h at room temperature and incubated with rabbit monoclonal anti-Synaptophysin (1:500, ab32127, Abcam) for 48 h at 4°C. After extensive rinsing with TBS-Tween

20, cultures were incubated with Alexa Fluor 647-conjugated secondary antibody (1:500, Jackson ImmunoResearch Laboratories) for 2h at room temperature. After extensive washing with TBS to remove unbound secondary antibody, the coverslips were mounted onto glass slides (VWR Scientific) using Vectashield mounting medium with DAPI (Vector Laboratories). The slides were observed under a confocal fluorescence microscope (FV1200, Olympus) with a 63x objective.

Mouse brains were fixed in 4% PFA overnight at 4°C and subsequently cryoprotected in 30% sucrose solution. The brains were then sectioned into 40- μ m thick coronal slices and subjected to immunostaining using an established protocol described elsewhere, with some modifications (36). In brief, brain sections were blocked in 5% donkey serum/1%BSA/TBS solution for 2h at room temperature. In staining using mouse primary antibody, sections were subsequently blocked in F(ab) fragment donkey anti-mouse IgG (50ug/ml, Jackson ImmunoResearch Laboratories) for 2 h at room temp to reduce background caused by secondary antibody binding to endogenous mouse IgG in the tissue. After blocking step, brain sections were then incubated in primary antibody solution at 4°C for 72 h. Primary antibodies used were as follow: mouse monoclonal anti-NeuN (1:500, ab104224, Abcam); rabbit polyclonal anti-GFAP (1:1000, ab7260, Abcam); rabbit monoclonal anti-Synaptophysin (1:500, ab32127, Abcam) and goat polyclonal anti-Pgrmc1 (1:200, ab48012, Abcam). Alexa Fluor 647, Alexa Fluor 594 or Rhodamine Red-conjugated secondary antibodies (Jackson ImmunoResearch Laboratories) were used at 1:500 dilution. After immunostaining, sections were mounted onto microscope slides with Vectashield mounting medium (Vector Laboratories) and observed under a confocal fluorescence microscope (FV1200, Olympus) with a 63x objective.

Mice and treatments

All procedures with animals were reviewed and approved by the Institutional Animal Care and Use Committee of the University of North Texas Health Science Center. All institutional and federal guidelines for the care and the use of animals were followed. Female C57BL/6J mice (18-

week-old) were purchased from Jackson Laboratory. Animals were habituated to housing conditions one week before experiments.

All mice were first ovariectomized to deplete endogenous ovarian hormone levels. Two weeks after ovariectomy (OVX), P4 pellets were subcutaneously implanted into these animals to replenish their progesterone levels. In parallel, different groups received cholesterol pellet implantations to serve as vehicle control. One week after pellet implantation, stroke was induced in these mice using middle cerebral artery occlusion (MCAo) procedure. In parallel, different groups received sham operation (non-stroke). 30 min after MCAo, 5 μ g of either scrambled or let-7i inhibitor was injected into each animal brain via intracerebroventricular (ICV) injection. Experimental groups included sham-operated mice with cholesterol pellet implantation (sham), stroked mice with cholesterol pellet implantation and scrambled ICV injection (cholesterol + scrambled), stroked mice with P4 pellet implantation and scrambled ICV injection (P4 + scrambled), and stroked mice with P4 pellet implantation and let-7i inhibitor ICV injection (P4 + scrambled).

Ovariectomy

Bilateral ovariectomy (OVX) was performed using a dorsal approach under isoflurane anesthesia, as described elsewhere (37). Briefly, small incisions were made bilaterally to expose ovaries. The arteries adjacent to ovaries were ligated before ovaries removal. Incisions were then closed using 4-0 Vicryl absorbable suture.

Transient middle cerebral artery occlusion (MCAo)

MCAo was performed to induce transient focal cerebral ischemia, as previously described (38). In brief, mice were anesthetized with isoflurane inhalation. A mid-line incision was made on the neck. Left common carotid artery (CCA), external carotid artery (ECA) and internal carotid artery (ICA) were dissected from the connective tissue. The left MCA was occluded by a 6-0

monofilament suture (Doccol Corporation) introduced via internal carotid artery. After 45 minutes occlusion, the suture was withdrawn for reperfusion. In sham-operated animals, monofilament was advanced to MCA region and withdraw immediately without MCA occlusion.

Intracerebroventricular (ICV) injection

5 µg of either scrambled or let-7i inhibitor (GE Healthcare Dharmacon) was suspended in 0.5 µL of PBS and injected into lateral ventricles using a stereotaxic instrument, as previously described, with minor modifications(23). In brief, the solution was injected using a 5-µL Hamilton syringe attached to the Ultra Micro Pump UMP3 system (World Precision Instruments) at a flow rate of 0.2 µl/min. Coordinates used for ICV injection were AP -0.58 mm, ML + 1.2 mm, DV -2.1 mm.

Assessment of brain tissue damage: 2,3,5-Triphenyltetrazolium chloride (TTC) staining

TTC staining was performed to assess ischemic injury among groups, as described in an established protocol (39). Briefly, 24 h after MCAo, mouse brains were harvested and sectioned into 2-mm thick coronal sections. These sections were immersed in 2% TTC solution for 30 min at 37°C and then fixed in 10% formalin. The stained slices were photographed and subsequently measured for the surface area of the slices and the ischemic lesion (Image-Pro Plus 3.0.1, Silver Springs, MD, U.S.A.). Imaged of stained sections were captured and infarct sizes were analyzed using ImageJ (National Institutes of Health) software (32).

Functional recovery assessment: wire suspension test

In order to assess motor function recovery with different treatments, wire suspension test, a test of grip strength and endurance, was used, as described elsewhere (40). In brief, mice were allowed to suspend their bodies on a single wire that was elevated above a padded platform. The latency for animals to fall off the wire was recorded. Mice were trained two days prior to MCAo to establish a baseline across groups. Training was achieved with several rounds of habituation

and trials. In the actual testing phase, each mouse was tested 3 times, and average performance was taken as final values. Performances of these mice was evaluated at day 3, 7 and 14 post stroke.

Synaptophysin (SYP) optical density analysis and puncta quantification

For experiments using primary cortical neurons, mounted coverslips were imaged using a confocal fluorescence microscope (FV1200, Olympus) with a 63x objective. Healthy cells that were at least two cell diameters from their nearest neighbor were identified and selected at random by eye by DAPI fluorescence. Ten non-overlapping fields per sample were imaged. Quantification of SYP immunoreactivity (IR) was performed using ImageJ (National Institutes of Health) software (32). Average IR was calculated by dividing total IR value by the number of cells presented in the captured image. Synaptophysin puncta quantification was analyzed with a custom plug-in (written by Barry Wark; available upon request from c.eroglu@cellbio.duke.edu) for ImageJ program. The details of this imaging and quantification method can be found in a previous publication (41).

To quantify SYP fluorescence intensity and number of puncta in mouse brain, three independent coronal brain sections per animal were stained with SYP. 5- μm confocal scans were performed (optical section width, 0.33 μm ; 15 optical sections each) at 63x magnification, as previously described (42). Maximum projections of three consecutive optical sections corresponding to 1- μm sections were analyzed by using the ImageJ puncta analyzer option to quantify for numbers of SYP puncta (≥ 5 optical sections per brain section and ≥ 15 total images per brain). Average SYP puncta density per imaged area was calculated for each treatment group.

Statistical Analysis

In-vitro data obtained from no fewer than three independent experiments, and in-vivo data obtained from at least 5 animals per group were analyzed using an analysis of variance (ANOVA),

followed by a *post hoc* analysis for the assessment of group differences, and presented as a bar graph depicting the mean \pm S.E.M, using the GraphPad Software (San Diego, CA).

RESULTS

BDNF and Pgrmc1 are negatively regulated by let-7i in primary cortical astrocytes

An *in silico* analysis using three prediction software programs (miRDB, TargetScan, and microRNA.org) revealed putative Let-7 binding sites in the 3'- UTR of Pgrmc1 and BDNF that were conserved in rat, mouse, and human sequences. Based on this observation, coupled with a prior report citing the regulation of Pgrmc1 by Let-7i in ovarian cancer cells, we evaluated the effect of Let-7i on both Pgrmc1 and BDNF. We evaluated the effect of Let-7f as a control, recognizing that the Sohrabji lab had previously shown an inverse relationship between Let-7f and BDNF. Our studies showed that overexpression of let-7i, by transfecting a let-7i mimic, led to decreased mRNA levels of both Pgrmc1 (Fig.1A) and BDNF (Fig.1B). Interestingly, overexpression of let-7f had no effect. Additionally, inhibition of let-7i (anti-let-7i) and let-7f (anti-let 7f), using miRNA inhibitor, did not alter basal mRNA levels of Pgrmc1 and BDNF (Fig.1A and 1B). Western blot analysis (Fig.1C) showed a consistent finding in that reduction in Pgrmc1 protein level was only observed in the group transfected with let-7i mimic. Quantitative assessments of BDNF, using an ELISA (Fig.1D), showed that BDNF levels were downregulated in cultures transfected with let-7i mimic. These data suggested that let-7i, and not let-7f, negatively regulates BDNF/Pgrmc1 system in cortical astrocytes.

Progesterone (P4)-induced BDNF release is inhibited in cultures over-expressing let-7i

Since our laboratory has shown that Pgrmc1 plays a central role in mediating the effect of P4 on the release of BDNF from cortical astrocytes (18), and let-7i negatively regulates expression of this component (Fig.1A and 1C); we tested whether overexpression of let-7i inhibits P4-elicited BDNF release from these cells. In situ assessment of BDNF release (Fig.2) showed that P4 (10nM, 24hrs) elicited a significant release of BDNF into the culture media compared to

the vehicle control (DMSO), an effect that was not blocked by overexpressing the let-7i antagomir. In contrast, let-7i overexpression led to the inhibition of P4's effect on BDNF release. These findings support our hypothesis that overexpression of let-7i, through the negative regulation of Pgrmc1/BDNF axis, abolishes P4-induced BDNF release from primary cortical astrocytes.

Let-7i represses progesterone (P4)'s neuroprotection and its enhancement on synaptogenesis

To investigate the role of let-7i in P4's neuroprotective effects, we manipulated miRNA expression in primary cortical astrocytes, then treated them with either vehicle (DMSO) or P4 to generate astrocyte-derived conditioned media (ACM). The conditioned media was then applied to primary cortical neurons (DIV14) that had been exposed to oxygen-glucose deprivation (OGD). The neurons were then assessed for cell viability to ascertain if conditioned media from P4-treated astrocytes was greater than in neurons treated with conditioned media from DMSO-treated astrocytes (Fig.3). We found that conditioned media collected from P4-treated astrocytes conferred similar neuroprotection as seen in the positive control group (consisting of direct administration of BDNF (50ng/ml) to the neuronal cultures). However, conditioned media from P4-treated astrocytes that overexpressed let-7i failed to promote the protection of neurons from OGD.

Next, we determined if conditioned media from the different experimental groups represented in Figure3 resulted in changes in expression of synaptophysin, a presynaptic marker closely linked to synaptogenesis (4). Exposure to conditioned media derived from P4-treated astrocytes (P4-ACM) resulted in a robust increase in SYP (green) immunofluorescence (Fig.4A). Quantitative analysis revealed that compared to non-let-7i transfected, DMSO-treated group, P4-ACM significantly increased both SYP immunoreactivity (Fig.4B) and the number of SYP puncta (Fig.4C). The same observations were seen in the positive control group (BDNF-50ng/ml). Application of P4-ACM collected from astrocytes that overexpressed let-7i, however, failed to elicit the increase in synaptophysin expression.

Combined treatment of progesterone (P4) and let-7i inhibition alleviate ischemia-induced suppression of Pgrmc1 and BDNF expressions in the penumbra of the ischemic brain.

Since we determined that let-7i is a negative regulator of BDNF and Pgrmc1 (Fig.1), and that OGD, as an *in-vitro* model of ischemia, induced expression of let-7i (data not shown), we next determined the expression of let-7i in the middle cerebral artery occlusion model of ischemic stroke, focusing on changes in the penumbra. Assessments of let-7i expression were conducted at different time points – 2, 7 and 14 days following stroke. Representative images of immunoblots probed for Pgrmc1, along with pro-and mature-BDNF, are shown in Fig.5A. We found that compared to sham (non-stroked controls), ischemic injury resulted in an up-regulation of let-7i expression (Fig.5E), starting at day 7 and remained elevated up to 14 days following stroke. P4 treatment alone (P4 + a control sequence for let-7i (scrambled)) did not attenuate the stroke-induced increase in Let-7i. As expected, ischemia-induced-increase in let-7i expression was repressed in the group receiving combined treatment P4 and let-7i inhibition (P4 + anti-7i) (Fig.5E). Importantly, along with upregulating let-7i level, ischemia also resulted in a reduction of Pgrmc1 protein level observed at day 7 and day 14 (Fig. 5B). P4 treatment alone did not restore Pgrmc1 level at either of the two time points. Combined treatment (P4+anti-let-7i), however, reversed ischemia-induced suppression of Pgrmc1 protein levels. Furthermore, expression of mature BDNF was reduced as a consequence of stroke at the 14 days post stroke evaluation period (Fig.5D), while pro-BDNF levels (Fig. 5C) remained unchanged across all time points and all treatments. Compared to sham, the treatment of P4 alone was able to maintain the same level of mature BDNF, even at 14 days post stroke. Remarkably, combined treatment (P4+anti-let-7i) led to a robust increase in expression of mature BDNF observed at day 7 and day 14.

Combined treatment of progesterone (P4) and let-7i inhibition reduces ischemic injury and enhances functional recovery.

To examine the effect of P4 with or without the let-7i antagomir on the extent of ischemic injury, we utilized 2,3,5-Triphenyltetrazolium chloride (TTC) staining to visualize the size of the ischemic lesion. Representative images of TTC stained are shown in Fig.6A. Quantification of relative infarct size (Fig.6B) revealed that the combined treatment (P4+anti-let-7i) significantly reduced ischemic injury; whereas P4 treatment alone did not.

Motor function (grip strength) was also evaluated using the wire suspension test. Results (Fig.7) showed that compared to the vehicle group (DMSO + scrambled), treatment of P4 led to a partial recovery of motor function, observed on day 7 and day 14. Interestingly, the combined treatment of P4 and the let-7i antagomir resulted in a rapid, but partial, motor function recovery as early as 3 days post-treatment. By day 7, combined treatment led to complete functional recovery, and the improvement was still evident at day 14. Results from Fig.6 and Fig.7 support our hypothesis that let-7i inhibition enhances P4's neuroprotective effects that importantly, enhances functional recovery.

Inhibition of let-7i enhances progesterone (P4)'s effect on synaptogenic marker

Synaptic plasticity in the ischemic penumbra region has long been known to contribute to the functional recovery after stroke (14, 16, 25). Therefore, to determine whether synaptogenesis occurring in the penumbra could be a factor contributing to functional recovery observed in Fig.7, we extended our in vitro findings, to evaluate the expression of synaptophysin (SYP), a synaptogenic marker, in the penumbra of stroked mice. To do so, we performed immunofluorescence to visualize SYP expression (red) (Fig.8A) and quantified the relative number of SYP puncta, which is an indication of potential synapses (Fig.8B). In parallel, Western blot analysis was performed to evaluate total SYP protein levels. Representative immunoblots probed for SYP are shown in Fig.8C, and its relative quantification of protein level is depicted in Fig.8D. Results revealed that ischemia resulted in a sustained downregulation of synaptophysin puncta (Fig.8B) in the penumbra at day 2,7 and 14 post-stroke. In addition, ischemic injury led to

decreased SYP protein level at day 2 and 14. There was a transient increase in SYP expression at day 7, which could be due to a compensatory response to the ischemic injury. P4 treatment alone led to a delayed, but sustained, restoration in SYP total protein expression, observed at day 7 and day 14. With regards to the number of SYP puncta, the positive effect of P4 was only evident at day 14 post-treatment. Interestingly, at day 7 and 14, combined treatment (P4+anti-let-7i) resulted in significantly higher expression of SYP, compared to sham controls and P4 treatment alone. This combined treatment also led to a complete restoration of synaptophysin puncta at day 7, an effect that was further enhanced at day 14. Taken together, these findings indicate that P4 induces synaptogenesis in the penumbra of ischemic brain and that let-7i inhibition further enhances this beneficial function of P4.

DISCUSSION

An increasing number of publications infer the brain protective effects of P4, including studies showing that P4 is neuroprotective in a variety of experimental models of stroke (2-4). However, the underlying mechanism(s) for P4's protective effects remain unclear. In point of fact, our ability to optimize the effectiveness of P4 requires a better understanding of the factors that influence the expression of key mediators (e.g., receptors) of P4's protective effects. In addition, most of the literature associated with P4's protective effects has focused on a direct effect of P4 on neurons. The notion that glia may be an equally important target underlying P4's protective effects on the brain has only been studied minimally. Indeed, astrocytes have been considered an important component of post-ischemic recovery, as these cells are critical for regeneration and remodeling of neural circuits following stroke (26). More direct support of our hypothesis of a vital role of glia is based on the observation that P4 protects cerebral cortical organotypic explants (containing both glia and neurons) against oxidative cell death (27), while P4 did not induce as robust protection in neuron-enriched primary cultures (unpublished data), which strongly suggests that glia is required for P4's neuroprotective program.

One mechanism that underlies the protective function of P4 is its ability to initiate intercellular crosstalk between astrocytes and neurons, where BDNF is a key mediator (28). For example, we have reported that P4 elicits a significant release of mature BDNF from astrocytes through a *Pgrmc1*-dependent ERK5 signaling mechanism. From this same study, BDNF from the conditioned media of P4-treated astrocytes, was specifically as the protective factor that not only promoted neuronal viability, but also, an increase in markers of synaptogenesis (28). In this study, we identified an upstream regulator of this *Pgrmc1*/BDNF axis in glia and characterized its influence in a mouse model of ischemic stroke (MCAo). Our results support the role of *let-7i* as a negative regulator of *Pgrmc1* and BDNF in primary cortical astrocytes. Interestingly, despite

sharing a similar seeding sequence, let-7f did not have the same effect, suggesting that regulation of Pgrmc1/BDNF in astrocytes is specific to let-7i. Not only did increased expression of let-7i significantly reduced P4-induced BDNF release from cultured astrocytes, it prevented P4 from protecting neurons against OGD and from increasing the expression of synaptophysin, a surrogate marker for synaptogenesis. We also found that OGD, serving as an *in vitro* model of ischemia, resulted in an upregulation of let-7i such that P4 was no longer able to elicit BDNF release from astrocytes (data not shown), presumably due to the fact that Pgrmc1, a critical mediator of P4-induced BDNF release, was downregulated. Collectively, these findings suggest that let-7i and condition that leads to the elevation of this miRNA, such as ischemia, represses P4-induced BDNF release from glia; thus, leading to attenuation of the beneficial effects of P4 on neuronal survival and markers of synaptogenesis. It is noteworthy that inhibition of let-7i alone (using the let-7i antagomir/inhibitor) did not confer any protection against OGD. Rather, let-7i inhibition enhanced the protective effects of P4.

The results from our *in vitro* studies corroborated our results from our *in vivo* data, using the MCAo model of stroke in mice. For example, like OGD, ischemic injury induced in the mouse led to an upregulation of let-7i in the penumbra, which was correlated with decreased Pgrmc1 expression and a reduction in the level of mature BDNF which was seen at day 14 following stroke. Given that BDNF has such a vital role on brain function (8-10), the observed reduction in Pgrmc1 could not only compromise the protective efficacy of hormones like P4, but could more generally, underlie the long term sequelae that lead to functional impairment over time in stroke victims. It is worth noting, however, that the reduction in BDNF levels was observed only at day 14. This could be due to a compensatory effort of the brain to maintain BDNF at earlier time points (day 2 and 7).

Treatment of P4 was able to restore the level of mature BDNF. Despite the reduction in Pgrmc1 levels in ischemic brain, P4's mild positive effect on BDNF expression might be due to its

action via classical progesterone receptor (PR), as supported by our previous work (27). Importantly, combined treatment, P4 and let-7i inhibition, restored Pgrmc1 expression and resulted in a marked increase in mature BDNF level. Taken together with our *in-vitro* results, these observations support the hypothesis that inhibition of let-7i alleviates ischemia-induced suppression of Pgrmc1 level, therefore allowing P4 to increase expression of mature BDNF via Pgrmc1 signaling. The striking increase in mature BDNF expression observed with the combined treatment could also be due to the effect of the intervention on the conversion from pro to mature BDNF and/or the stability of mature BDNF. Ongoing studies in the lab are aimed at further exploring these possible mechanisms in greater detail.

In agreement with other published studies (2, 29), our results showed treatment of P4 alone led to a modest and delayed improvement in functional recovery, along with an increase in synaptogenesis depicted by the increase in expression and number of synaptophysin puncta. However, treatment with P4 alone failed to reduce ischemic injury. Interestingly, the combined treatment not only significantly reduced the size of the ischemic lesion but also led to a quicker, and more pronounced functional recovery as well as a more pronounced increase in markers of synaptogenesis in the penumbra region. These findings are consistent with other studies proposing the link between synaptogenesis in the penumbra and functional recovery following stroke (14, 30).

Collectively, our findings reported herein identify let-7i as a negative upstream regulator of both Pgrmc1 and BDNF in glia, leading to suppression of P4-induced BDNF release from glia and attenuation of P4's beneficial effects on neuroprotection and synaptogenesis in the ischemic brain. Furthermore, the increased expression of let-7i with stroke may explain why post-stroke therapy may not be so effective. As such, dampening the up-regulation of let-7i may prove to be an effective strategy to enhance the efficacy of P4 and other therapeutic candidates that engage

the BDNF system, and as such, could potentially extend the “window of opportunity” for stroke therapy.

ACKNOWLEDGMENTS

This work was supported in part by funds from the American Heart Association (13SDG17050059) to CS, the National Institute of Health (AG027956) to MS and a fellowship to TN through the Neurobiology of Aging training grant (T32 AG020494, Program Director: MS).

FIGURES

Figure.1. let-7i negatively regulates the expression of Pgrmc1 and BDNF in primary cortical astrocytes.

The effect of let7 mimics and antagomirs on Pgrmc1 (A) and BDNF (B) mRNA (n=4). (C) Representative immunoblot for Pgrmc1 protein and associated quantitation depicting the signal (densitometric) intensity, expressed as the ratio of Pgrmc1 to GAPDH (n=4). (D) Total cellular BDNF measured by ELISA (n=5). n.s: not significant, ***P<0.001 compared to control, and ### P<0.001 compared to let-7i mimic by analysis of variance (ANOVA) followed by Dunn's post hoc analysis. Data are presented as the mean \pm SEM.

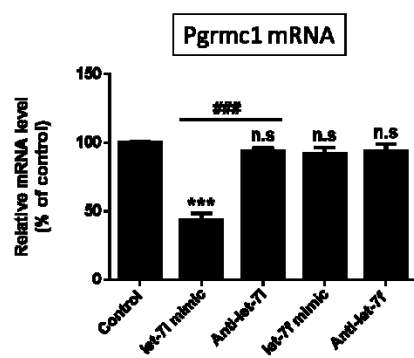
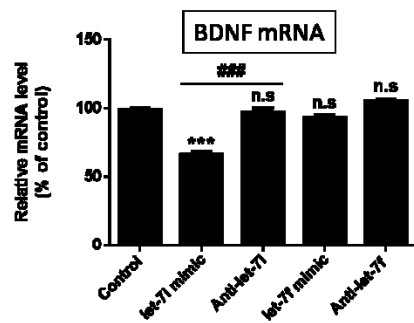
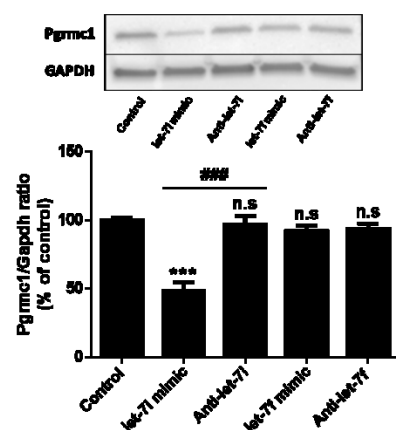
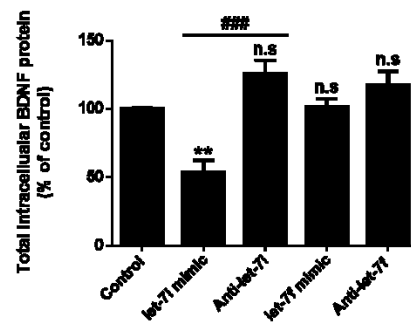
A**B****C****D**

Figure 2. let-7i and OGD abolished progesterone (P4)-induced BDNF release from primary cortical astrocytes.

Quantitation of BDNF release measured by BDNF *in situ* ELISA (n=4). n.s: not significant, ***P<0.001 and ## P<0.01 compared to corresponding DMSO groups by one-way ANOVA followed by Tukey's post hoc analysis. Data are presented as the mean \pm SEM.

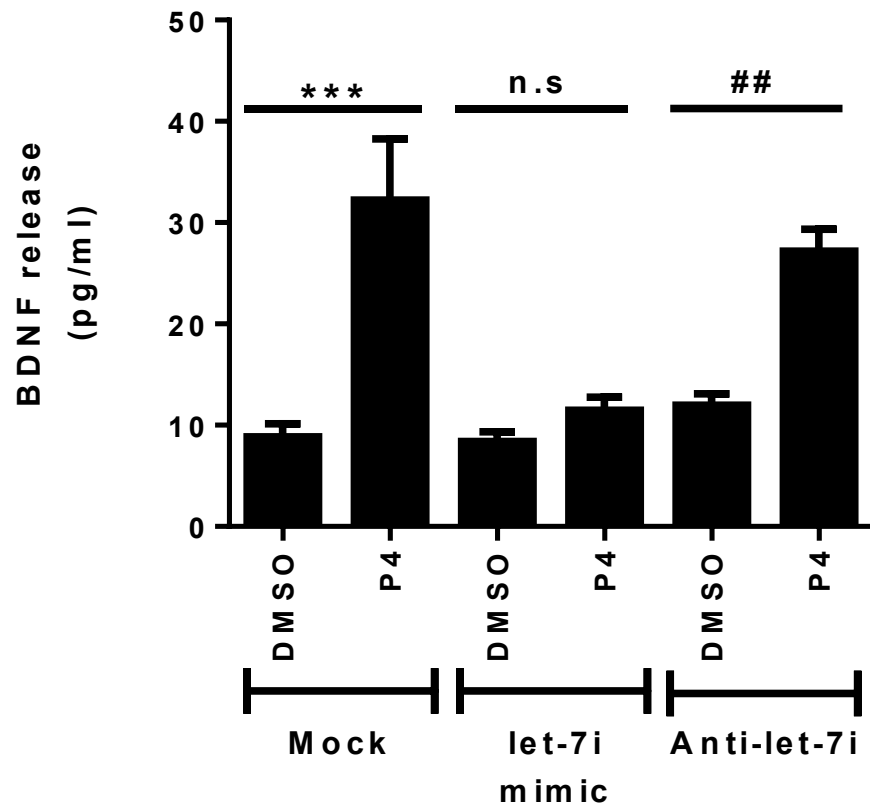


Figure 3. let-7i prevents progesterone (P4)-induced neuroprotection against oxygen-glucose-deprivation (OGD).

Conditioned-media derived from hormone or control-treated astrocytes were applied to primary cortical neurons (DIV 14) after one-hour exposure to OGD. BDNF (50ng/ml) was directly added to neurons after OGD to serve as positive control. Neuronal viability was measured by CellTiter-Glo viability assay (n=5). n.s: not significant, ***P<0.001 and ** P<0.01 compared to normoxia by one-way ANOVA followed by Tukey's post hoc analysis. Data are presented as the mean \pm SEM.

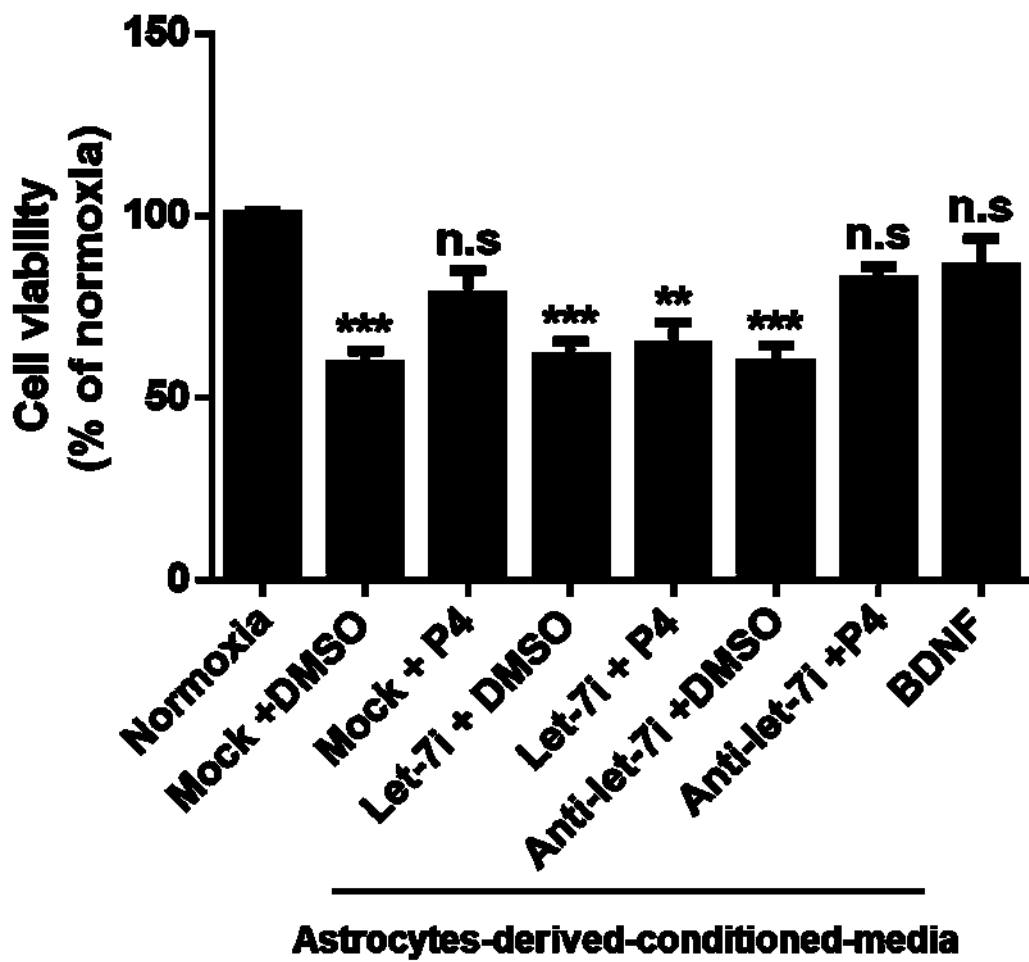
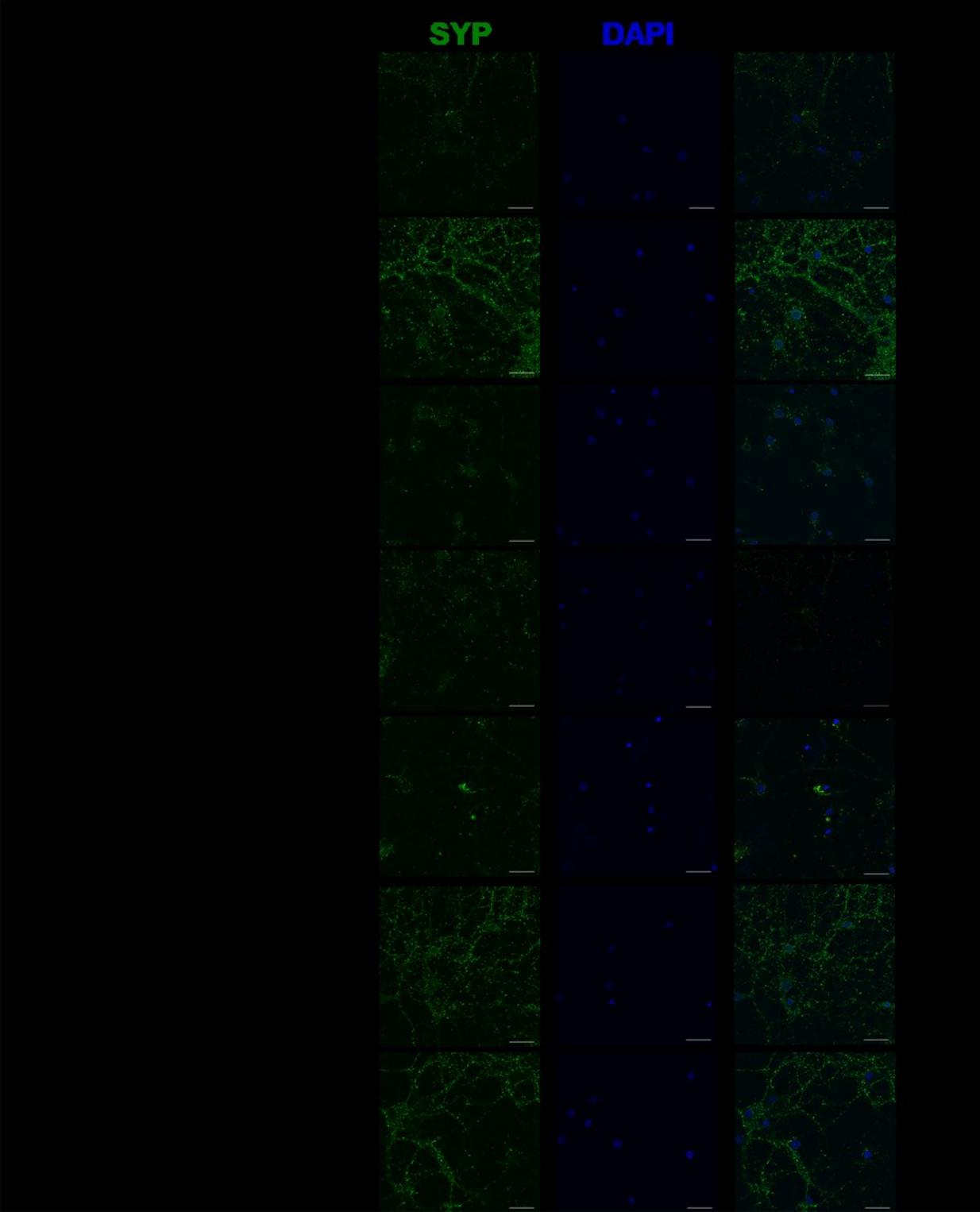


Figure 4. let-7i inhibits progesterone (P4) induces synaptophysin (SYP) expression in primary cortical astrocytes.

(A) Representative confocal images of primary cortical neurons (DIV 14) immunostained with synaptophysin (SYP,green) and DAPI (blue). (60x, Scale bars=30 μ m). (B) Quantification of average SYP fluorescence intensity per neuron (n=3). RFU : relative fluorescence unit. n.s: not significant, ***P<0.001 and ** P<0.01 compared to mock+DMSO group by one-way ANOVA followed by Tukey's post hoc analysis. (C) Quantification of average number of SYP puncta per neuron (n=3). n.s: not significant, ***P<0.001 compared to mock transfected+DMSO group by one-way ANOVA followed by Tukey's post hoc analysis. Data are presented as the mean \pm SEM.



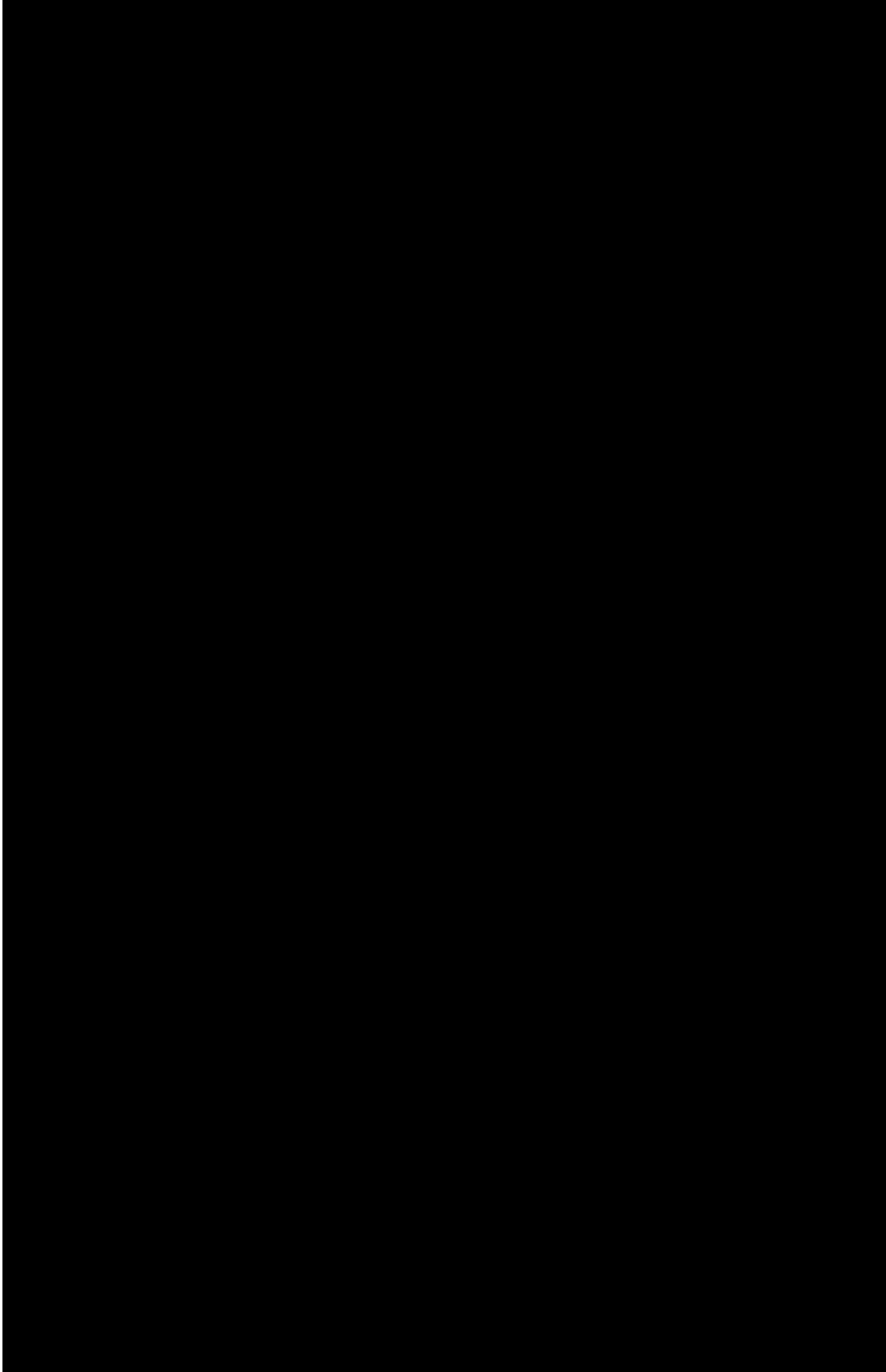
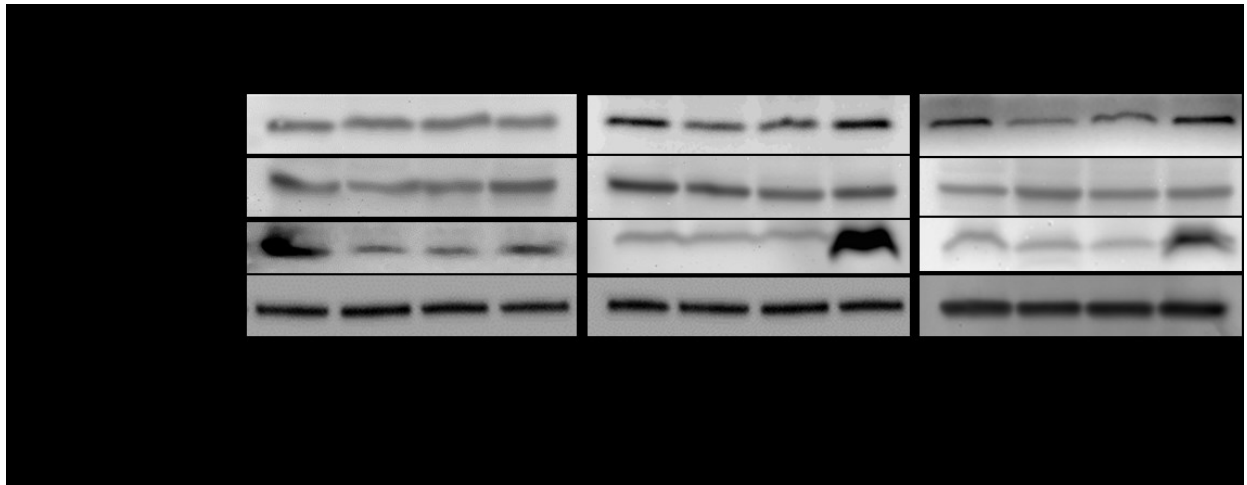


Figure 5. Combined treatment with progesterone (P4) and the let-7i inhibitor reversed the ischemia-induced suppression of Pgrmc1 and BDNF expressions in the peri-infarct region.

(A) Representative immunoblots probed for Pgrmc1, pro- and mature-BDNF. (B) Quantitation graph of relative Pgrmc1 protein ratio to Gapdh (n=4-5 per group). (C) Quantitation graph of relative pro-BDNF protein ratio to Gapdh (n=4-5 per group). (D) Quantitation graph of relative mature BDNF protein ratio to Gapdh (n=4-5 per group). (E) Quantitation graph of relative let-7i expression in ischemic brain (n=4-5 per group). n.s: not significant, ** P<0.01 and *P<0.05 compared to sham, and #P<0.05 compared to P4+ scrambled by analysis of variance followed by Dunn's post hoc analysis. Data are presented as the mean \pm SEM.



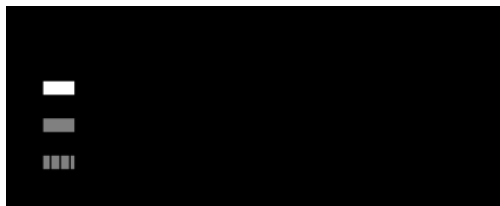
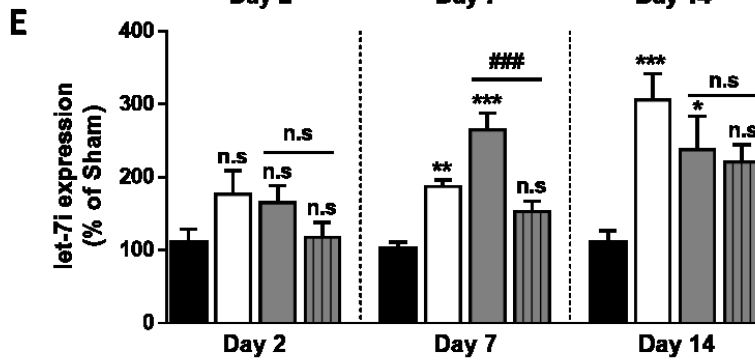
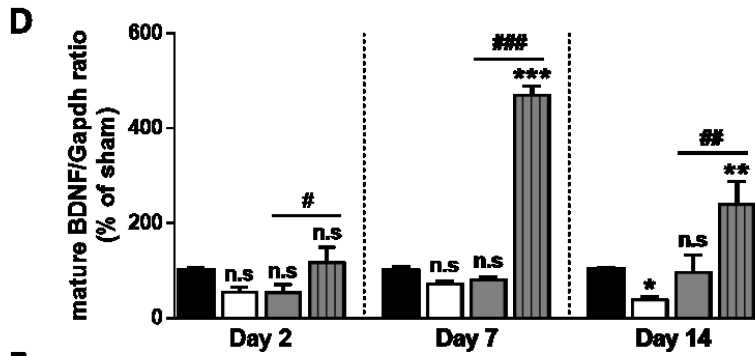
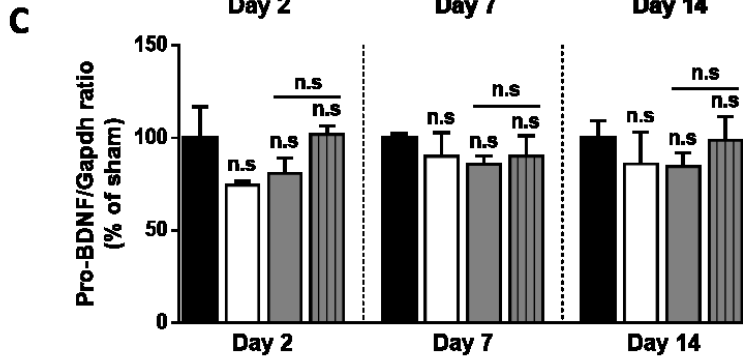
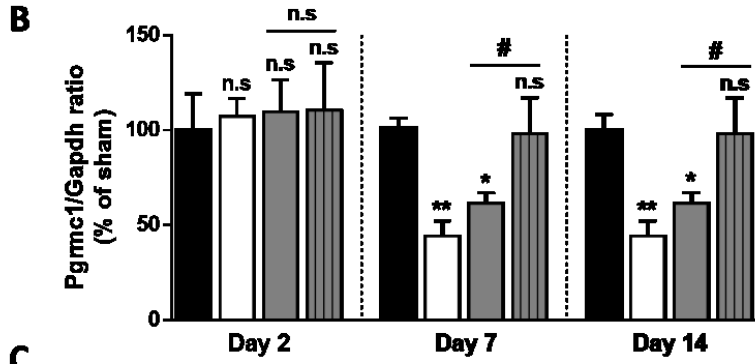
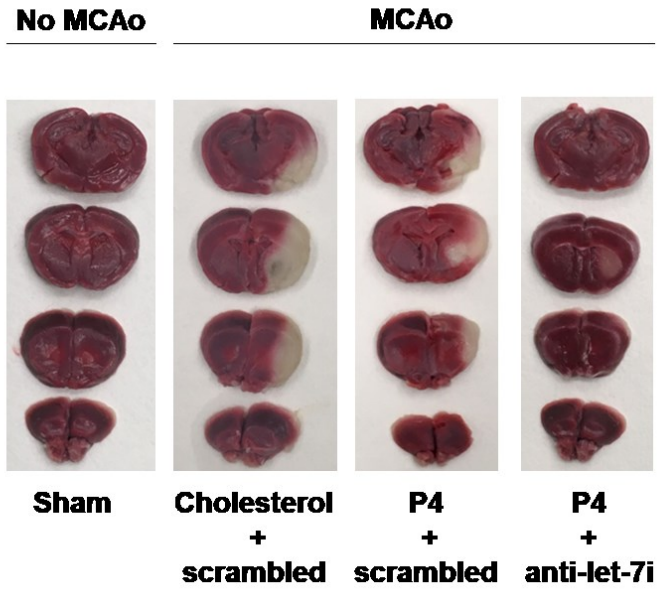


Figure 6. Co-administration of let-7i antagomir (anti-let-7i) and progesterone (P4) reduces ischemic injury.

(A) Representative images of serial coronal brain sections stained with triphenyltetrazolium chloride (TTC). (B) Quantification of infarct sizes of TTC-stained images (n=4 per group). n.s: not significant, ***P<0.001 and ** P<0.01 compared to cholesterol+scrambled group by one-way ANOVA followed by Tukey's post hoc analysis. Data are presented as the mean \pm SEM.

A



B

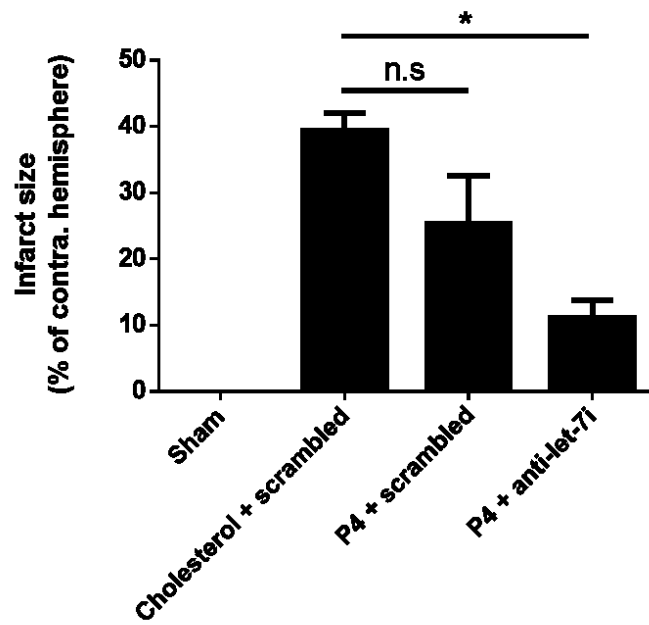


Figure. 7. Co-administration of let-7i antagomir (anti-let-7i) and progesterone (P4) enhances recovery of motor function/grip strength following stroke.

Results of wire suspension test at day 3, 7 and 14 post stroke (n=15-20 per group). n.s: not significant, ***P<0.001 and ** P<0.01 compared to sham, ### P<0.001, ##P<0.01 compared to P4+ scrambled, and \$\$P<0.01 compared to cholesterol+ scrambled by one-way ANOVA followed by Tukey's post hoc analysis. Data are presented as the mean \pm SEM

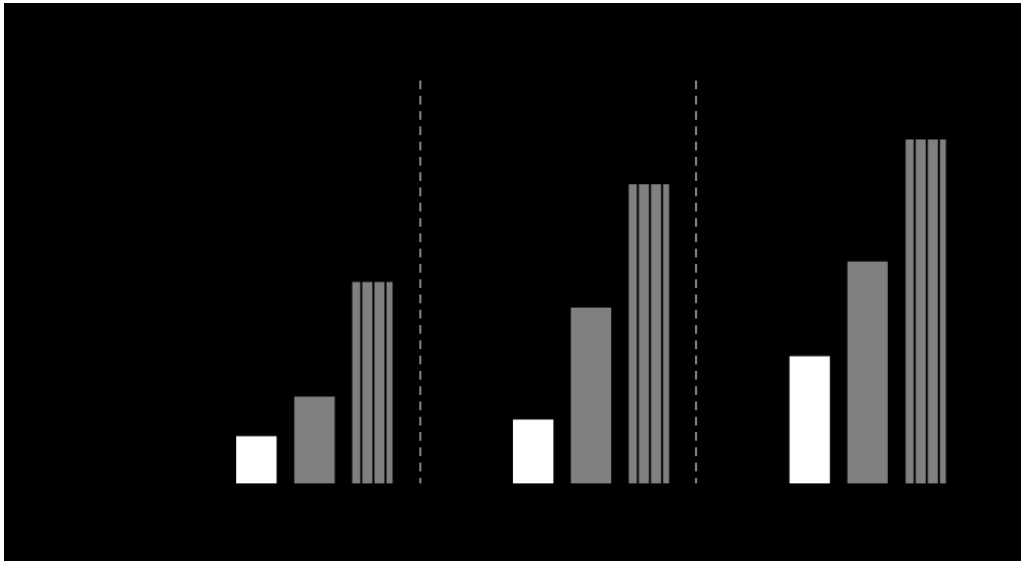
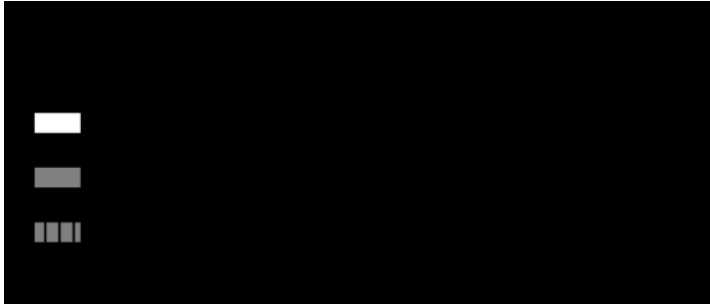
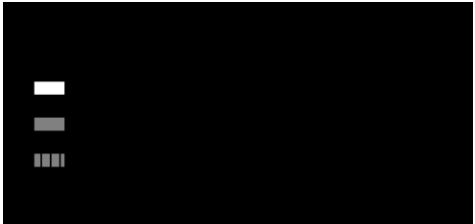
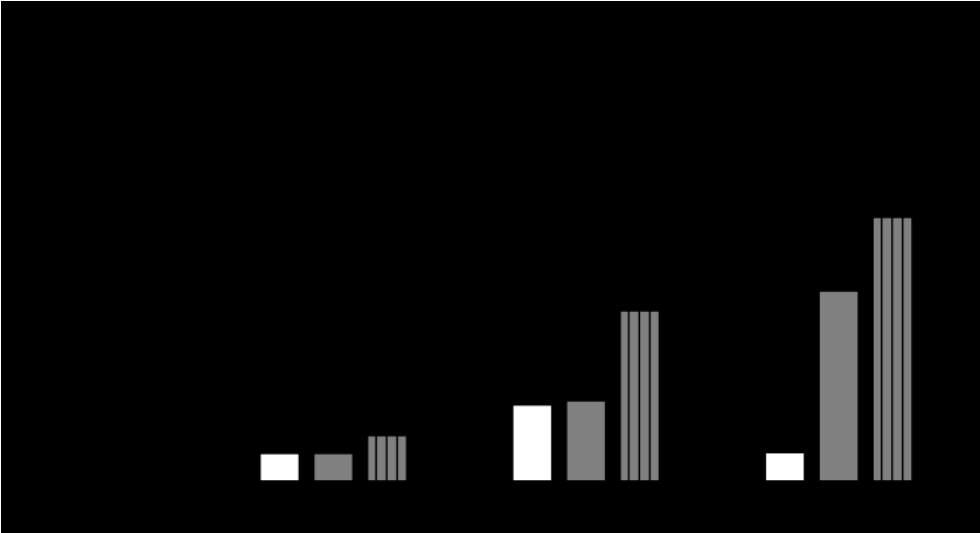
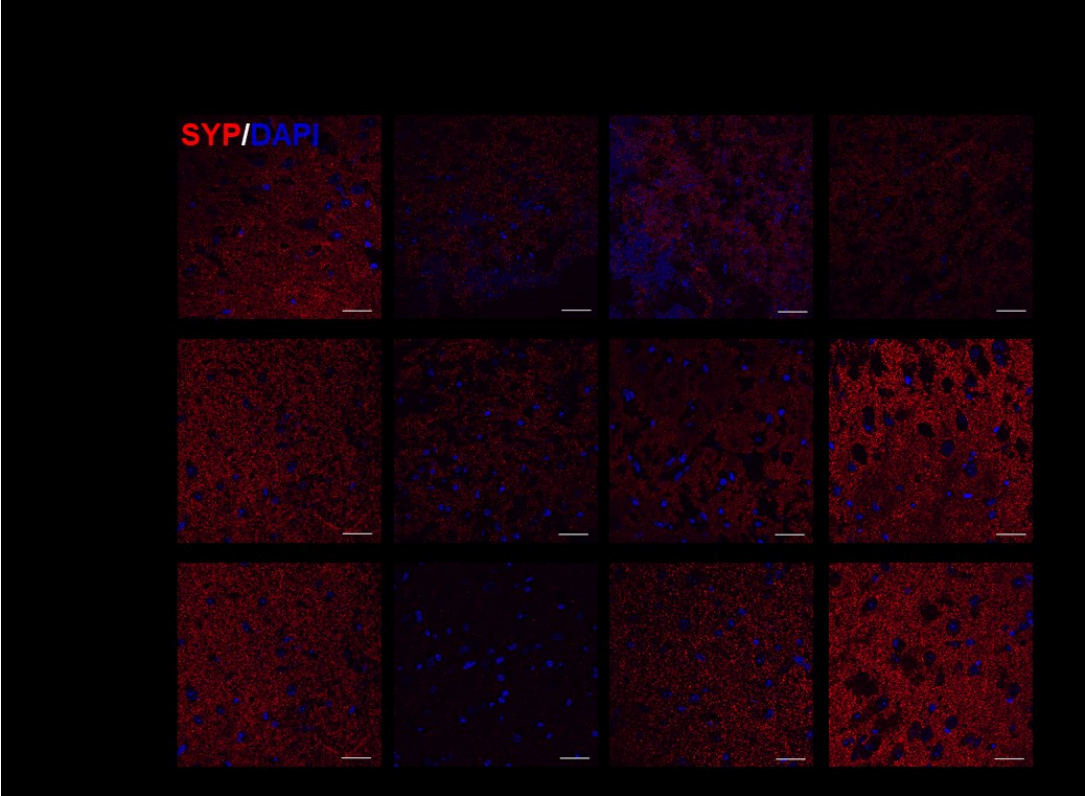
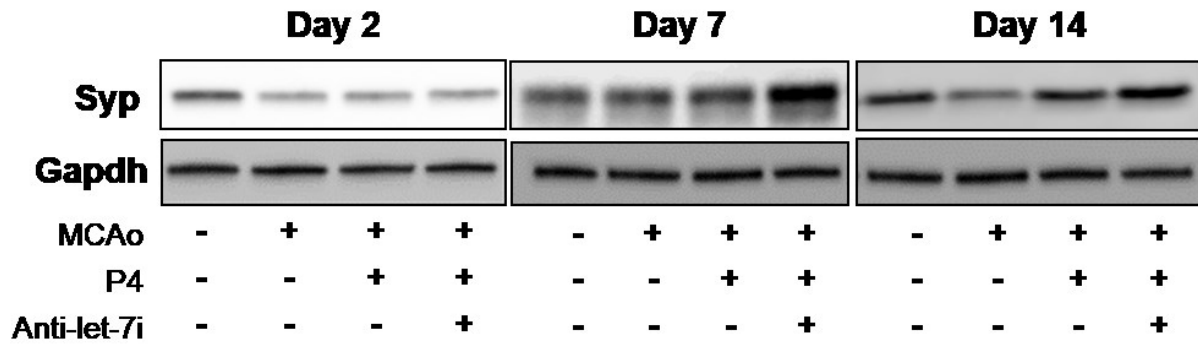


Figure 8. Inhibition of let-7i enhances progesterone (P4)'s effect on the expression of synaptophysin in the peri-infarct region.

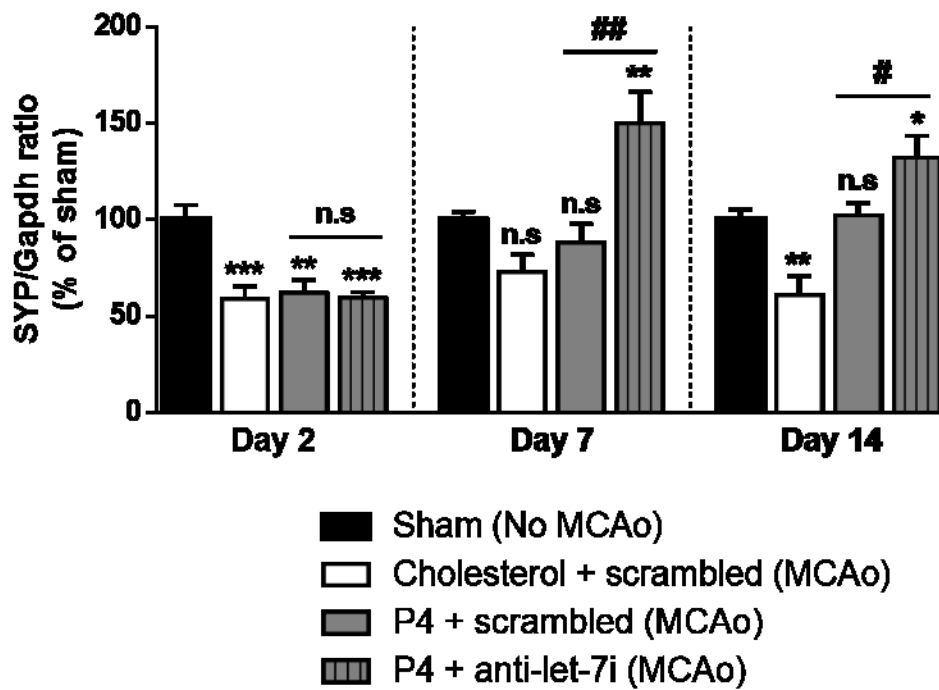
(A) Representative confocal images of peri-infarct area staining for synaptophysin (SYP, red) and DAPI (blue). (60x, Scale bars=30 μ m). (B) Quantification of average relative SYP puncta presents in each field (n=3 per group). n.s: not significant and ***P<0.001 compared to sham, ### P<0.001 and ##P<0.01 compared to P4+ scrambled by analysis of variance followed by Dunn's post hoc analysis. (C) Representative immunoblots probed for SYP protein. (D) Quantification graph of Syp signal, expressed as a ratio to Gapdh (n=4-5 per group). n.s: not significant, ***P<0.001 and **P<0.01 compared to sham, ## P<0.01 and #P<0.05 compared to P4+ scrambled by analysis of variance followed by Dunn's post hoc analysis



C



D



REFERENCES

1. Mozaffarian D, *et al.* (2015) Heart disease and stroke statistics--2015 update: a report from the American Heart Association. *Circulation* 131(4):e29-322.
2. Atif F, *et al.* (2013) Combination treatment with progesterone and vitamin D hormone is more effective than monotherapy in ischemic stroke: the role of BDNF/TrkB/Erk1/2 signaling in neuroprotection. *Neuropharmacology* 67:78-87.
3. Ishrat T, Sayeed I, Atif F, & Stein DG (2009) Effects of progesterone administration on infarct volume and functional deficits following permanent focal cerebral ischemia in rats. *Brain research* 1257:94-101.
4. Zhao Y, *et al.* (2011) Progesterone influences postischemic synaptogenesis in the CA1 region of the hippocampus in rats. *Synapse* 65(9):880-891.
5. Kaur P, *et al.* (2007) Progesterone increases brain-derived neurotrophic factor expression and protects against glutamate toxicity in a mitogen-activated protein kinase- and phosphoinositide-3 kinase-dependent manner in cerebral cortical explants. *Journal of neuroscience research* 85(11):2441-2449.
6. Liu L, *et al.* (2010) The neuroprotective effects of Tanshinone IIA are associated with induced nuclear translocation of TORC1 and upregulated expression of TORC1, pCREB and BDNF in the acute stage of ischemic stroke. *Brain Res Bull* 82(3-4):228-233.
7. Sato Y, *et al.* (2009) White matter activated glial cells produce BDNF in a stroke model of monkeys. *Neurosci Res* 65(1):71-78.
8. Causing CG, *et al.* (1997) Synaptic innervation density is regulated by neuron-derived BDNF. *Neuron* 18(2):257-267.

9. Coffey ET, Akerman KE, & Courtney MJ (1997) Brain derived neurotrophic factor induces a rapid upregulation of synaptophysin and tau proteins via the neurotrophin receptor TrkB in rat cerebellar granule cells. *Neurosci Lett* 227(3):177-180.
10. Heldt SA, Stanek L, Chhatwal JP, & Ressler KJ (2007) Hippocampus-specific deletion of BDNF in adult mice impairs spatial memory and extinction of aversive memories. *Mol Psychiatry* 12(7):656-670.
11. McAllister AK (2007) Dynamic aspects of CNS synapse formation. *Annual review of neuroscience* 30:425-450.
12. Sheng M & Hoogenraad CC (2007) The postsynaptic architecture of excitatory synapses: a more quantitative view. *Annual review of biochemistry* 76:823-847.
13. Waites CL, Craig AM, & Garner CC (2005) Mechanisms of vertebrate synaptogenesis. *Annual review of neuroscience* 28:251-274.
14. Stroemer RP, Kent TA, & Hulsebosch CE (1995) Neocortical neural sprouting, synaptogenesis, and behavioral recovery after neocortical infarction in rats. *Stroke* 26(11):2135-2144.
15. Liu HS, *et al.* (2011) Post-treatment with amphetamine enhances reinnervation of the ipsilateral side cortex in stroke rats. *NeuroImage* 56(1):280-289.
16. Zhang L, *et al.* (2011) Delayed administration of human umbilical tissue-derived cells improved neurological functional recovery in a rodent model of focal ischemia. *Stroke* 42(5):1437-1444.
17. Zhang L, *et al.* (2012) Intravenous administration of human umbilical tissue-derived cells improves neurological function in aged rats after embolic stroke. *Cell transplantation*.
18. Su C, Cunningham RL, Rybalchenko N, & Singh M (2012) Progesterone increases the release of brain-derived neurotrophic factor from glia via progesterone receptor membrane component 1 (Pgrmc1)-dependent ERK5 signaling. *Endocrinology* 153(9):4389-4400.

19. Selvamani A, Sathyan P, Miranda RC, & Sohrabji F (2012) An antagomir to microRNA Let7f promotes neuroprotection in an ischemic stroke model. *PLoS One* 7(2):e32662.
20. Wendler A, Keller D, Albrecht C, Peluso JJ, & Wehling M (2011) Involvement of let-7/miR-98 microRNAs in the regulation of progesterone receptor membrane component 1 expression in ovarian cancer cells. *Oncol Rep* 25(1):273-279.
21. Di Y, *et al.* (2014) MicroRNAs expression and function in cerebral ischemia reperfusion injury. *J Mol Neurosci* 53(2):242-250.
22. Caballero-Garrido E, *et al.* (2015) In Vivo Inhibition of miR-155 Promotes Recovery after Experimental Mouse Stroke. *J Neurosci* 35(36):12446-12464.
23. Ni J, *et al.* (2015) MicroRNA let-7c-5p protects against cerebral ischemia injury via mechanisms involving the inhibition of microglia activation. *Brain Behav Immun* 49:75-85.
24. Pena-Philippides JC, Caballero-Garrido E, Lordkipanidze T, & Roitbak T (2016) In vivo inhibition of miR-155 significantly alters post-stroke inflammatory response. *J Neuroinflammation* 13(1):287.
25. Sigler A & Murphy TH (2010) In vivo 2-photon imaging of fine structure in the rodent brain: before, during, and after stroke. *Stroke* 41(10 Suppl):S117-123.
26. Franke H, Verkhatsky A, Burnstock G, & Illes P (2012) Pathophysiology of astroglial purinergic signalling. *Purinergic signalling* 8(3):629-657.
27. Jodhka PK, Kaur P, Underwood W, Lydon JP, & Singh M (2009) The differences in neuroprotective efficacy of progesterone and medroxyprogesterone acetate correlate with their effects on brain-derived neurotrophic factor expression. *Endocrinology* 150(7):3162-3168.
28. Sun F, *et al.* (2016) Pgrmc1/BDNF Signaling Plays a Critical Role in Mediating Glia-Neuron Cross Talk. *Endocrinology* 157(5):2067-2079.

29. Yousuf S, Atif F, Sayeed I, Wang J, & Stein DG (2013) Post-stroke infections exacerbate ischemic brain injury in middle-aged rats: immunomodulation and neuroprotection by progesterone. *Neuroscience* 239:92-102.
30. Stroemer RP, Kent TA, & Hulsebosch CE (1998) Enhanced neocortical neural sprouting, synaptogenesis, and behavioral recovery with D-amphetamine therapy after neocortical infarction in rats. *Stroke* 29(11):2381-2393; discussion 2393-2385.
31. Roy Choudhury G, *et al.* (2015) Methylene blue protects astrocytes against glucose oxygen deprivation by improving cellular respiration. *PLoS One* 10(4):e0123096.
32. Rueden CT, *et al.* (2017) ImageJ2: ImageJ for the next generation of scientific image data. *BMC Bioinformatics* 18(1):529.
33. Crouch SP, Kozlowski R, Slater KJ, & Fletcher J (1993) The use of ATP bioluminescence as a measure of cell proliferation and cytotoxicity. *J Immunol Methods* 160(1):81-88.
34. Parker CG, *et al.* (2017) Ligand and Target Discovery by Fragment-Based Screening in Human Cells. *Cell* 168(3):527-541 e529.
35. Ryou MG, *et al.* (2015) Methylene blue-induced neuronal protective mechanism against hypoxia-reoxygenation stress. *Neuroscience* 301:193-203.
36. Jin K, *et al.* (2004) Increased hippocampal neurogenesis in Alzheimer's disease. *Proc Natl Acad Sci U S A* 101(1):343-347.
37. Singh M, Meyer EM, Millard WJ, & Simpkins JW (1994) Ovarian steroid deprivation results in a reversible learning impairment and compromised cholinergic function in female Sprague-Dawley rats. *Brain Res* 644(2):305-312.
38. Li W, *et al.* (2014) PTEN degradation after ischemic stroke: a double-edged sword. *Neuroscience* 274:153-161.
39. Yang SH, *et al.* (2001) 17-beta estradiol can reduce secondary ischemic damage and mortality of subarachnoid hemorrhage. *J Cereb Blood Flow Metab* 21(2):174-181.

40. Hauben U, D'Hooge R, Soetens E, & De Deyn PP (1999) Effects of oral administration of the competitive N-methyl-D-aspartate antagonist, CGP 40116, on passive avoidance, spatial learning, and neuromotor abilities in mice. *Brain Res Bull* 48(3):333-341.
41. Ippolito DM & Eroglu C (2010) Quantifying synapses: an immunocytochemistry-based assay to quantify synapse number. *J Vis Exp* (45).
42. Kucukdereli H, *et al.* (2011) Control of excitatory CNS synaptogenesis by astrocyte-secreted proteins Hevin and SPARC. *Proc Natl Acad Sci U S A* 108(32):E440-449.

CHAPTER IV

PGRMC1/BDNF SIGNALING PLAYS A CRITICAL ROLE IN MEDIATING GLIA- NEURON CROSSTALK

Fen Sun *, **Trinh Nguyen ***, **Xin Jin**, **Renqi Huang**, **Zhenglan Chen**, **Rebecca L. Cunningham**, **Meharvan Singh**, and **Chang Su**

Department of Pharmacology & Neuroscience, University of North Texas Health Science Center,
Fort Worth, Texas, 76107

*: Contributed equally to this manuscript

Short title: Pgrmc1 signaling mediates glia-neuron crosstalk

Endocrinology 2016, 157 (5): 2067-79

Corresponding author: Chang Su

Department of Pharmacology & Neuroscience, Center Focused On Resources for her Health,
Education and Research (FOR HER), the Institute for Aging & Alzheimer's Disease Research,
University of North Texas Health Science Center, Fort Worth, Texas, 76107

Phone: +1-8177350610

Fax:+1-8177350408

email: Chang.Su@unthsc.edu

ABSTRACT

Progesterone (P4) exerts robust cytoprotection in brain slice cultures (containing both neurons and glia), yet such protection is not as evident in neuron-enriched cultures, suggesting that glia may play an indispensable role in P4's neuroprotection. We previously reported that a membrane-associated P4 receptor, P4 receptor membrane component 1, mediates P4-induced brain-derived neurotrophic factor (BDNF) release from glia. Here, we sought to determine whether glia are required for P4's neuroprotection and whether glia's roles are mediated, at least partially, via releasing soluble factors to act on neighboring neurons. Our data demonstrate that P4 increased the level of mature BDNF (neuroprotective) while decreasing pro-BDNF (potentially neurotoxic) in the conditioned media (CMs) of cultured C6 astrocytes. We examined the effects of CMs derived from P4-treated astrocytes (P4-CMs) on 2 neuronal models: 1) *all-trans* retinoic acid-differentiated SH-SY5Y cells and 2) mouse primary hippocampal neurons. P4-CM increased synaptic marker expression and promoted neuronal survival against H₂O₂. These effects were attenuated by Y1036 (an inhibitor of neurotrophin receptor [tropomyosin-related kinase] signaling), as well as tropomyosin-related kinase B-IgG (a more specific inhibitor to block BDNF signaling), which pointed to BDNF as the key protective component within P4-CM. These findings suggest that P4 may exert its maximal protection by triggering a glia-neuron cross talk, in which P4 promotes mature BDNF release from glia to enhance synaptogenesis as well as survival of neurons. This recognition of the importance of glia in mediating P4's neuroprotection may also inform the design of effective therapeutic methods for treating diseases wherein neuronal death and/or synaptic deficits are noted.

INTRODUCTION

Progesterone (P4), the natural progestin, is a major gonadal hormone synthesized primarily by the ovary in females, and the testes and adrenal cortex in males. P4 is also synthesized in astrocytes within the brain, thus considered to be a neurosteroid as well [1]. While the function of P4 has historically been considered within the context of the reproductive system, it is now clear that P4 has important effects on multiple organ systems including the brain. P4 has been reported to exert protective effects in numerous experimental models that mimic a variety of age-associated brain diseases, including ischemic stroke [2-4], Alzheimer's disease (AD) and traumatic brain injury (TBI) [5] [6-9]. For example, acute administration of P4 enhanced learning and spatial working memory performance in both male and female middle-aged and aged mice [10, 11]. Despite the promising experimental and preclinical data, a recent phase III clinical trial (ProTECT III) assessing the efficacy of P4 treatment for acute TBI showed rather disappointing results with no favorable effects noted, while increasing the frequencies of phlebitis [12]. Such discrepancies between animal and human data further underscore the critical need to better understand the mechanisms of P4 action in the central nervous system, to better inform future studies that address either acute insults (such as TBI) or chronic neurodegenerative diseases (such as AD).

Characteristic neuropathological changes of AD include both neuronal loss and synapse loss [13]. Of note, P4 has been shown to promote neuronal survival as well as synaptogenesis [14, 15]. One potential downstream mediator of P4's effect on neuronal survival and synaptogenesis is a brain-derived neurotrophic factor (BDNF). BDNF belongs to the family of neurotrophins, which play key roles in the brain to support cell survival and synaptic plasticity [16, 17] and is synthesized in both neurons and glia [18, 19]. BDNF is synthesized as a glycosylated precursor (pre-pro-BDNF), processed into a 35 kDa pro-BDNF, and then can be converted into

the 14 kDa mature BDNF [20, 21]. BDNF released from cells elicits its effects by binding to TrkB (a tyrosine kinase (tropomyosin-related kinase) family of receptors) and/or the p75NTR receptor [19, 20, 22, 23]. Delineating the effects of pro-versus mature BDNF is critical because they can exert opposite biological functions such that mature BDNF binds to the TrkB receptor to influence neuronal survival, differentiation, and promote LTP, while pro-BDNF binds preferentially to p75NTR and can induce neuronal apoptosis and promote LTD [21]. Moreover, it has been proposed that neuronal dysfunction or atrophy consequent to aging or age-associated diseases may result from not only decreases in mature neurotrophin expression or function [24-26], but potentially, to increased accumulation of the pro-neurotrophins.

We recently found that glia and neurons showed an interesting and striking difference in not only basal release of BDNF but also in their response to P4. Glia exhibited low levels of basal BDNF secretion and responded significantly to treatment with P4 [27]. In characterizing the mechanism by which P4 increased the release of BDNF, we found that a novel membrane-associated progesterone receptor (progesterone receptor membrane component 1, Pgrmc1), was responsible for the P4-elicited BDNF release from glia [27]. Pgrmc1 has been implicated as an important biomarker for cancer progression and as a potential target for anticancer therapies [28]. With regards to the brain, expression of Pgrmc1 has been mapped to the cerebral cortex, hypothalamus, amygdala, and cerebellum [29-31]. Concerning neuroprotection, Guennoun et al. showed the potential role of Pgrmc1 in mediating the protective effects of P4 in the injured spinal cord and in the brain after TBI [32]. Furthermore, this same group also showed that Pgrmc1 expression was up-regulated after TBI in both cortical neurons as well as in the astrocytes near the lesion [32], suggesting that Pgrmc1 may influence P4-stimulated glial responses after injury as well.

In this study, we tried to determine whether glia is required for P4's neuroprotection and if the role of glia is mediated by releasing soluble factors to act on neighboring neurons. Our data

demonstrated that P4 increased the ratio of mature vs. pro-BDNF in astrocytes and that the conditioned media from P4-treated astrocytes (P4-CM) was effective at promoting an increase in synaptic marker expression and neuronal viability. Interestingly, the protective effects of P4-CM were prevented by inhibiting BDNF signaling. Together, our data support a critical role for astrocytes in mediating the protective effects of progesterone, and further, that these protective effects are mediated, at least in part, through the regulation of BDNF signaling.

MATERIALS AND METHODS

Cell culture and treatment

Rat C6 glioma cells (male) and human SH-SY5Y neuroblastoma cells (female) were purchased from American Type Culture Collection (Manassas, VA). C6 cells were propagated in DMEM (Invitrogen Life Technologies, Carlsbad, CA) supplemented with 10% charcoal-stripped fetal bovine serum (Hyclone, Logan, UT) and maintained at 37°C in a humidified environment containing 5% CO₂ for 24 h, then treated with vehicle control-dimethylsulfoxide (DMSO, 0.1%), P4 (Sigma-Aldrich, St.Louis, MO) at 10nM for the indicated time. SH-SY5Y cells were propagated in DMEM/F12 (Invitrogen Life Technologies, Carlsbad, CA) supplemented with 15% charcoal-stripped fetal bovine serum (Hyclone, Logan, UT) and differentiated with retinoic acid (RA, Sigma-Aldrich, St.Louis, MO) at 10µM for 7 d.

The use of animals to generate primary cultures was approved by the Institutional Animal Care and Use Committee at the University of North Texas Health Science Center. All mice were handled according to the Guide for the Care and Use of Laboratory Animals. Primary cultures of cortex and hippocampal neurons were prepared from neonatal murine pups (C57BL/6NHSd mice, Harlan) as described by Sarkar et al. with modifications [33]. Briefly, hippocampal tissues isolated from newborn mice (postnatal days 2–4, mixed gender) were dissociated with trypsin and DNase I for 10 min at 37 °C. The tissues were then washed twice with Neurobasal-A medium containing B-27 and further dissociated by gentle titration using a graded series of finely polished Pasteur pipettes. After centrifugation at 200 ×g for 3 min at 4 °C, cortex and hippocampal neurons were resuspended in Neurobasal-A/B-27 medium, passed through a cell strainer with 70 µm mesh, and plated at 1.0×10⁵ cells/cm² on culture dishes precoated with poly-D-lysine. The culture dishes were kept at 37°C in humidified 95% air and 5% CO₂. The initial culture medium was

replaced after 5 h; subsequently, half of the medium was changed every 3 days. At day in vitro (DIV) 2, 1- β -arabinofuranosylcytosine (AraC) was added to a final concentration of 5 μ M to prevent glial proliferation. Treatments of the primary cultures started at DIV 7.

For SH-SY5Y cells or primary neurons experiments, there were 6 groups: 1. Non-treated, 2. Brain-derived neurotrophic factor (BDNF, Millipore, Billerica, MA, USA) -treated, added at 100 ng/ml, 3. DMSO condition medium (DMSO-CM)-treated, 4. P4 condition medium (P4-CM)-treated, 5. DMSO-CM with neurotrophin antagonist, Y-1036 (Millipore, Billerica, MA, USA), at 40 μ M, and 6. P4-CM with neurotrophin antagonist, Y-1036; or 1. Non-treated, 2. Brain-derived neurotrophic factor (BDNF, Millipore, Billerica, MA, USA) -treated, added at 100 ng/ml, 3. DMSO condition medium (DMSO-CM) with IgG control-treated, 4. P4 condition medium (P4-CM) with IgG control -treated, 5. DMSO-CM with TrkB-Fc, at 4 μ g/ml, and 6. P4-CM with TrkB-Fc. For primary neurons, DMSO- or P4-CM needed enriching via Pierce protein concentrators (Thermo Fisher Scientific, Rockford, IL, USA).

Recombinant human TrkB-Fc chimera (R&D Systems) to remove BDNF. Briefly, 4.0 μ g/ml TrkB-Fc was added to media for 2 h in 4 $^{\circ}$ C with rotation, and equal amounts of normal human IgG were added as control.

Pgrmc1 pull-down assay

Dynabeads Protein A was purchased from Life Technologies (Carlsbad, CA, USA). In advance of the experiment, Dynabeads Protein A was coated with anti-Pgrmc1 antibody (Abcam, ab48058, Cambridge, MA). Briefly, 400 μ l of Dynabeads Protein A suspension was attached to DynaMag-2 (Life Technologies; Carlsbad, CA), and the supernatant was removed. Dynabeads Protein A was resuspended in 800 μ l of wash buffer (100 mM phosphate buffer containing 0.05% Tween 20, pH 7.4) containing 40 μ l of the antibody, and incubated at 4 $^{\circ}$ C overnight with head-

to-tail rotation. Immediately prior to the experiment, Dynabeads Protein A was washed with wash buffer five times and resuspended in 800 μ l of wash buffer. 25 μ l suspension of Dynabeads Protein A: anti-Pgrmc1 Ab complex was added to 1 mL of C6 cell supernatants (enriched from 20 mL total culture supernatants; see following). After incubation at room temperature for 60 min, the Dynabeads Protein A were washed with 250 μ l of wash buffer five times and resuspended in 25 ml of 1 X SDS-PAGE sample buffer. Pro- and mature BDNF was separated by different molecular weight on Western blotting.

Column enrichment of C6 culture supernatants

20ml of C6 conditioned media (CM) was harvested and transferred to a pre-rinsed Pierce 9K MWCO 20ml concentrator (Thermo Scientific, Waltham, MA), following centrifuge at 3200rpm for 45 min to achieve a final concentrated volume of 1ml. The concentrated CM was sterilized via a 0.2 μ m sterile syringe filter and then applied to cultures in volumes to dilute back to 1X.

Immunocytochemistry quantification

SH-SY5Y cells were differentiated with 10 μ M all-trans retinoic acid (Sigma Aldrich, St.Louis, MO) for 7d prior to being treated with glial-derived DMSO-conditioned media (DMSO-CM) or P4-conditioned media (P4-CM) in the presence/absence of the Y1036 compound, a neurotrophin antagonist. Treatment of cells with 50ng/ml of BDNF was used as positive control. At the end of treatment, cells were briefly washed with cold PBS and fixed with 4% paraformaldehyde for 15 min at room temperature. Fixed cells were permeabilized with cold Methanol: Acetone (1:1) for 1 min. The cells were then washed with cold PBS and incubated with 2% normal goat serum (NGS) in PBS for 1h at room temperature. The cells were incubated with

the rabbit anti-GAP-43 antibody (ab75810; Abcam, Cambridge, MA), in PBS containing 2% NGS at 4°C overnight. After several washes with cold PBS, they were then incubated with green-fluorescent dye labeled goat anti-rabbit IgG antibody (Invitrogen Life Technologies, Carlsbad, CA) for 1 h at room temperature. After two washes with cold PBS, cells were then incubated with Hoechst dye at room temperature for 15 min. Stained cultures were preserved in PBS at 4°C. Images were acquired with a Nikon Eclipse TS100 microscope (20x) with strict preservation of imaging setting across samples. Mean fluorescence intensity values were measured by drawing a rectangle (20x10 pixels in dimension) and aligning the box such that it enclosed the area of interest, the Region of Interest function of the NIS elements software were then used to compute a mean fluorescence intensity value. For each treatment group, GAP-43 mean fluorescence intensities of 3 to 5 non-overlapping proximal and distal neuritic segments were measured and average values were computed. A proximal segment is defined as a section within 2 cell body lengths of a cell body and a distal neuritic segment is that which is anywhere greater than 2 cell body lengths from the cell body that it originates from. Mean intensity values were then normalized to non-treated control group and reported as percentage of control. Three to four independent experiments were performed.

RNA isolation and cDNA synthesis

Total RNA was isolated from SH-SY5Y cell, primary neuron cultures and mouse brains using the RNeasy Mini Kit and the RNeasy Lipid Kit (QIAGEN, Valencia, CA) according to the manufacturer's instructions. Concentrations of extracted RNA were determined using absorbance values at 260 nm. The purity of RNA was assessed by ratios of absorbance values at 260 and 280 nm (A_{260}/A_{280} ratios of 1.9 –2.0 were considered acceptable). Total RNA (1.6 µg) was reverse transcribed into cDNA in a total volume of 20 µl using the High-Capacity DNA Archive Kit (Roche Applied Science, Indianapolis, IN) according to the manufacturer's instructions.

Primers and probes for quantitative real-time RT-PCR

PCR primers and probes for the target gene were purchased as Assay-On-Demand (Applied Biosystems Inc., Foster City, CA). The assays were supplied as a 20 mix of PCR primers (900 nM) and TaqMan probes (200 nM). The BDNF (Mm00432069_m1), Pgrmc1 (Mm00443985_m1), GAP-43 (Hs00967138_m1), Synaptophysin (SYP, Hs00300531_m1) and GAPDH (Hs02758991_g1 and Mm03302249_g1) assays contained FAM (6-carboxy-fluorescein phosphoramidite) dye label at the 5' end of the probes, a minor groove binder and a nonfluorescent quencher at the 3' end of the probes.

Quantitative real-time RT-PCR

The reaction mixture contained water, 2x quantitative PCR Master Mix (Eurogentec, Fremont, CA), and 20x Assay-On-Demand for each target gene. A separate reaction mixture was prepared for the endogenous control, GAPDH. The reaction mixture was aliquoted in a 96-well plate, and cDNA (30 ng RNA converted to cDNA) was added to give a final volume of 30 μ l. Each sample was analyzed in triplicate. Amplification and detection were performed using the ABI 7300 Sequence Detection System (Applied Biosystems) with the following profile: 2 min hold at 50°C [uracil-N-glycosylase (UNG)] and 10 min hold at 95°C, followed by 40 cycles of 15 sec at 95°C (denaturation) and 1 min at 60°C (annealing and extension). Sequence Detection Software version 1.3 (Applied Biosystems) was used for data analysis. The comparative cycle threshold (Ct) method ($2^{-\Delta\Delta Ct}$) was used to calculate the relative changes in target gene expression. In the comparative Ct method, the amount of target, normalized to an endogenous control (GAPDH) and relative to a calibrator (untreated control), is given by the $2^{-\Delta\Delta Ct}$ equations. Quantity is expressed relative to a calibrator sample that is used as the basis for comparative results. Therefore, the calibrator was the baseline (non-treated control) sample, and all other treatment groups were expressed as an n-fold (or percentage) difference relative to the control (40). The

average and SD of $2^{-\Delta\Delta Ct}$ was calculated for the values from five independent experiments, and the relative amount of target gene expression for each sample was plotted in bar graphs using GraphPad Prism version 4 software (GraphPad, San Diego, CA).

Western blotting

Cells were harvested with lysis buffer containing protease and phosphatase inhibitors, as described previously [34]. After homogenization, samples were centrifuged at 12,000rpm for 15 min at 4 °C, and the resulting supernatants were evaluated for total protein concentrations using the Bio-Rad DC (Bio-Rad Laboratories, Hercules, CA, USA) protein assay kit. Sample lysates were loaded onto a sodium dodecyl sulfate/10 % polyacrylamide gel, subjected to electrophoresis, and subsequently transferred onto a polyvinylidene difluoride membrane (0.22 μm pore size; Bio-Rad Laboratories, Hercules, CA, USA). The membrane was blocked for 1 h with 5 % non-fat milk in 0.2 % Tween-containing Tris-buffered saline solution before application of the primary antibody. The following primary antibodies were used: The antibodies against Pro-BDNF and mature-BDNF (N20, 1:1000) were purchased from Santa Cruz Biotechnology (Dallas, TX); the antibodies against total BDNF, synaptophysin and GAP43 (1:1000) were purchased from Abcam (Cambridge, MA); the antibodies against GAPDH (14C10, 1:1000) were purchased from Cell Signaling Technology (Danvers, MA).

Antibody binding to the membrane was detected using a secondary antibody (either goat anti-rabbit or rabbit anti-goat) conjugated to horseradish peroxidase (1:20,000; Pierce Chemical Co., Rockford, IL, USA) and visualized using enzyme-linked chemiluminescence (Pierce ECL Western Blotting Substrate; Thermo Fisher Scientific, Rockford, IL, USA) with the aid of the AlphaInnotech imaging system.

Apoptotic Assay:

Apoptosis was quantified using the Vybrant apoptosis assay kit (Invitrogen) per manufacturer's instructions. Briefly, Hoechst 33342 solution (1:2000) was added to cells cultured in 6-well plate, and the mixture was incubated for 30 min on ice. Fluorescence was measured under a fluorescence microscope with a ×20 objective. The blue fluorescent dye Hoechst 33342 stains chromatin of apoptotic nuclei more vividly than non-apoptotic nuclei. Apoptotic cells were quantified from 3 random non-overlapping fields per well. Results are expressed as % of apoptotic cells ($100 \times \text{Hoechst-positive cells}/\text{number of cells per field}$).

Statistical Analysis:

Densitometric analysis of the Western blots was conducted using Alpha Innotech Image Analysis software (Cell Biosciences, Santa Clara, CA). For each figure, data from at least three independent experiments were subjected to two-way ANOVA, followed by Bonferroni post-test for the assessment of group differences, and presented as a bar graph depicting the average \pm SEM, using GraphPad Prism software (San Diego, CA).

RESULTS

P4 increased the ratio of mature vs. pro-BDNF released from glia

We previously reported that P4 elicits the release of total BDNF from astroglia. Here we extended these findings to demonstrate that the levels of mature BDNF increased, while the level of pro-BDNF decreased, in the conditioned media of P4-treated C6 astrocyte cultures (Fig. 1A and 1B). To determine whether the effect of P4 on this increased ratio of mature-to-proBDNF was mediated by a novel membrane-associated progesterone receptor, Pgrmc1, we used RNA interference (RNAi)-mediated gene depletion to knock down the expression of Pgrmc1 in C6 cells, as conducted in previously published studies [26]. Western blot of the BDNF-immunoprecipitated conditioned media was used to measure the relative amounts of the forms of BDNF (mature and pro-BDNF). Our data revealed that Pgrmc1 depletion completely prevented the effect of P4 on the ratio of mature vs. pro-BDNF (Fig. 1C and 1D). These results suggest that P4 increases the ratio of mature vs. pro-BDNF released from glia through a Pgrmc1-dependent mechanism.

P4 did not change the mRNA levels of synaptic markers in differentiated SH-SY5Y cells

To test whether P4 directly affects the expression of synaptic markers, we tested its effect on a widely used neuronal model, the all-trans RA-differentiated SH-SY5Y human neuroblastoma cells. We directly added P4 (ranged from 0.1nM to 100nM) into these cells and measured the mRNA levels of GAP43 (Figure 2A) and SYP (Figure 2B) using quantitative real-time PCR. GAP43 is a protein mainly synthesized during axonal outgrowth during neuronal development and regeneration [34], and SYP is a presynaptic marker usually expressed highly during neuronal remodeling [35]. Compared with the DMSO vehicle control, treatments with this wide concentration range of P4 did not show any difference in GAP43 and SYP levels. These data

suggest that P4, when directly added into neuronal cultures, does not affect the synaptic marker expression.

P4-CM triggers synaptic marker expression in primary neurons

Next, we sought to test the hypothesis that P4 affects neuronal function indirectly via a glial-mediated mechanism (i.e., triggering the soluble release factors such as BDNF from glia to act on neighboring neurons). We examined the effects of CMs derived from P4-treated C6 astrocytes (P4-CM) on synaptic marker expression in neurons. We first used mouse neuron-enriched primary hippocampal cultures. To avoid the potential confound of the P4 transferred from the glial CM to the neurons to increase BDNF release, we used a 9-kDa molecular mass cut-off column to collect the neurotrophic factors released (found in the retentate) while allowing the free P4 to be filtered through and discarded. We used the ELISA to confirm that P4 indeed was significantly reduced from the retentate of the filtered CMs (data not shown). The retentate was then reconstituted and applied to the neuronal cultures. Cells exposed to purified recombinant BDNF were used as positive control in all the following experiments, as we compared the effects of glial P4-CM with the purified BDNF. Using double immunofluorescent labeling, we found that glial P4-CM enhanced expression of GAP43 (Figure 3A) and SYP (Figure 3B) in primary hippocampal neurons.

Glial P4-CM increased SYP and GAP43 expression in differentiated SH-SY5Y cells

To further elucidate the underlying mechanisms of P4-CM on induction of synaptic marker expression, we tested its effect on differentiated SH-SY5Y cells. At the end of the 7 days *all-trans* RA differentiation, SH-SY5Y cells form a network of long and smooth neurites (Figure 4, long arrows). P4-CM or BDNF treatments induced an increase in dendritic sprouting, promoting

a complex synaptic connection network in differentiated SH-SY5Y culture. These changes were also observed in the DMSO-CM group, but to a lesser extent, in agreement with our previous findings that glia secretes BDNF independently of exogenous stimulation at a modest rate. Importantly, effects of P4-CM were attenuated by Y1036, a neurotrophin signaling antagonist [36], indicating that the beneficial effect of glial P4-CM on synaptogenesis in SH-SY5Y cells may be mediated by neurotrophic factors. These morphological changes were prominent up to 24 hours after P4-CM exposure.

We also quantified the transcript levels of SYP and GAP43 in the differentiated SH-SY5Y cells by qPCR (Figure 5A). We found that glial P4-CM increased SYP and GAP43 expression by 2- and 4-fold, respectively, in differentiated SH-SY5Y cells. Western blot analysis confirmed that the protein levels of SYP and GAP43 were increased by P4 as well, which was blocked by Y1036 (Figure 5B).

P4-CM up-regulated GAP43 expression in both proximal and distal segments of SH-SY5Y neuritis via BDNF signaling

Because our qPCR and Western blotting results showed that P4-CM increased the overall expression of synaptic markers in differentiated SH-SY5Y cells at the levels of both mRNA and protein, we sought to further determine the effect of P4-CM on synaptic markers by assessing their expression at proximal and distal aspects of the neurites. This would give us an insight into any regional specificity associated with the observed effects. We found that compared with nontreated control, treatments with either BDNF or P4-CM elicited a significant increase of GAP43 fluorescence intensity in both proximal and distal neurite segments (Figures 6 and 7). Again, this effect was attenuated in the presence of Y1036, the nerve growth factor (NGF) and BDNF signaling inhibitor (Figure 6). To specifically examine the involvement of BDNF in this process,

we also tested the effect of TrkB-IgG in a similar experimental setting (Figure 7). TrkB-IgG blocked the up-regulation of GAP43 expression in the neurites of differentiated SH-SY-5Y cells by P4-CM, suggesting that such an effect was indeed mediated by BDNF present in the CMs.

P4-CM up-regulated GAP43 expression in both proximal and distal segments of primary hippocampus neuritis via BDNF signaling

Next, we tested the GAP43 fluorescence intensity in both proximal and distal neurite segments of primary hippocampus neurons. We found that compared with the nontreated control, treatments with BDNF or P4-CM elicited a significant increase of GAP43 fluorescence intensity in both proximal and distal neurite segments, and these effects were attenuated by TrkB-IgG (Figure 8). These data were consistent with our findings in SH-SY5Y cells and further supported involvement of BDNF in mediating the effects of glial P4-CM on neurons.

P4-CM increased neuronal survival against oxidative stress

In addition to assessing the expression of surrogate markers of neuronal function (i.e., synaptogenesis), we also asked whether P4-CM has any effect on neuronal survival. We pretreated the SH-SY5Y cells with P4-CM for 24 hours, then examined the viability of SH-SY5Y cells exposed to 100 μ M H₂O₂ for another 24 hours. We found that pretreatment of SH-SY5Y cells with P4-CM significantly protected against H₂O₂ to a level similar to that elicited by recombinant BDNF (Figure 9). In agreement with our hypothesis that glia secretes basal level BDNF to support neighboring neurons, DMSO-CM also protected the SH-SY5Y cells from H₂O₂, although P4 enhanced this effect further (P4-CM vs. DMSO-CM, $P < .05$). Importantly, Y1036 abolished the effects of either DMSO-CM or P4-CM on the survival of SH-SY5Y cells. These data strongly

implicate the release of neurotrophins (and their subsequent action) as the mediator of P4-CM-induced neuronal survival against oxidative insult.

DISCUSSION

Pgrmc1 is a highly conserved heme-binding protein and belongs to MAPR family [37, 38]. Pgrmc1 is recognized as an important biomarker for cancer progression and as a potential target for anticancer therapies [28, 39]. However, information regarding its role(s) in the brain remains limited. Munton et al., showed that the expression of Pgrmc1 is broadly mapped in the brain at low levels and enriched in the postsynaptic fragment [40]. Bashour and Wray [29] found that P4 decreases calcium oscillations and thereby inhibits neuronal activity through Pgrmc1 on a subpopulation of GnRH neurons in mice. With regard to glia, we discovered that Pgrmc1 is expressed on the cell surface of C6 glial cells (a model of astrocytes) as well as primary astrocytes. Functionally, we determined that P4-induced release of BDNF was mediated via Pgrmc1-dependent ERK5 signaling [26].

BDNF belongs to the family of neurotrophins (along with NGF, Neurotrophin-3, and Neurotrophin-4), which play key roles to support neuronal survival and synaptic plasticity [16, 41]. Among the neurotrophins, there is significant clinical evidence to support the statement that BDNF plays a pivotal role in synaptic plasticity and cognition [17]. Hippocampus-specific deletion of BDNF in adult mice impairs spatial memory [42], and exogenous BDNF rescued deficits in hippocampal long term potentiation in both homozygous and heterozygous BDNF knockout mice [43, 44]. Therefore, one option for developing pharmacotherapy of neurodegenerative diseases is to focus on BDNF modulation.

To date, considerable research has been conducted in understanding the etiology of neurodegenerative diseases from the standpoint of neuronal dysfunction, with a relatively smaller, but growing, the body of literature that implicates glia in the pathogenesis and/or progression of these diseases. We previously reported that P4 not only increases the expression of BDNF in

cerebral cortical explants but that the protective effects of P4 are mediated by neurotrophin signaling [17]. Given the critical roles that BDNF plays during aging and in neurodegenerative diseases such as AD, our data elucidated a novel mechanism for glia to affect neuronal survival and functions via secreting soluble factors such as BDNF and thus may help develop more efficient therapeutic interventions for neurodegenerative diseases.

As mentioned in the Results, the pro- and mature form of neurotrophins can often exert opposite effects on cell viability. As such, we investigated whether the previously described increase in BDNF release was attributed to preferential release of one or both forms of BDNF. Our data revealed that P4 increases the ratio of mature to pro-BDNF within the released pool of BDNF from glia (Figure 1A). Further, this P4-induced increase in the ratio of mature to pro-BDNF was dependent on *Pgrmc1* (Figure 1B).

To address the hypothesis that the neuroprotective effects of P4 may be mediated, at least in part, through astrocyte-derived neurotrophic factors, we assessed surrogate markers of synaptic structure/function and cell viability in neurons exposed to P4-CMs. We found that such CMs not only increase the expression of synaptic markers, such as GAP43 but also protected the cells from a cytotoxic insult. Although there was a trend noted for the effect of P4-CM to induce the transcription of the presynaptic marker, SYP, there was no effect on its protein levels, at least at the time point evaluated in these studies. This difference between changes in pre- vs. postsynaptic markers may be consistent with the report by Miyata et al. [45], which demonstrated an inverse correlation between GAP43 protein expression level vs. presynaptic terminal markers in immature synapses of rat hippocampal neurons [27].

Previous studies have shown that *all-trans* RA treatment of SH-SY5Y cells triggered the expression of functional TrkB (receptor for BDNF) but not TrkA (receptor for NGF) [36]. Because Y1036 is known to bind only to BDNF and NGF (thereby preventing the interaction with their cognate receptor), our data are showing that Y1036 attenuated P4-CM-induced GAP43

expression in differentiated SH-SY5Y cells strongly point to a role of BDNF in mediating this process. Furthermore, we chose to examine specific regions of neurons where markers of synaptic functions/structure were affected by P4-CM. GAP43 has been shown to localize in cellular membranes of axons and growth cones [45]. By focusing on the cellular processes (e.g., neurites), we found that treatments with BDNF (used as the positive control) or P4-CM elicited a significant increase in GAP43 expression in both proximal and distal neurite segments compared with the nontreated control group (Figure 7). To more specifically block the BDNF signaling, we then tested the effect of TrkB-IgG in glial P4-CM-treated neuronal cultures. We examined both the differentiated SH-SY5Y cells as well as the mouse primary hippocampal neurons as 2 complimentary neuron models. In both cell types, P4-CM + control IgG induced significant increases in the GAP43 fluorescence intensity in proximal and distal segments compared with DMSO-CM + control IgG, which was blocked by the TrkB-IgG (Figures 8 and 9). These observations demonstrated that the P4-CM-induced increase in synaptic marker expression occurred at expected and appropriate locations. These data further support our conclusion that the up-regulation of GAP43 expression in neurites was mediated by BDNF available in the CMs.

Finally, we sought to determine whether the effects of P4-CM on markers of neuronal function would translate into actual cytoprotection. In this regard, we found that P4-CM did indeed increase neuron survival challenged with an oxidative insult (Figure 9). Furthermore, the neuroprotection effect of glial P4-CM was abolished by Y1036, again supporting the model that the protective effects of P4 may be mediated by glial-derived neurotrophic factors.

In summary, our data support the critical role of Pgrmc1/BDNF signaling in mediating glia-neuron crosstalk. In addition, Pgrmc1 may play a critical role in mediating complicated crosstalk between all the brain cell types and implicate glial Pgrmc1 as a potential therapeutic target for treating neurodegenerative diseases.

ACKNOWLEDGEMENTS

This work was supported by funds from the American Federation of Aging Research and the American Heart Association (C.S.), National Institutes of Health National Institute of Aging Grants AG022550; and AG027956, the Alzheimer's Association, and the Texas Garvey Foundation (M.S.).

FIGURES

Figure 1. P4 increases the ratio of mature to pro-BDNF released from glia.

Western blotting of the BDNF-immunoprecipitated CMs was used to measure the relative amounts of the forms of BDNF (mature and pro-BDNF) in nontransfected C6 cells (A and B) and scrambled siRNA (siScramble), or siRNA against Pgrmc-1 (siPgrmc-1) transfected C6 cells between groups of DMSO-CM and P4-CM (C and D). P4 increased the ratio of mature to pro-BDNF released from glia cells and siPgrmc1 abolished P4-induced beneficial effect of BDNF releasing. Data are presented as the mean \pm SEM, n = 3 per group; ***, P < .001; ****, P < .0001, DMSO vs P4.

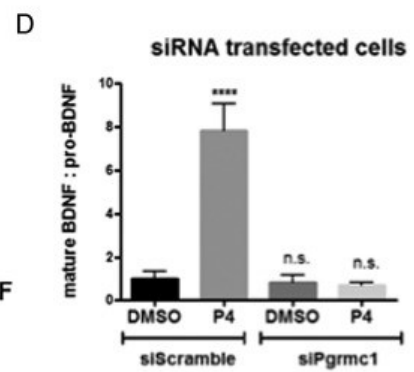
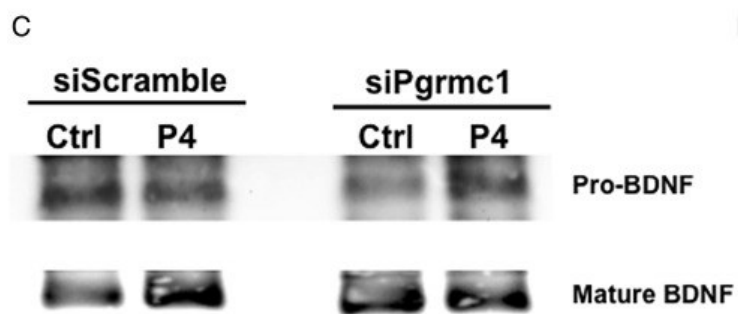
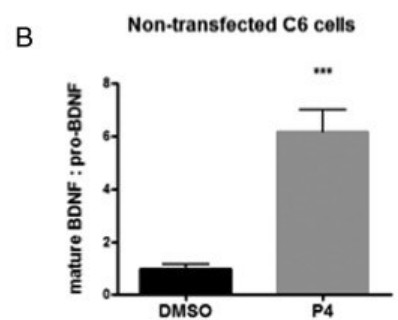
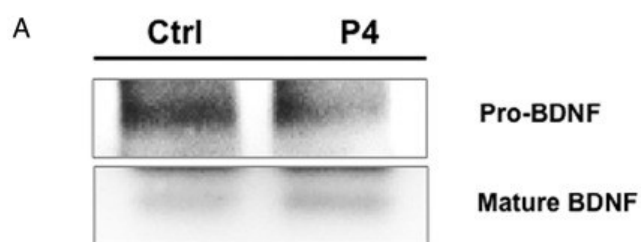


Figure 2. P4 did not affect the mRNA levels of GAP43 and SYP in differentiated SH-SY5Y cells.

P4 (diluted to a final concentration of 0.1nM, 1nM, 10nM, or 100nM in DMSO) was added into differentiated SH-SY5Y cultures for 24 hours. The same dilutions of DMSO were used as the control for each P4 concentration. mRNA levels of GAP43 (A) and SYP (B) were determined by quantitative reverse transcription polymerase chain reaction. Data from the DMSO groups were set at 100%, and data from each corresponding P4 concentration were presented as percentage compared with the DMSO control. There was no statistical difference across all the treatments.

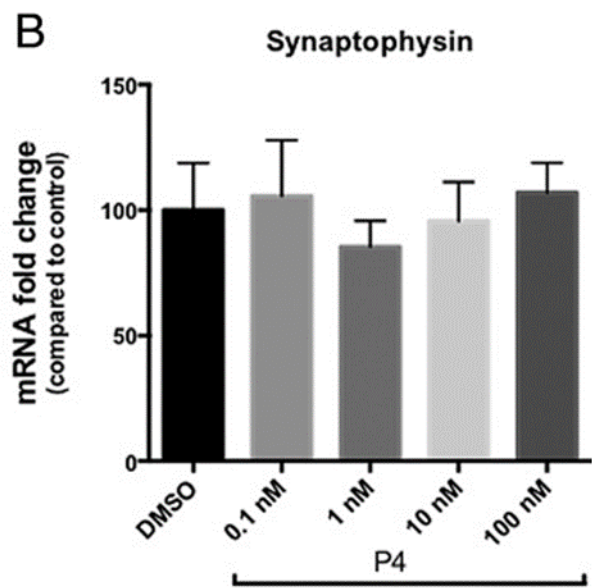
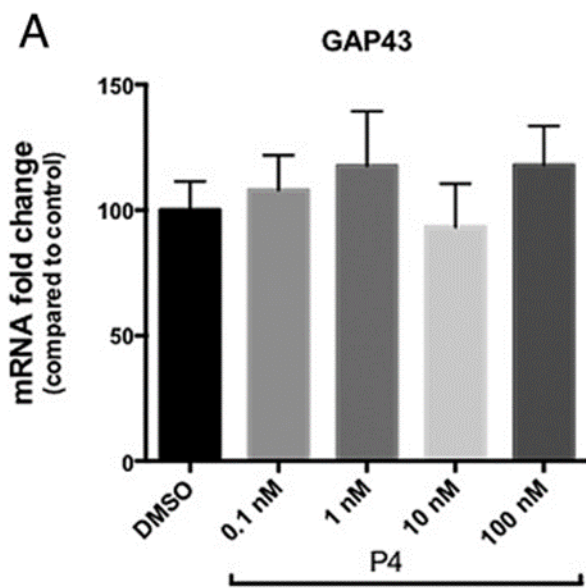


Figure 3. P4-CM triggers synaptic marker expression in mouse hippocampal neurons.

Mouse primary hippocampal neurons were exposed with non-treated control, BDNF, DMSO-CM, or P4-CM for 24 hours at DIV 7. Double-label immunofluorescence staining shows that expression of synaptic markers, (A) GAP43 (green) and (B) SYP (red), were enhanced by glial P4-CM in primary hippocampal neurons. Hoechst dye (blue) was used to counterstain nuclei. Insets show staining without GAP43 or SYP primary antibodies at a higher magnification. Scale bar, 100 μ m.

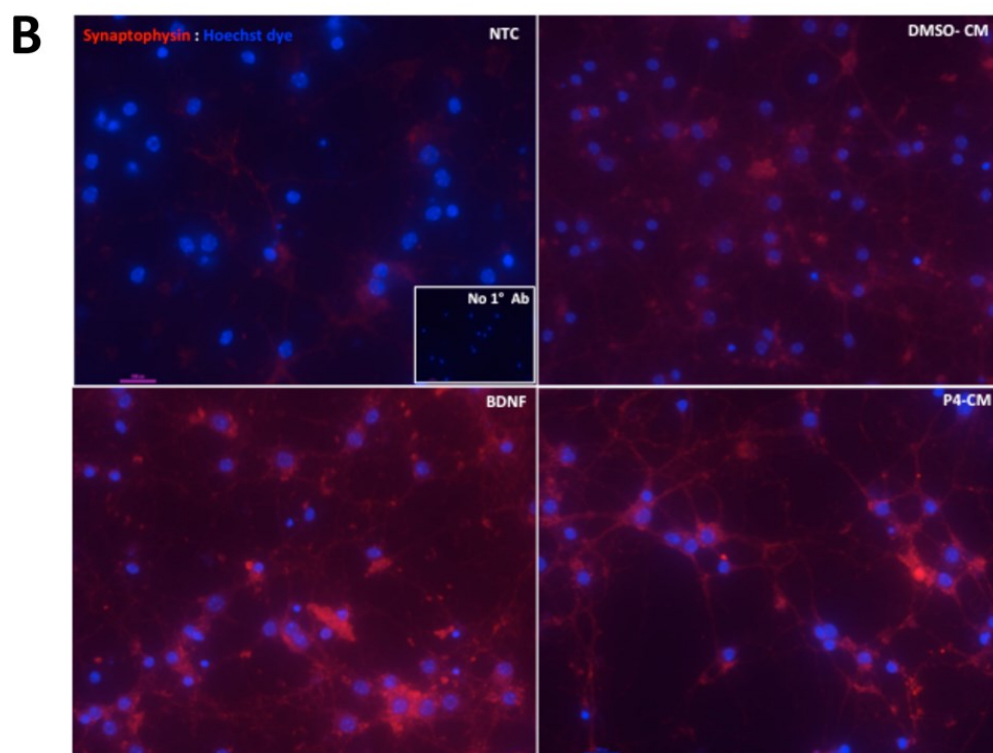
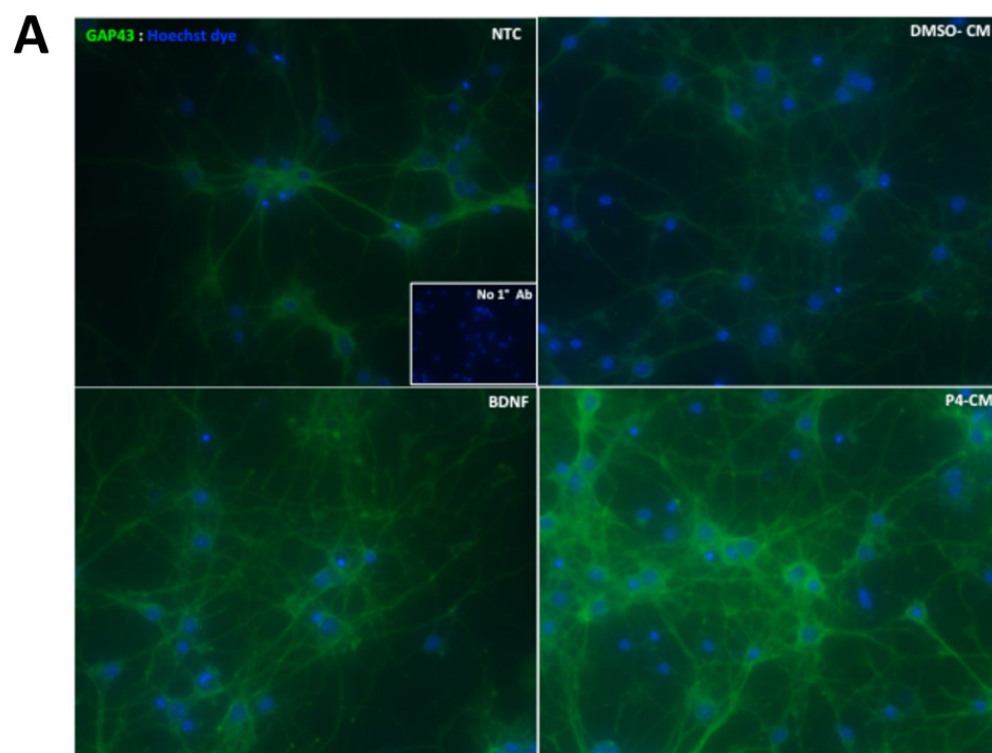


Figure 4. P4-CM induced morphological change in SH-SY5Y cells.

SH-SY5Y human neuroblastoma cells were differentiated with RA for 7 days and formed a network of long and smooth neuritis (long arrows) at 24 hours exposed with nontreated control, BDNF, DMSO-CM, or P4-CM in the presence or absence of the neurotrophin antagonist Y1036. P4-CM or BDNF treatment induced an increase in dendritic sprouting, promoting a complex synaptic connection network in differentiated SH-SY5Y culture. These changes were also observed in the DMSO-CM group but to a lesser extent. The effects of P4-CM on dendritic process formation were attenuated by Y1036. Scale bar, 100 μm .

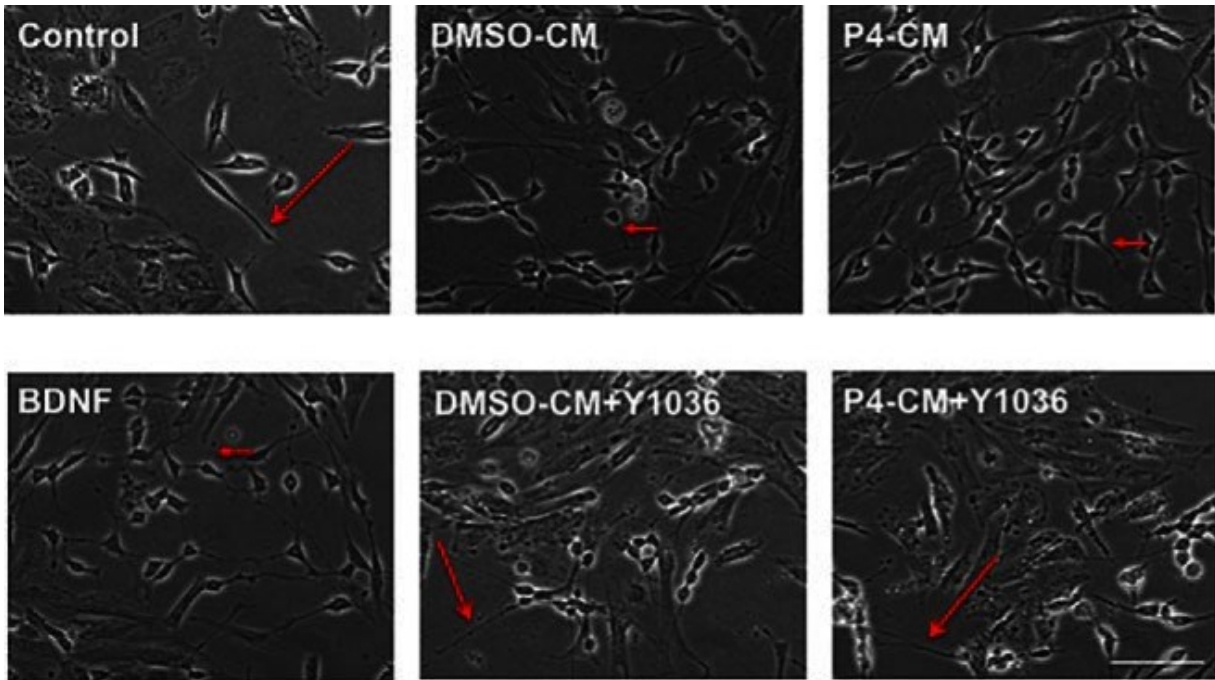


Figure 5. Effect of glial-CM on the expression of synaptic markers.

SH-SY5Y human neuroblastoma cells were differentiated with RA for 7 days and were exposed to BDNF, DMSO-CM, or P4-CM in the presence or absence of Y1036 for 24 hours. Nontreated cultures were used as control. mRNA levels of SYP and GAP43 were determined by qPCR (A), and protein level of Pgrmc1 was determined by Western blotting (B). Representative blots were shown on the left, and the densitometry data were shown on the right. Data are presented as the mean \pm SEM, n = 3 per group. #, P < .05, Y + P4 P4-CM compared with P4-CM; *, P < .05; ***, P < .001; ****, P < .0001, P4-CM compared with DMSO-CM.

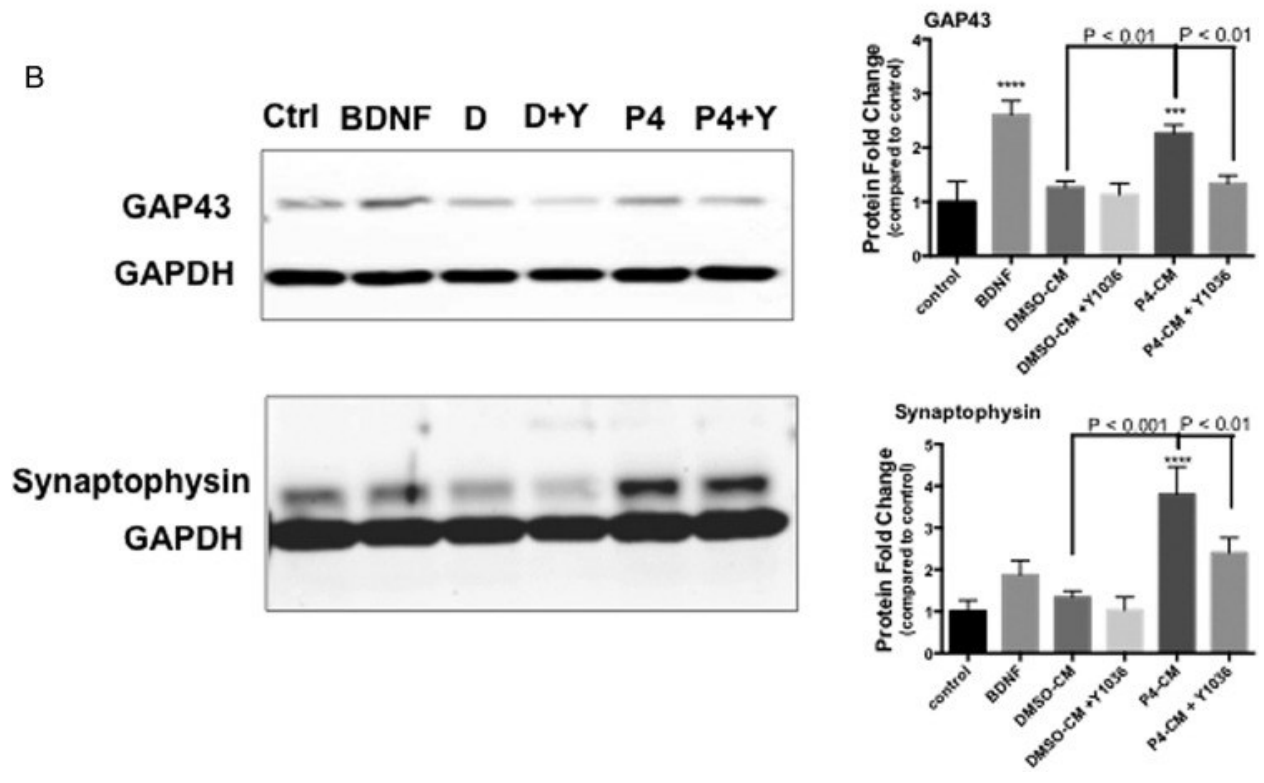
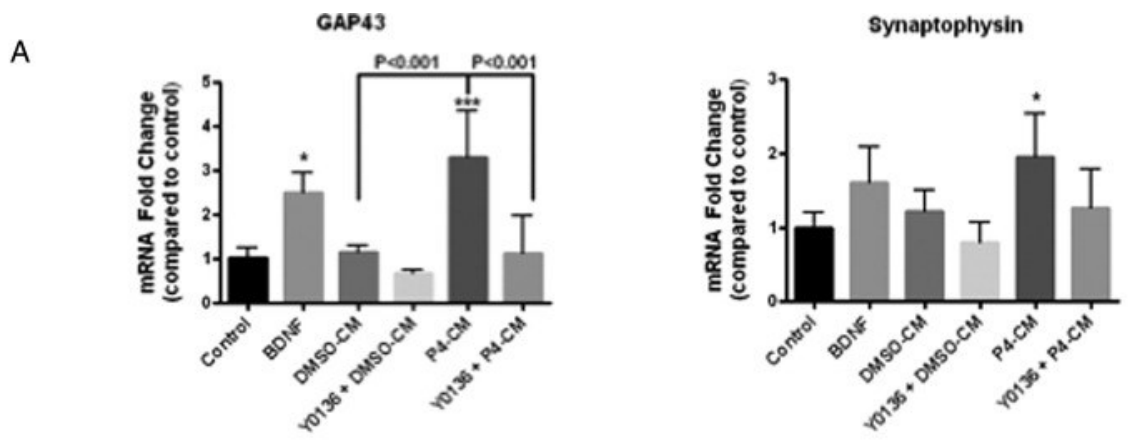


Figure 6. Glial P4-CM increased GAP43 density in both proximal and distal neuritic segments of SH-SY5Y cells.

A, Immunocytochemistry of SH-SY5Y cultures. Cells were treated with DMSO-CM or P4-CM in the presence or absence of Y1036 for 24 hours. 50-ng/mL BDNF was used as positive control. Cultures were stained for GAP43 (green) and DAPI (blue). The white box represents a proximal neuritic segment, and the red box indicates a distal neuritic segment. B, Quantification of GAP43 mean fluorescence intensity in proximal neuritic portions. C, Quantification of GAP43 mean fluorescence intensity in distal neuritic segments. Data are presented as the mean \pm SEM, n = 3 per group; **, P < .01; ***, P < .001, compared with control. Scale bar, 100 μ m.

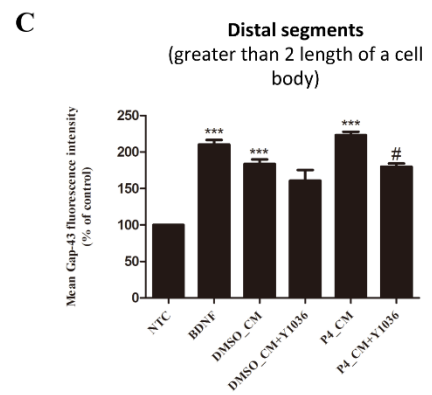
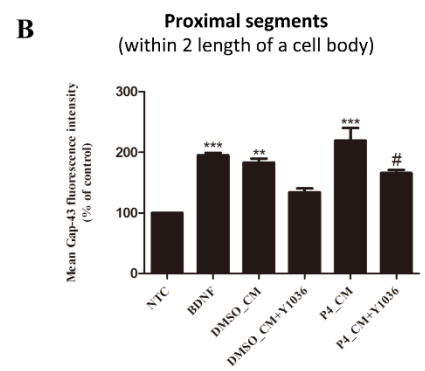
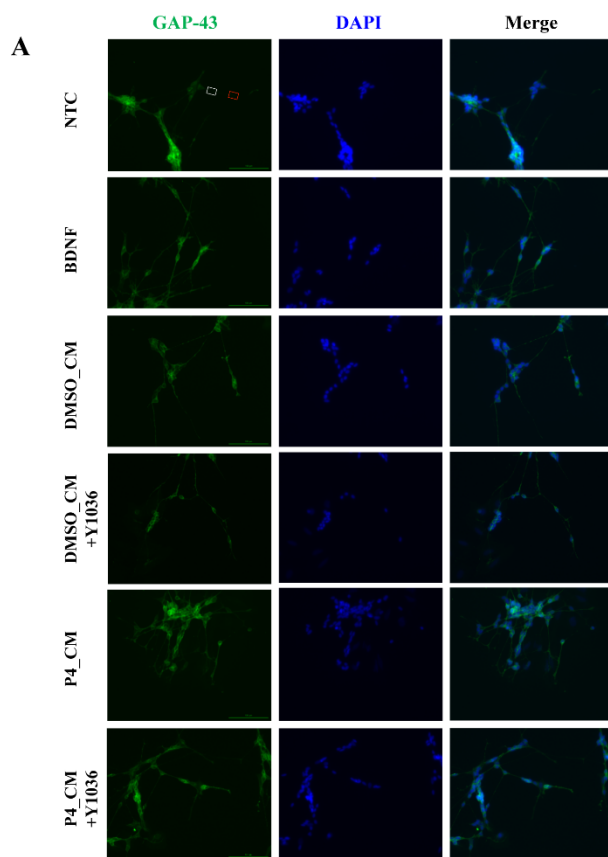


Figure 7. Blocking of BDNF signaling inhibited glial P4-CM-induced GAP43 density in both proximal and distal neuritic segments of SH-SY5Y cells.

A, Immunocytochemistry of SH-SY5Y cultures. Cells were treated with DMSO-CM or P4-CM in the presence of human IgG control or TrkB-IgG for 24 hours. Cells treated with BDNF were used as positive control. Cultures were stained for GAP43 (green) and DAPI (blue). The white box represents a proximal neuritic segment, and the red box indicates a distal neuritic segment. B, Quantification of GAP43 mean fluorescence intensity in proximal neuritic portions. C, Quantification of GAP43 mean fluorescence intensity in distal neuritic segments. Data are presented as the mean \pm SEM, n = 4 per group; **, P < .01; ***, P < .001, compared with control; ##, P < .01; ###, P < .001, compared with DMSO-CM + IgG ctrl; &&&, P < .001, compared with DMSO-CM + TrkB-IgG; \$\$\$, P < .001, compared with P4-CM+TrkB-IgG. Scale bar, 100 μ m.

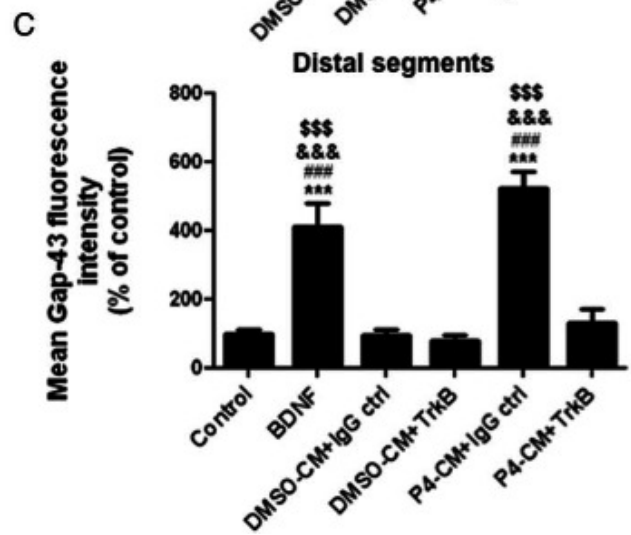
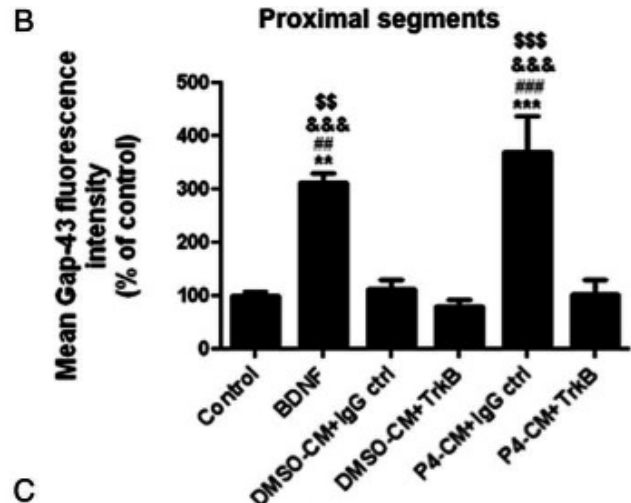
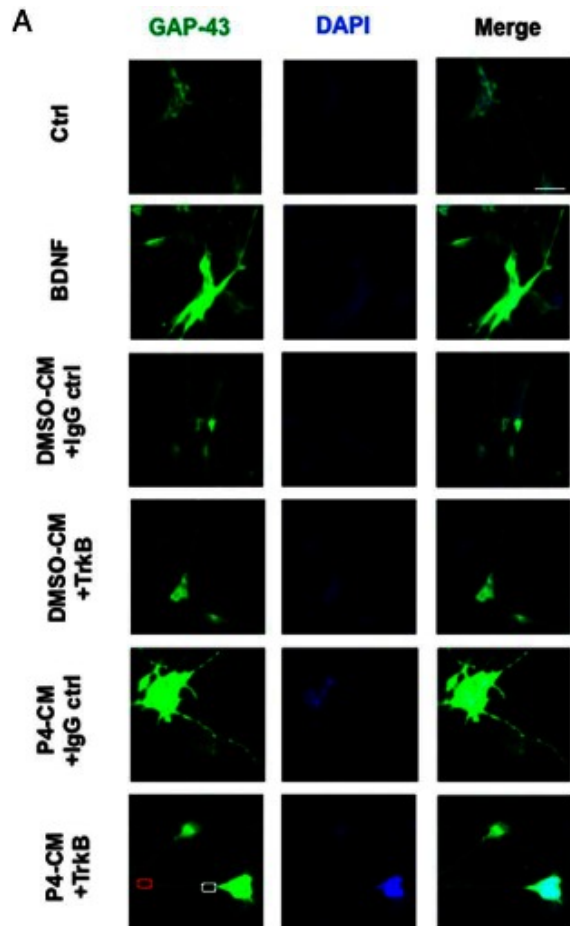


Figure 8. Blocking of BDNF signaling inhibited glial P4-CM-induced GAP43 density in both proximal and distal neuritic segments of primary hippocampus neurons.

A, Immunocytochemistry of primary neuronal cultures. Cells were treated with DMSO-CM or P4-CM in the presence of human IgG control or TrkB-IgG for 24 hours. Cells treated with BDNF were used as positive control. Cultures were stained for GAP43 (green) and DAPI (blue). The white box represents a proximal neuritic segment and the red box indicates a distal neuritic segment.

B, Quantification of GAP43 mean fluorescence intensity in proximal neuritic portions. C, Quantification of GAP43 mean fluorescence intensity in distal neuritic segments. Data are presented as the mean \pm SEM, n = 4 per group; **, P < .01; ***, P < .001, compared with control; #, P < .05; ##, P < .01, compared with DMSO-CM+IgG ctrl; &, P < .05; &&, P < .01, compared with DMSO-CM+TrkB-IgG; \$, P < .05; \$\$, P < .01, compared with P4-CM+TrkB-IgG. Scale bar, 100 μ m.

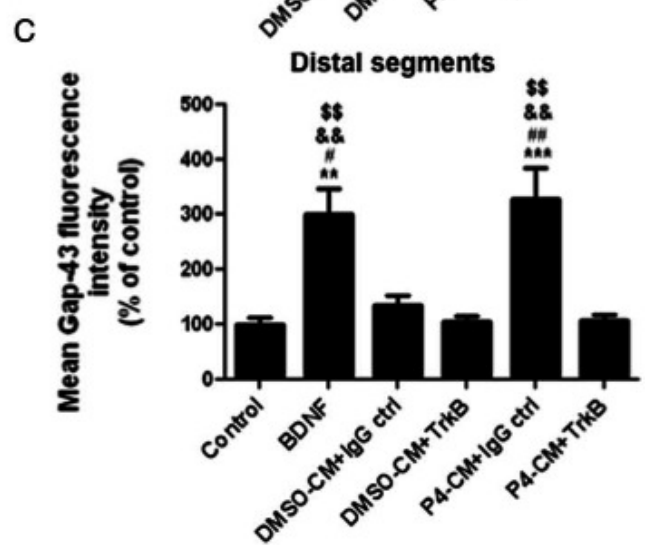
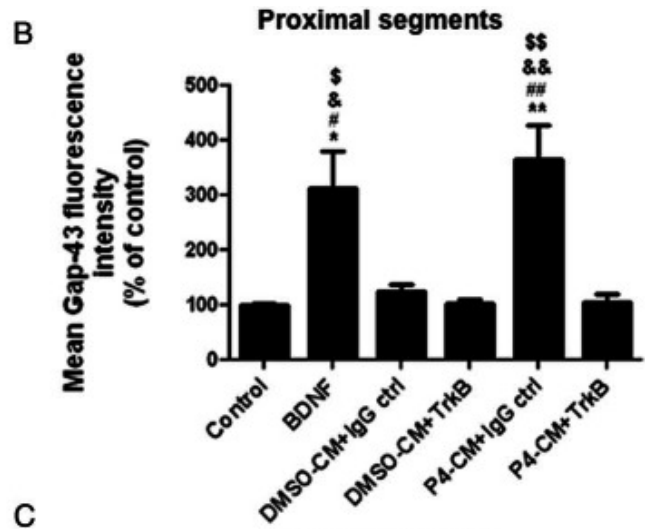
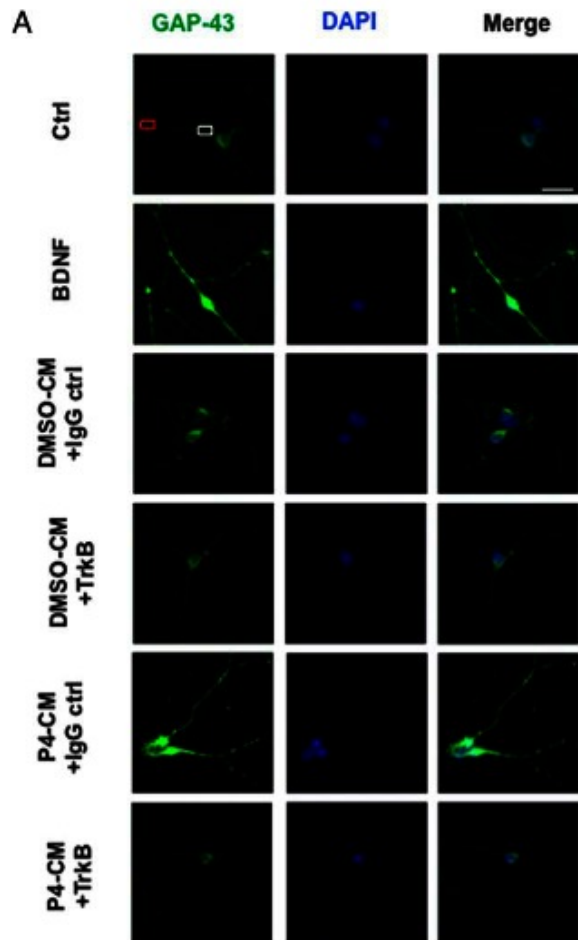
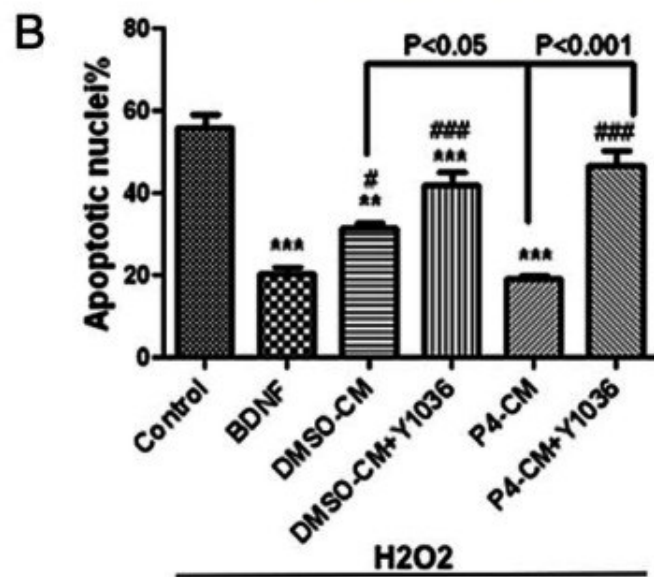
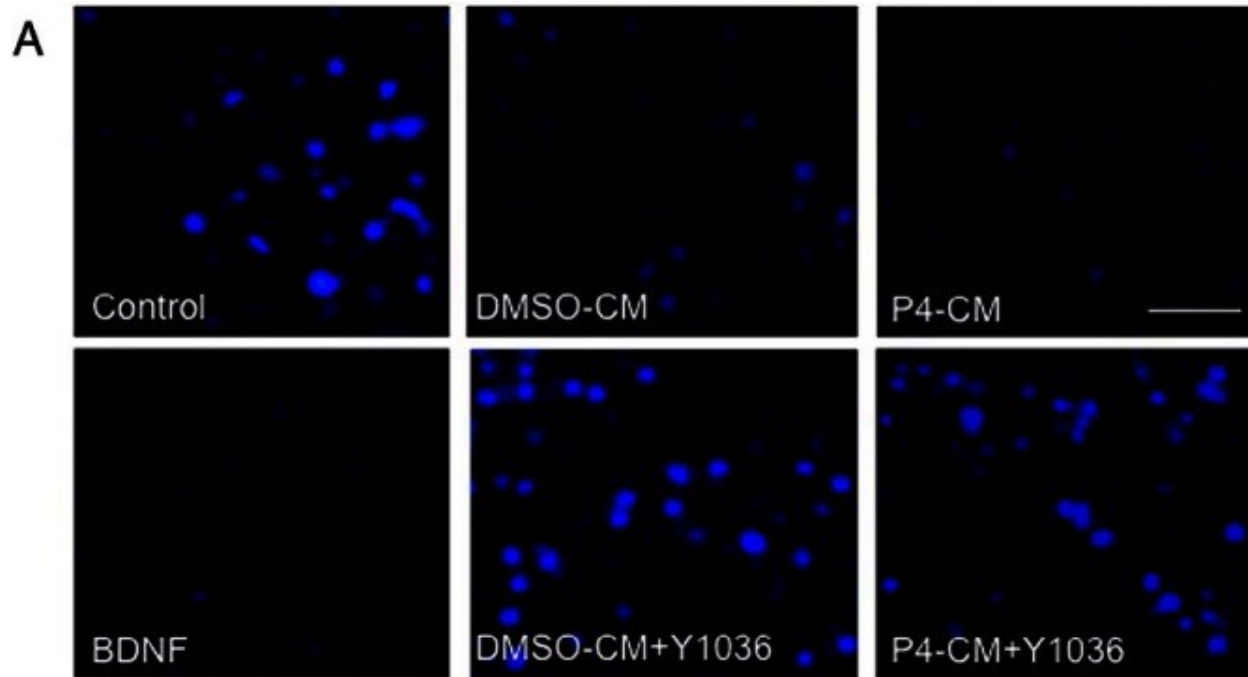


Figure 9. P4-CM increased neuronal survival against oxidative stress.

Differentiated SH-SY5Y cells were exposed to no-treatment (control), BDNF, DMSO-CM, or P4-CM in the presence or absence of Y1036 for 24 hours. All groups were then exposed to 100 μ M H₂O₂ for another 24 hours before the viability of SH-SY5Y cells was examined. Pretreatment of SH-SY5Y cells with P4-CM significantly protected against H₂O₂ to a level similar to that elicited by recombinant BDNF (A and B). Data are presented as the mean \pm SEM, n = 4 per group; **, P < .01; ***, P < .001, compared with control; #, P < .05; ###, P < .001, compared with BDNF. Scale bar, 100 μ m.



REFERENCES

1. Roof, R.L. and E.D. Hall, *Gender differences in acute CNS trauma and stroke: neuroprotective effects of estrogen and progesterone*. J Neurotrauma, 2000. **17**(5): p. 367-88.
2. Atif, F., et al., *Combination treatment with progesterone and vitamin D hormone is more effective than monotherapy in ischemic stroke: the role of BDNF/TrkB/Erk1/2 signaling in neuroprotection*. Neuropharmacology, 2013. **67**: p. 78-87.
3. Liu, A., et al., *Progesterone receptors: a key for neuroprotection in experimental stroke*. Endocrinology, 2012. **153**(8): p. 3747-57.
4. Wali, B., I. Sayeed, and D.G. Stein, *Improved behavioral outcomes after progesterone administration in aged male rats with traumatic brain injury*. Restor Neurol Neurosci, 2011. **29**(1): p. 61-71.
5. Wright, D.W., et al., *ProTECT: a randomized clinical trial of progesterone for acute traumatic brain injury*. Ann Emerg Med, 2007. **49**(4): p. 391-402, 402 e1-2.
6. Vandromme, M., S.M. Melton, and J.D. Kerby, *Progesterone in traumatic brain injury: time to move on to phase III trials*. Crit Care, 2008. **12**(3): p. 153.
7. Xiao, G., et al., *Improved outcomes from the administration of progesterone for patients with acute severe traumatic brain injury: a randomized controlled trial*. Crit Care, 2008. **12**(2): p. R61.
8. Junpeng, M., S. Huang, and S. Qin, *Progesterone for acute traumatic brain injury*. Cochrane Database Syst Rev, 2011(1): p. CD008409.
9. Lewis, M.C., P.T. Orr, and K.M. Frick, *Differential effects of acute progesterone administration on spatial and object memory in middle-aged and aged female C57BL/6 mice*. Horm Behav, 2008. **54**(3): p. 455-62.

10. Frye, C.A. and A.A. Walf, *Progesterone enhances performance of aged mice in cortical or hippocampal tasks*. *Neurosci Lett*, 2008. **437**(2): p. 116-20.
11. Wright, D.W., et al., *Very early administration of progesterone for acute traumatic brain injury*. *N Engl J Med*, 2014. **371**(26): p. 2457-66.
12. Serrano-Pozo, A., et al., *Neuropathological alterations in Alzheimer disease*. *Cold Spring Harb Perspect Med*, 2011. **1**(1): p. a006189.
13. Barha, C.K., et al., *Progesterone treatment normalizes the levels of cell proliferation and cell death in the dentate gyrus of the hippocampus after traumatic brain injury*. *Exp Neurol*, 2011. **231**(1): p. 72-81.
14. Zhao, Y., et al., *Progesterone influences postischemic synaptogenesis in the CA1 region of the hippocampus in rats*. *Synapse*, 2011. **65**(9): p. 880-91.
15. Cohen, S. and M.E. Greenberg, *Communication between the synapse and the nucleus in neuronal development, plasticity, and disease*. *Annu Rev Cell Dev Biol*, 2008. **24**: p. 183-209.
16. Lu, Y., K. Christian, and B. Lu, *BDNF: a key regulator for protein synthesis-dependent LTP and long-term memory?* *Neurobiol Learn Mem*, 2008. **89**(3): p. 312-23.
17. Causing, C.G., et al., *Synaptic innervation density is regulated by neuron-derived BDNF*. *Neuron*, 1997. **18**(2): p. 257-67.
18. Pruginin-Bluger, M., D.L. Shelton, and C. Kalcheim, *A paracrine effect for neuron-derived BDNF in development of dorsal root ganglia: stimulation of Schwann cell myelin protein expression by glial cells*. *Mech Dev*, 1997. **61**(1-2): p. 99-111.
19. Matsumoto, T., et al., *Biosynthesis and processing of endogenous BDNF: CNS neurons store and secrete BDNF, not pro-BDNF*. *Nat Neurosci*, 2008. **11**(2): p. 131-3.
20. Lu, B., P.T. Pang, and N.H. Woo, *The yin and yang of neurotrophin action*. *Nat Rev Neurosci*, 2005. **6**(8): p. 603-14.

21. Minichiello, L., *TrkB signalling pathways in LTP and learning*. Nat Rev Neurosci, 2009. **10**(12): p. 850-60.
22. Yoshii, A. and M. Constantine-Paton, *Postsynaptic BDNF-TrkB signaling in synapse maturation, plasticity, and disease*. Dev Neurobiol, 2010. **70**(5): p. 304-22.
23. Phillips, H.S., et al., *BDNF mRNA is decreased in the hippocampus of individuals with Alzheimer's disease*. Neuron, 1991. **7**(5): p. 695-702.
24. Connor, B., et al., *Brain-derived neurotrophic factor is reduced in Alzheimer's disease*. Brain Res Mol Brain Res, 1997. **49**(1-2): p. 71-81.
25. Hock, C., et al., *Decreased trkA neurotrophin receptor expression in the parietal cortex of patients with Alzheimer's disease*. Neurosci Lett, 1998. **241**(2-3): p. 151-4.
26. Su, C., et al., *Progesterone increases the release of brain-derived neurotrophic factor from glia via progesterone receptor membrane component 1 (Pgrmc1)-dependent ERK5 signaling*. Endocrinology, 2012. **153**(9): p. 4389-400.
27. Peluso, J.J., et al., *Progesterone inhibits apoptosis in part by PGRMC1-regulated gene expression*. Mol Cell Endocrinol, 2010. **320**(1-2): p. 153-61.
28. Intlekofer, K.A. and S.L. Petersen, *Distribution of mRNAs encoding classical progesterin receptor, progesterone membrane components 1 and 2, serpine mRNA binding protein 1, and progesterin and ADIPOQ receptor family members 7 and 8 in rat forebrain*. Neuroscience, 2011. **172**: p. 55-65.
29. Bashour, N.M. and S. Wray, *Progesterone directly and rapidly inhibits GnRH neuronal activity via progesterone receptor membrane component 1*. Endocrinology, 2012. **153**(9): p. 4457-69.
30. Bali, N., et al., *Differential responses of progesterone receptor membrane component-1 (Pgrmc1) and the classical progesterone receptor (Pgr) to 17beta-estradiol and progesterone in hippocampal subregions that support synaptic remodeling and neurogenesis*. Endocrinology, 2012. **153**(2): p. 759-69.

31. Guennoun, R., et al., *The membrane-associated progesterone-binding protein 25-Dx: expression, cellular localization and up-regulation after brain and spinal cord injuries*. Brain Res Rev, 2008. **57**(2): p. 493-505.
32. Sarkar, S.N., et al., *Estrogens directly potentiate neuronal L-type Ca²⁺ channels*. Proc Natl Acad Sci U S A, 2008. **105**(39): p. 15148-53.
33. Singh, M., et al., *Estrogen-induced activation of mitogen-activated protein kinase in cerebral cortical explants: convergence of estrogen and neurotrophin signaling pathways*. J Neurosci, 1999. **19**(4): p. 1179-88.
34. Stroemer, R.P., T.A. Kent, and C.E. Hulsebosch, *Increase in synaptophysin immunoreactivity following cortical infarction*. Neurosci Lett, 1992. **147**(1): p. 21-4.
35. Chamniansawat, S. and S. Chongthammakun, *Estrogen stimulates activity-regulated cytoskeleton associated protein (Arc) expression via the MAPK- and PI-3K-dependent pathways in SH-SY5Y cells*. Neurosci Lett, 2009. **452**(2): p. 130-5.
36. Encinas, M., et al., *Extracellular-regulated kinases and phosphatidylinositol 3-kinase are involved in brain-derived neurotrophic factor-mediated survival and neuritogenesis of the neuroblastoma cell line SH-SY5Y*. J Neurochem, 1999. **73**(4): p. 1409-21.
37. Cahill, M.A., *Progesterone receptor membrane component 1: an integrative review*. J Steroid Biochem Mol Biol, 2007. **105**(1-5): p. 16-36.
38. Rohe, H.J., et al., *PGRMC1 (progesterone receptor membrane component 1): a targetable protein with multiple functions in steroid signaling, P450 activation and drug binding*. Pharmacol Ther, 2009. **121**(1): p. 14-9.
39. Ahmed, I.S., et al., *Progesterone receptor membrane component 1 (Pgrmc1): a heme-1 domain protein that promotes tumorigenesis and is inhibited by a small molecule*. J Pharmacol Exp Ther, 2010. **333**(2): p. 564-73.

40. Munton, R.P., et al., *Qualitative and quantitative analyses of protein phosphorylation in naive and stimulated mouse synaptosomal preparations*. Mol Cell Proteomics, 2007. **6**(2): p. 283-93.
41. Murer, M.G., Q. Yan, and R. Raisman-Vozari, *Brain-derived neurotrophic factor in the control human brain, and in Alzheimer's disease and Parkinson's disease*. Prog Neurobiol, 2001. **63**(1): p. 71-124.
42. Heldt, S.A., et al., *Hippocampus-specific deletion of BDNF in adult mice impairs spatial memory and extinction of aversive memories*. Mol Psychiatry, 2007. **12**(7): p. 656-70.
43. Diamond, D.M., et al., *Competitive interactions between endogenous LTD and LTP in the hippocampus underlie the storage of emotional memories and stress-induced amnesia*. Hippocampus, 2005. **15**(8): p. 1006-25.
44. Patterson, S.L., et al., *Recombinant BDNF rescues deficits in basal synaptic transmission and hippocampal LTP in BDNF knockout mice*. Neuron, 1996. **16**(6): p. 1137-45.
45. Fumagalli, F., G. Racagni, and M.A. Riva, *The expanding role of BDNF: a therapeutic target for Alzheimer's disease?* Pharmacogenomics J, 2006. **6**(1): p. 8-15.
46. Morita, S. and S. Miyata, *Synaptic localization of growth-associated protein 43 in cultured hippocampal neurons during synaptogenesis*. Cell Biochem Funct, 2013. **31**(5): p. 400-11.

CHAPTER V
ADDITIONAL DATA

Figure 1. Oxygen-glucose deprivation (OGD) induces expression of let-7i in primary cortical astrocytes.

Primary cortical astrocytes were exposed to 1 hour of OGD. RNA extraction was performed at 3,6,12 and 24 hours after reperfusion and expression of let-7i was examined using the qRT-PCR method. Let-7i miRNA levels were normalized to the normoxia group. The results are representative of 4 independent experiments. Statistical significance was determined using an analysis of variance followed by Dunn's post hoc analysis (n.s: not significant, **P<0.01, *P<0.05)

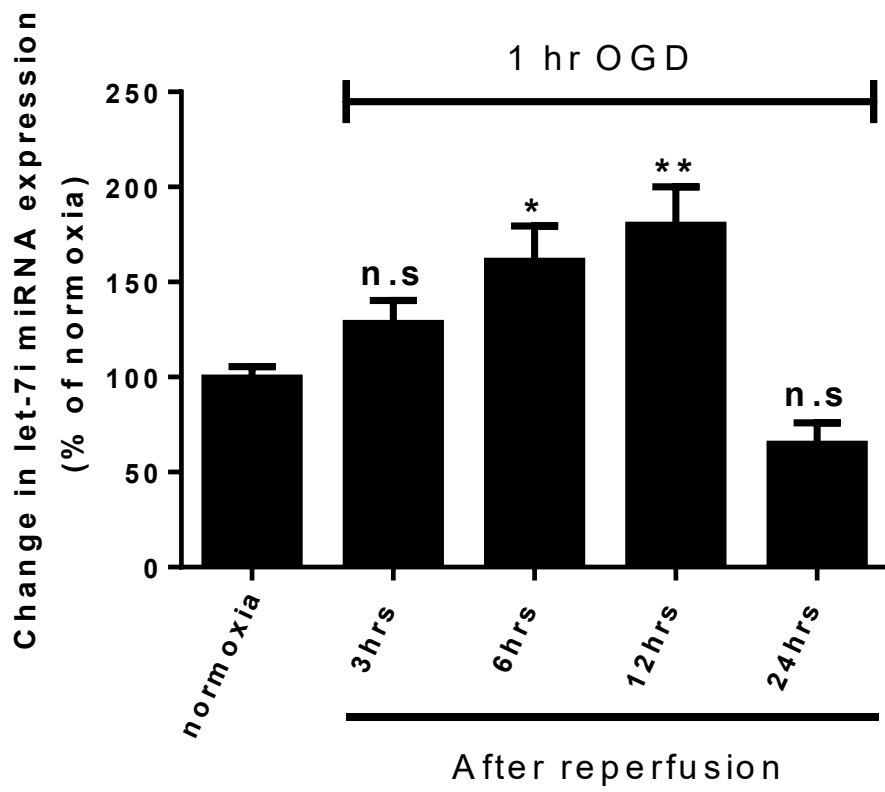


Figure 2. Oxygen-glucose deprivation (OGD) suppresses the P4-induced BDNF release from primary cortical astrocytes.

Primary cortical astrocytes were exposed to 1 hour of OGD. 24 hours after OGD, cultures were treated with 0.01% DMSO to serve as control, and a parallel group received 10nM P4 treatment. 24 hours afterward, BDNF release from these cells were measured using the BDNF in-situ ELISA assay. The results are representative of 4 independent experiments. Statistical significance was determined using an unpaired t-test (**P<0.01)

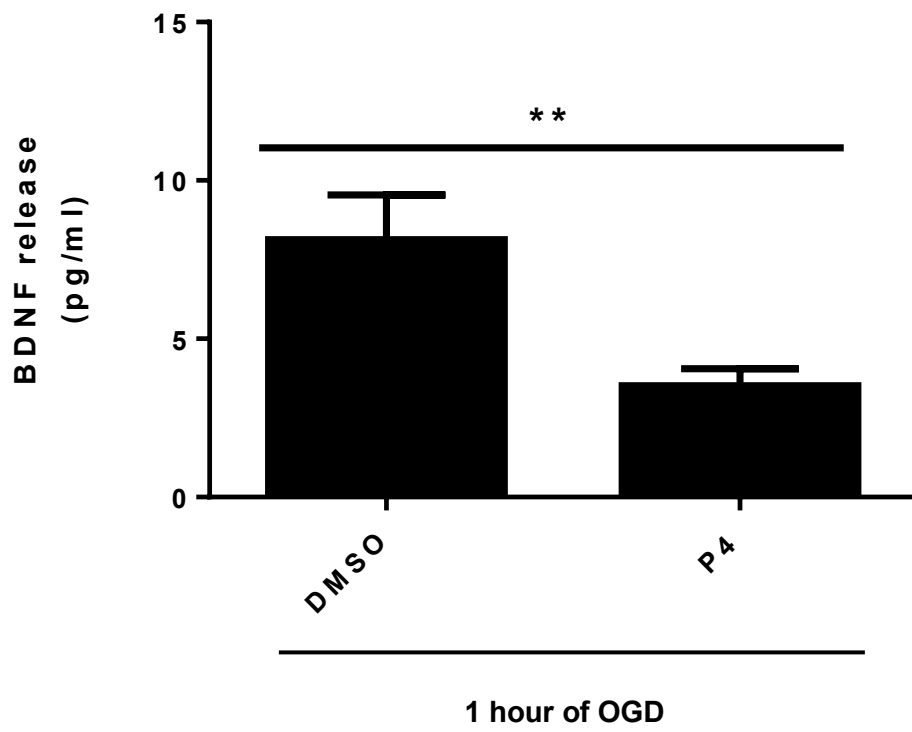


Figure 3. Optimization of let-7i mimic transfection duration in primary cortical astrocytes

In order to determine an optimal transfection duration with minimal toxicity , primary cortical astrocytes were transfected with let-7i mimic for 24, 36, 48 and 72 hours.. At the end of transfection, proteins were isolated and western blotting was done to probe for Pgrmc1.

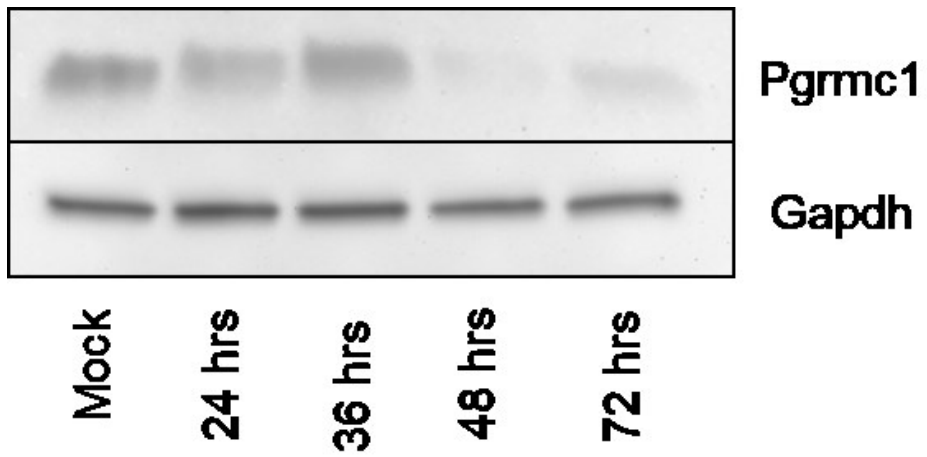


Figure 4. Progesterone (P4) levels in ovariectomized (OVX) mice, with and without P4 pellet implantation.

Young adult female mice (14 weeks old) were ovariectomized. Two weeks after OVX, one group received subcutaneous implantation of cholesterol pellet (OVX + cholesterol) to serve as control, and a parallel group received P4 pellet implantation (OVX + P4). One week afterward, P4 levels in these mice were measured using the P4 ELISA method (10 mice/group).

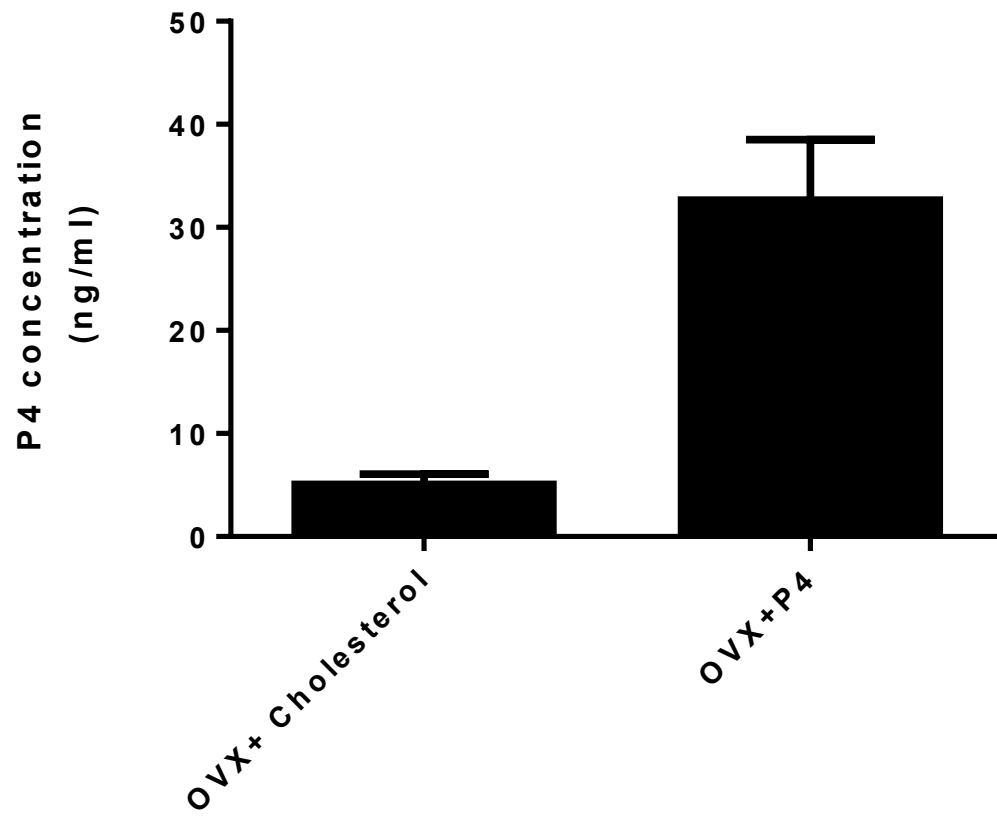
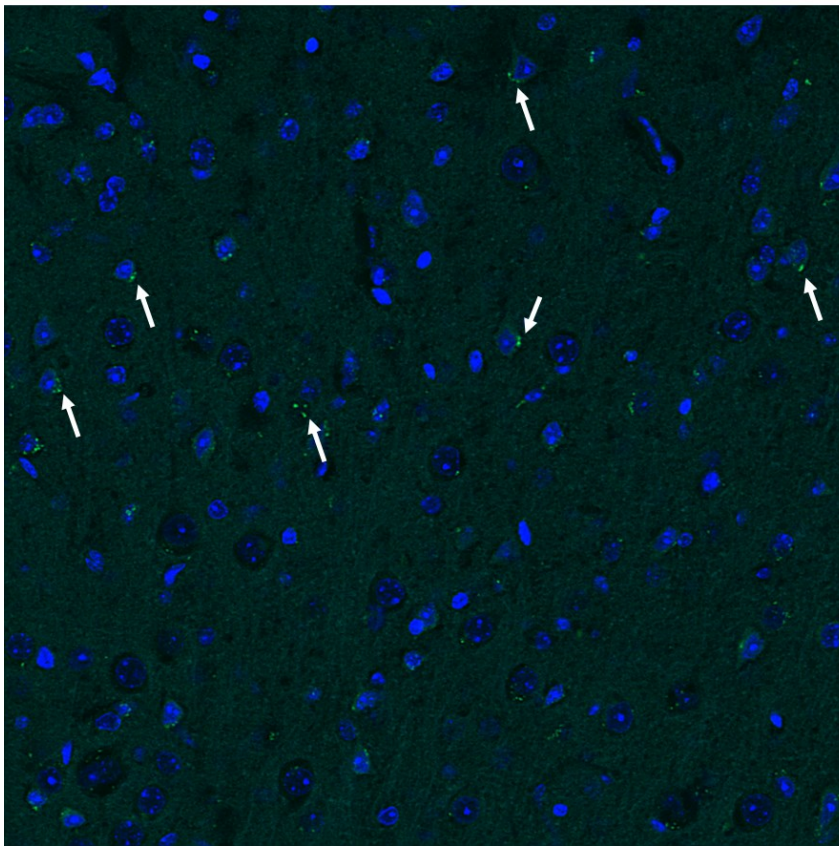


Figure 5. The distribution of let-7i antagomir via the intracerebroventricular injection (ICV)

To assess whether ICV is effective in delivering the antagomir to the ischemic lesion, FITC-tagged antagomir (green fluorescent, see white arrow) was visualized using immunofluorescence method. Images were captured using confocal microscopy with a 40x objective.

Let-7i inhibitor / DAPI



IC: Ischemic core

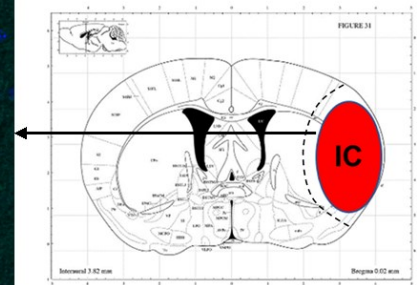


Figure 6. TTC (2,3,5-triphenyltetrazolium chloride) staining of an ischemic brain. White area indicates the ischemic core (IC), dotted area indicates the peri-infarct region (P) and (*) defines the remote region.

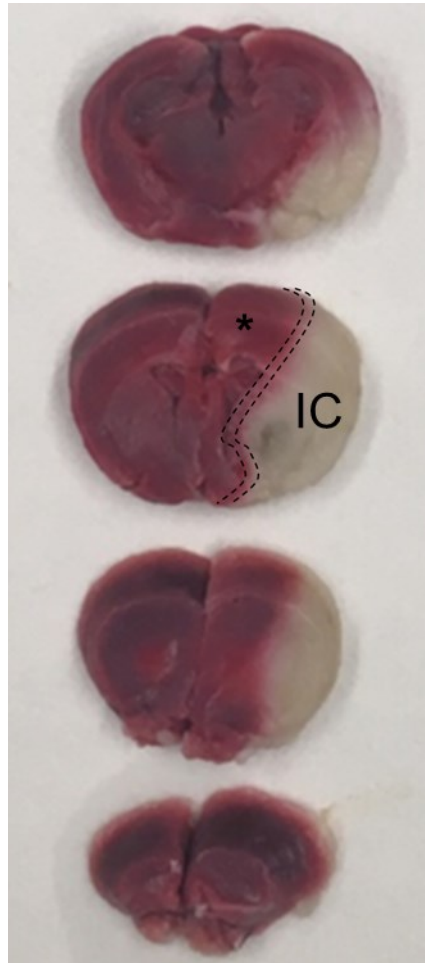
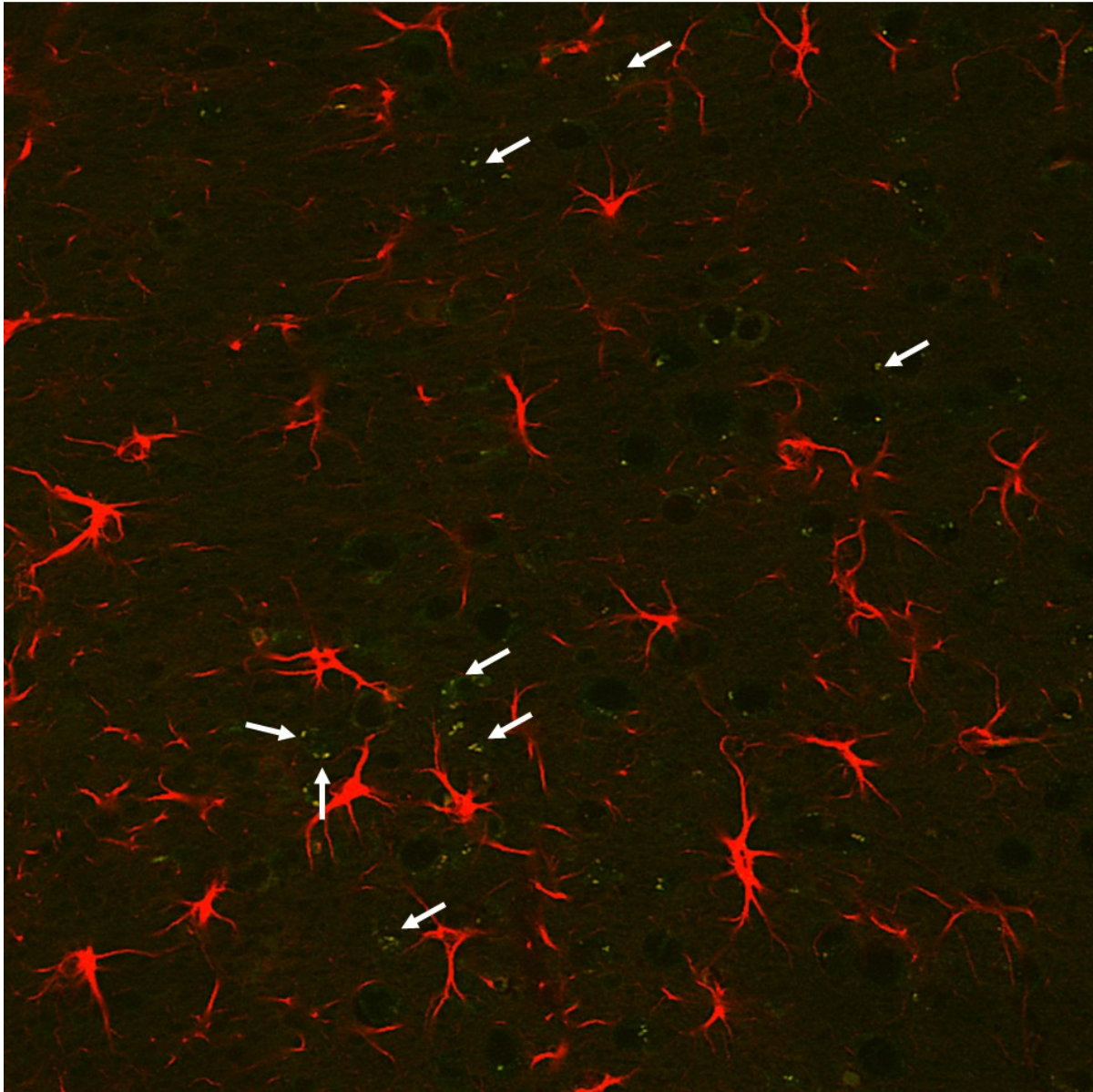


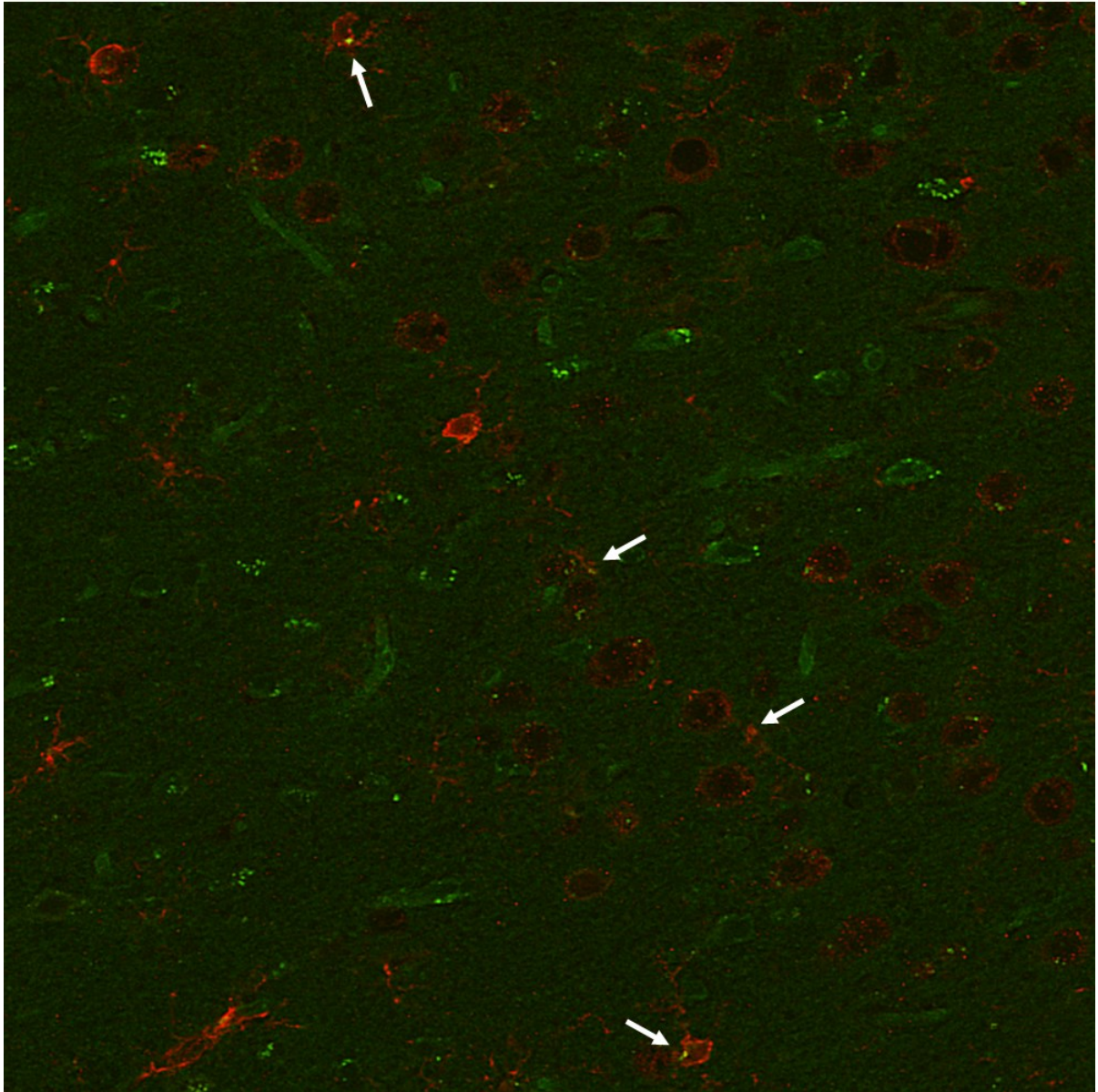
Figure 7. The colocalization (see white arrows) of FITC-tagged let-7i antagomir (green fluorescent) with markers of different cell types in the ischemic brain.

To determine what cell types uptake the let-7i inhibition, immunofluorescence was performed to probe for GFAP (marker for astrocytes), NeuN (marker for neurons) and Iba1 (marker for microglia). Images were taken using a confocal microscope with a 40X objective. White arrows indicate colocalization.

Let-7i inhibitor / GFAP



Let-7i inhibitor / Iba1



Let-7i inhibitor / NeuN

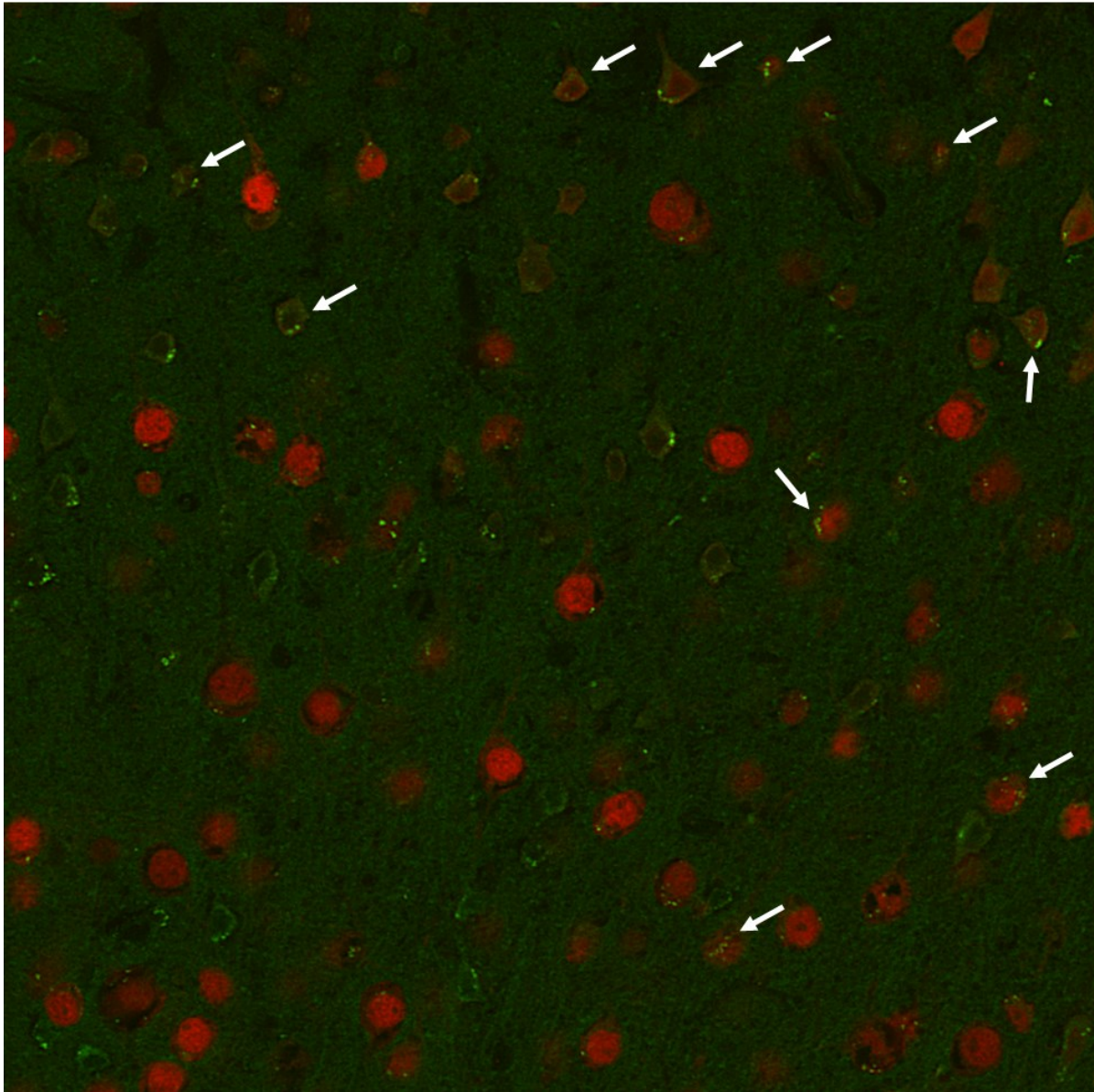


Figure 8. The homology of let-7i mature sequence in mouse vs. human

mmu-let-7i	UGAGGUAGUAGUUUGUGCUGUU
hsa-let-7i	UGAGGUAGUAGUUUGUGCUGUU

Figure 9. Both human BDNF and Pgrmc1 mRNAs have potential binding sites for let-7i

```
3' uugucguguuuGAU-GAUGGAGu 5' hsa-let-7i
      :|| ||| |||
427:5' ugauuucuguuUUAUCUACCUCu 3' PGRMC1
```

```
3' uugucguGUUUGAUGAUGGAGu 5' hsa-let-7i
      :| : | :||| |||
1134:5' uguguuuUAUGAUUUUACCUCa 3' PGRMC1
```

```
3' uuGUCGUGUUUGA-UGAUGGAGu 5' hsa-let-7i
      |||: || | || | ||| |||
2199:5' caCAGUACCAUCUGAAUACCUCu 3' BDNF
```

CHAPTER VI

SUMMARY AND FUTURE DIRECTION

SUMMARY

The main goal of my dissertation was to elucidate the role of let-7i in the neuroprotective effects of P4 in the ischemic brain. Taken as a whole, my data suggest that let-7i is a negative regulator of the Pgrmc1/BDNF axis in glia, and results in the suppression of P4-induced BDNF release from glia. This not only led to the attenuation of P4-induced neuroprotection but also a diminished capacity of P4 to induce the expression of such markers of synaptogenesis as synaptophysin.

The data presented in the preceding chapters also support the indispensable role of glia in the neuroprotective program of P4. Of note, in studies investigating the neuroprotective effects of P4 in experimental models of stroke, a heavy emphasis has been placed on the direct effect of P4 on neurons. The notion that glia may be an equally important target underlying P4's protective effects on the brain has only been studied minimally. However, evidence from emerging literature as well as from our own recent studies has highlighted the critical role of glia, both as a site of local P4 synthesis and as a mediator of P4's pro-survival functions in CNS (1-3). In addition, astrocytes have been considered as an important component in the post-ischemic recovery, as these cells are critical for regeneration and remodeling of neural circuits following stroke (4). More direct support of our hypothesis of a critical role of glia is based on the observation that P4 protects cerebral cortical organotypic explants (containing both glia and neurons) against oxidative cell death (5), while P4 did not induce as robust protection in neuron-enriched primary cultures (unpublished data), which strongly suggests that glia is required for P4's neuroprotective program.

Through the studies conducted and presented in this dissertation, we have added to our understanding of the role astrocytes play as cellular mediators of P4's protective effects. This information is useful and important because only through a detailed understanding of how neuroprotective cues, such as P4, influence both neurons and glia, and how each key component in the downstream signaling cascade is regulated, will the development of effective mechanism-based therapeutics for stroke become available.

These data also highlight the necessary role of glial BDNF, more specifically the mature form, in mediating the P4-initiated intercellular relationship between astrocytes and neurons for neuroprotection and synaptogenesis. A deficit in BDNF has been linked to stroke pathophysiology (6, 7). In the central nervous system (CNS), BDNF also has an established role in promoting neuronal differentiation, survival, synaptic plasticity (8-10) and synaptogenesis (11-13). Of note, synaptogenesis occurring in the peri-infarct region is known to strongly contribute to enhanced functional recovery from stroke. We have reported that P4 can influence the action of BDNF via two distinct mechanisms; one of which is its regulation of BDNF expression, both mRNA and protein, via a genomic mechanism (i.e., PR action) (14); another and more novel mechanism is its regulation of BDNF release via *Pgrmc1* (15), a non-genomic pathway. Our results show that conditioned medium derived from P4-treated astrocytes increases the expression of synaptic markers and enhances neuronal survival against OGD, and blocking of BDNF signaling using TrkB IgG (a selective inhibitor of BDNF's cognate receptor) attenuates these effects. Thus, we interpreted that these beneficial effects were attributed to P4 eliciting its effects through a mechanism that involved *Pgrmc1*-dependent BDNF release from glia.

Given the key role that *Pgrmc1* plays in P4's mechanism of action, a more detailed understanding regarding the regulation of *Pgrmc1* in the brain and the consequence of such regulation is critically important. To this end, our data suggest that the miRNA, *let-7i*, serves as a negative regulator *Pgrmc1* and BDNF in glia, leading to suppression of P4-induced BDNF release

from glia and attenuation of P4's beneficial effects on neuroprotection and synaptogenesis. These studies represent the very first to show how *Pgrmc1* is regulated in glia. Interestingly, OGD, an *in vitro* model of ischemia, also induces expression of *let-7i* in glia (Chapter 5, figure 1) and suppresses P4-induced BDNF release from these cells (Chapter 5, figure 2). Collectively, we infer that the suppression of P4-induced BDNF release is attributed to the elevated expression of *let-7i* in these cells. Intriguingly, we also observed an upregulation of *let-7i* in ischemic brain, which is associated with a reduction in *Pgrmc1* and mature BDNF expression. While P4 alone was minimally effective in our mouse model of stroke, inhibition of *let-7i* greatly facilitated the effect of P4 through restoration of *Pgrmc1* expression and increase in mature BDNF expression. In fact, this combined treatment (*let-7i* inhibition + P4) significantly reduced ischemic injury and led to enhanced synaptogenesis and complete functional recovery following stroke. Taken together, we infer that the reduced expression of *Pgrmc1* and BDNF in the ischemic brain may be attributed to increased *let7i* levels., and that these molecular changes associated with ischemia reduce the protective efficacy of P4. As such, these data support the potential utility of targeting and downregulating *let-7i* as a viable method to enhance P4's protective actions in the ischemic brain. Moreover, dampening the up-regulation of *let-7i* may have the potential to extend the "window of opportunity" for stroke therapy (discussed further below). These data have helped us gain a detailed understanding of how *Let7i* regulates *Pgrmc1* and BDNF expression in glia and how this regulatory loop is altered in the ischemic brain. They also provide a strong scientific framework/foundation for the identification and development of a novel, miRNA-targeting approach for the treatment of ischemic stroke which could also impact the effectiveness of hormone-based therapeutic approaches. The latter may have particular significance to the future of hormone therapy in postmenopausal women as it may reveal an important predictor of the beneficial effects of P4 in the CNS.

Despite the promising experimental and preclinical data, a recent phase III clinical trial (ProTECT III) assessing the efficacy of P4 treatment for acute TBI showed rather disappointing results with no favorable effects noted (16). Since some studies have reported an elevated expression of let-7i in traumatic brain injury (TBI) models (17, 18), we suggest that the data from my dissertation project may help to explain this lack of efficacy in that following TBI, upregulation of let-7i may downregulate the Pgrmc1/BDNF signaling, thus dampening the protective function of P4.

As discussed in chapter 1, we have confirmed that let-7i sequence is conserved from mouse to human (Chapter 5, figure 8), and both human Pgrmc1 and BDNF genes are potential targets of let-7i (Chapter 5, figure 9). In addition, our unpublished data also suggest that let-7i is a negative regulator of Pgrmc1 in human cell lines. Taken together, these findings support the translatability of our intervention into humans.

We recognize that the data presented in chapters 3 – 5, though significant, lead to many additional questions that need to be addressed in order to translate our findings into a clinically relevant treatment for ischemic stroke. One potential direction would include a discovery-driven approach to elucidating other potential targets/pathways of let-7i that are relevant to P4's action (using a transcriptome-wide approach like the Ago-HITS CLIP). In addition, our data suggest that inhibition of let-7i could also expand the therapeutic window. These preclinical studies will serve as the foundation for developing a humanized version of the intervention, taking into consideration not only the method by which the antagomir is delivered, but also for whom such an intervention is most likely to be effective.

FUTURE DIRECTIONS

THERAPEUTIC WINDOW

To date, the only FDA approved drug for ischemic stroke treatment is recombinant tissue-type plasminogen activator (19). tPA has a very narrow therapeutic window of 3 - 4.5 h after stroke onset (20). This limited therapeutic window translates to the finding that only a small percentage of patients (3-8% of all ischemic cases) benefit from such an intervention (20). This underscores the need to develop an intervention with wider therapeutic window to benefit a larger population, or alternatively, the need to develop an adjuvant therapy that expands the therapeutic window for existing drugs for stroke. In this dissertation project, we administered let-7i inhibitor 30 minutes after stroke onset. This time point was chosen initially to assess the efficacy of the intervention. Now that the effects on neuroprotection and functional recovery are established, the next necessary study is to determine therapeutic window offered by this intervention. We speculate that dampening the ischemia associated upregulation of let-7i may prevent early detrimental changes (i.e., key receptor system/ mediators) that are relevant to P4's action, therefore creating an ideal environment for P4 to maximize its effect and leading to a wider therapeutic window.

ALTERNATIVE DELIVERY APPROACHES

We used ICV as a method to deliver let-7i inhibitor into the brain to avoid potential peripheral effects. This method of delivery is widely used in preclinical studies and does not seem to lead to any complications (21-23). However, in humans, this method of delivery imposes several serious complications including hemorrhage, malpositioning, post-operative infection, chemical arachnoiditis and leukoencephalopathy (24). As such, there is a need to develop a better approach to efficiently bypassing the blood-brain barrier (BBB) to delivery drug centrally, and the approach also needs to be less invasive and less risky to patients. One promising approach is a

systemic injection of RVG (rabies viral glycoprotein – a central nervous system-specific peptide)-fused exosomes. This has been shown to efficiently deliver siRNA to a mouse brain without peripheral effects (25). Another method to consider is using the RVG-glycoprotein-disulfide-linked PEI (polyethyleneimine) as the packaging of miRNA antagomir. It has been shown that systemic injection of this nanocarrier effectively and safely delivers miRNA to a mouse brain (26). The use of the RVG-mediated targeting of antagomir containing exosomes is currently being investigated by members of the Singh lab. Another alternative approach is the intranasal delivery, which can bypass the BBB and deliver drug centrally due to the direct transport into the cerebrospinal fluid (CSF) compartment along the olfactory pathway (27).

POTENTIAL EFFECTS IN OTHER CNS CELL TYPES

Another important direction that this research needs to go is to determine the role of let-7i in P4's direct function in neurons as we have now elucidated in glia. Our immunofluorescence data revealed that let-7i inhibitors were taken up by neurons and astrocytes. While we have determined that let-7i interferes with P4's protective function by regulating expression of Pgrmc1 and BDNF in astrocytes, whether it has a similar role in neurons is not known and needs to be explored further. This will inform us as to whether the observed effect of let-7i inhibition in enhancing P4's protective function is solely due to the involvement of glia, or it may be attributed to mechanisms in neurons as well. Such information is extremely useful because only through a better understanding of the factors that influence the expression of key mediators (e.g., receptors) of P4, we will be able to maximize the effectiveness of P4.

MECHANISM UNDERLIES THE CONVERSION OF BDNF PROTEIN IN ISCHEMIC BRAIN

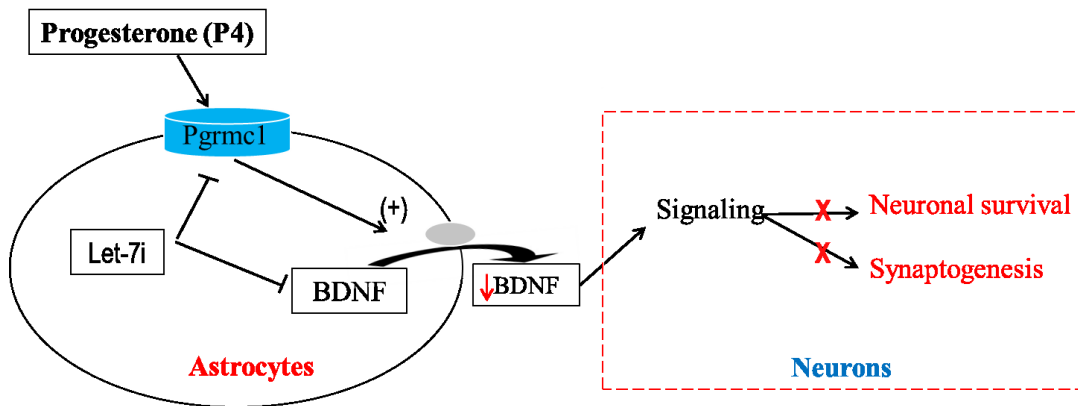
Our data demonstrate that P4 induced a significant release of mature BDNF from glia, which we suggest mediates P4-induced neuroprotection and synaptogenesis. Furthermore, the levels of mature BDNF level observed in the ischemic brain with the combined treatment (of the let-7i antagomir and P4) was far greater than the effect of P4 alone. And while the enhanced expression of Pgrmc1 can explain the increased P4-induced release of BDNF with the combination of let-7i antagomir and P4, what is still unclear is the mechanism underlying the increased expression of BDNF protein. One possible mechanism is based on the hypothesis that inhibition of let-7i increases the stability of BDNF mRNA (creating a larger translatable pool of BDNF mRNA), or alternatively, promotes the conversion from the pro- to mature-form of BDNF. While the literature does not provide any information on the stability of BDNF transcripts, we have consolidated evidence from the literature to support our second hypothesis, which focuses on the conversion of the pro-form of BDNF to the mature form of the protein. An *in silico* analysis reveals that Kruppel-like factor 8 (KLF8) is a potential target of let-7i. KLF8 has been shown to increase the expression of matrix metalloproteinase (MMP)9, at least in a peripheral (non-CNS) cell type (28). MMP9, in turn, has been shown to promote the conversion of pro-BDNF to mature-BDNF. Taken together, we propose that ischemia-induced upregulation of let-7i leads to the suppression in KLF8 expression, resulting in a downregulation of MMP9. Under such conditions, the conversion of BDNF protein to mature form would be limited. If this is true, then it could explain why P4 treatment increases total BDNF protein, but only a small fraction of that is converted to mature BDNF in ischemic brain.

OTHER CNS DISEASE MODELS

As discussed above, TBI-induced increased expression of let-7i may be responsible for the dampening protective effect of P4 in clinical studies. Thus, we propose to study whether let-7i inhibition can enhance P4's beneficial effect in TBI. Due to the significant effect of the combined let-7i/P4 treatment on synaptophysin levels, this intervention may also be applied to Alzheimer's Disease (AD), a disease characterized by profound neuronal and synaptic loss (29).

CONCLUSION

In conclusion, I have determined that that let-7i represses P4's neuroprotective effects by down-regulating the expression of both Pgrmc1 and BDNF in glia, leading to the suppression of P4-induced BDNF release from glia, and the attenuation of the beneficial effects of P4 on neuronal survival and synaptogenesis in the ischemic brain. My results have provided an important step toward advancing not only our fundamental understanding of the receptor pharmacology associated with P4's effects in the CNS, but also revealed the role of a major miRNA in the regulation of P4's protective effects. Furthermore, these studies also reveal new and important mechanistic details that are relevant to the development of novel miRNA-based therapeutic strategies in mitigating the structural and functional deficits associated with stroke, and possibly other CNS pathologies such as TBI and AD.



STROKE BRAIN

REFERENCES

1. Cekic M, Sayeed I, & Stein DG (2009) Combination treatment with progesterone and vitamin D hormone may be more effective than monotherapy for nervous system injury and disease. *Front Neuroendocrinol* 30(2):158-172.
2. Micevych P, Bondar G, & Kuo J (2010) Estrogen actions on neuroendocrine glia. *Neuroendocrinology* 91(3):211-222.
3. Wong AM, *et al.* (2009) Progesterone influence on neurite outgrowth involves microglia. *Endocrinology* 150(1):324-332.
4. Franke H, Verkhatsky A, Burnstock G, & Illes P (2012) Pathophysiology of astroglial purinergic signalling. *Purinergic Signal* 8(3):629-657.
5. Jodhka PK, Kaur P, Underwood W, Lydon JP, & Singh M (2009) The differences in neuroprotective efficacy of progesterone and medroxyprogesterone acetate correlate with their effects on brain-derived neurotrophic factor expression. *Endocrinology* 150(7):3162-3168.
6. Liu L, *et al.* (2010) The neuroprotective effects of Tanshinone IIA are associated with induced nuclear translocation of TORC1 and upregulated expression of TORC1, pCREB and BDNF in the acute stage of ischemic stroke. *Brain research bulletin* 82(3-4):228-233.
7. Sato Y, *et al.* (2009) White matter activated glial cells produce BDNF in a stroke model of monkeys. *Neuroscience research* 65(1):71-78.
8. Causing CG, *et al.* (1997) Synaptic innervation density is regulated by neuron-derived BDNF. *Neuron* 18(2):257-267.

9. Coffey ET, Akerman KE, & Courtney MJ (1997) Brain derived neurotrophic factor induces a rapid upregulation of synaptophysin and tau proteins via the neurotrophin receptor TrkB in rat cerebellar granule cells. *Neuroscience letters* 227(3):177-180.
10. Heldt SA, Stanek L, Chhatwal JP, & Ressler KJ (2007) Hippocampus-specific deletion of BDNF in adult mice impairs spatial memory and extinction of aversive memories. *Mol Psychiatry* 12(7):656-670.
11. McAllister AK (2007) Dynamic aspects of CNS synapse formation. *Annual review of neuroscience* 30:425-450.
12. Sheng M & Hoogenraad CC (2007) The postsynaptic architecture of excitatory synapses: a more quantitative view. *Annual review of biochemistry* 76:823-847.
13. Waites CL, Craig AM, & Garner CC (2005) Mechanisms of vertebrate synaptogenesis. *Annual review of neuroscience* 28:251-274.
14. Kaur P, *et al.* (2007) Progesterone increases brain-derived neurotrophic factor expression and protects against glutamate toxicity in a mitogen-activated protein kinase- and phosphoinositide-3 kinase-dependent manner in cerebral cortical explants. *J Neurosci Res* 85(11):2441-2449.
15. Su C, Cunningham RL, Rybalchenko N, & Singh M (2012) Progesterone increases the release of brain-derived neurotrophic factor from glia via progesterone receptor membrane component 1 (Pgrmc1)-dependent ERK5 signaling. *Endocrinology* 153(9):4389-4400.
16. Wright DW, *et al.* (2014) Very early administration of progesterone for acute traumatic brain injury. *The New England journal of medicine* 371(26):2457-2466.
17. Johnson D, *et al.* (2017) Acute and subacute microRNA dysregulation is associated with cytokine responses in the rodent model of penetrating ballistic-like brain injury. *J Trauma Acute Care Surg* 83(1 Suppl 1):S145-S149.

18. Balakathiresan N, *et al.* (2012) MicroRNA let-7i is a promising serum biomarker for blast-induced traumatic brain injury. *Journal of neurotrauma* 29(7):1379-1387.
19. Jala VR, *et al.* (2017) The yin and yang of leukotriene B4 mediated inflammation in cancer. *Semin Immunol* 33:58-64.
20. Gravanis I & Tsirka SE (2008) Tissue-type plasminogen activator as a therapeutic target in stroke. *Expert Opin Ther Targets* 12(2):159-170.
21. Adler MW, Rowan CH, & Geller EB (1984) Intracerebroventricular vs. subcutaneous drug administration: apples and oranges? *Neuropeptides* 5(1-3):73-76.
22. Selvamani A, Sathyan P, Miranda RC, & Sohrabji F (2012) An antagomir to microRNA Let7f promotes neuroprotection in an ischemic stroke model. *PLoS One* 7(2):e32662.
23. Dirren E, *et al.* (2014) Intracerebroventricular injection of adeno-associated virus 6 and 9 vectors for cell type-specific transgene expression in the spinal cord. *Hum Gene Ther* 25(2):109-120.
24. Atkinson AJ (2017) Intracerebroventricular drug administration. *Translational and Clinical Pharmacology* 25(3).
25. Alvarez-Erviti L, *et al.* (2011) Delivery of siRNA to the mouse brain by systemic injection of targeted exosomes. *Nat Biotechnol* 29(4):341-345.
26. Hwang DW, *et al.* (2011) A brain-targeted rabies virus glycoprotein-disulfide linked PEI nanocarrier for delivery of neurogenic microRNA. *Biomaterials* 32(21):4968-4975.
27. Miyake MM & Bleier BS (2015) The blood-brain barrier and nasal drug delivery to the central nervous system. *Am J Rhinol Allergy* 29(2):124-127.
28. Wang X, *et al.* (2011) KLF8 promotes human breast cancer cell invasion and metastasis by transcriptional activation of MMP9. *Oncogene* 30(16):1901-1911.
29. Serrano-Pozo A, Frosch MP, Masliah E, & Hyman BT (2011) Neuropathological alterations in Alzheimer disease. *Cold Spring Harbor perspectives in medicine* 1(1):a006189.

CHAPTER VII

PATENT/PUBLICATIONS

1. Singh, M., Su, C., **Nguyen, T.** Inhibition of Let7i as a Means to Enhance the Protective Effect of Progesterone Against Stroke. Provisional Serial No. 62/544,994. Filing date: 08-14-17.
2. **Nguyen, T.**, Sun, F., Jin, X., Huang, R., Chen, Z., Cunningham, R. C., Su, C. (2016). Pgrmc1/BDNF signaling plays a critical role in mediating glia-neuron crosstalk. *Endocrinology* 157(5), 2067–2079.
3. **Nguyen, T.**, Su, C., Singh, M. (2018). let-7i inhibition potentiates progesterone's action on functional recovery in a mouse model of ischemia. *Proc Natl Acad Sci USA*. (Under review)
4. Singh, M., Brock, C., **Nguyen, T.**, Toofan, J. Kubelka, N., Li, R., Sumien, N. (2017). Estrogen, Progesterone and Testosterone as key factors that impact sex differences in Alzheimer's Disease. *Alzheimer's and Dementia*. (Under review)
5. Sun, F., **Nguyen, T.**, Jin, K., Simpkins, J.W., Su, C., Singh, M. (2018). A Potential Role of Pgrmc1 in Hippocampal Function. *Brain Research*. (In preparation)
6. Kim, S., **Nguyen, T.**, Toofan, J., Rybalchenko, N., Singh, M. (2018). Pgrmc1 mediates the P4-induced protection against oxidative stress in glial and neuronal cells. *Endocrinology*. (In preparation)